

SUSTAINABILITY STRATEGIES ASEMERGING TRENDS FOR COMPETITIVE ADVANTAGES IN CHOCOLATE INDUSTRY

Dr. Raveesh Agarwal¹, Monica Thiel², Nitin Bisht³

¹Professor and Head, Department of Business Administration,
Rajshree Institute of Management & Technology, Bareilly, (India)

²Ph.D. Candidate, Social Science, Tilburg University, The Netherlands

³Associate Professor, Rajshree Institute of Management & Technology, Bareilly, (India)

ABSTRACT

This case focuses on sustainability strategies of global chocolate manufacturers. Many chocolate manufacturers purchase significant amounts of West African cocoa to meet challenges and find new opportunities to simultaneously create strategic value for the company, the supply chain, local farmers, and communities in a globally competitive marketplace. Today, companies use sustainability strategies to continuously create and display strong corporate responsibility derived from public and stakeholder pressure and demands within complex social, environmental and economic issues. This case will provide insights of innovative corporate responsibility and sustainability strategies to increase and sustain competitive advantage for farmers, communities, and companies resulting from increasing market competition, price fluctuations and public demands.

Keywords: *Cocoa, Corporate Responsibility, Strategy, Sustainability*

I. INTRODUCTION ABOUT COCOA & CHOCOLATE INDUSTRY

As we all know that Chocolate is made from the cacao beans, the dried and partially fermented seeds of the cacao tree which is generally referred as cocoa. Cacao trees are small, understory trees that need rich, well-drained soils. The three main varieties of cacao beans used in chocolate are Criollo, Forastero, and Trinitario. Criollo represents only 5% of all cocoa beans grown as it is the rarest and most expensive cocoa in the market. It is difficult to grow, as they are vulnerable to a variety of environmental threats and produce low yields of cocoa per tree (Kowalchuk & Kristine 2008). Forastero is the most commonly grown bean. The African cocoa crop is entirely of the forastero variety. They are significantly hardier and of higher yield than Criollo. Trinitario is a natural hybrid of criollo and forastero. Nearly all cacao produced over the past five decades is of the forastero or lower-grade trinitario varieties (Meta Efficient 2008).

Cocoa is produced by the farmers in the tropical climates of Western Africa, Asia, and Latin America (World Cocoa Foundation 2012). The cocoa sector forms the economic backbone of many countries as it contributes in their gross domestic product (GDP) and provide a basis to earn foreign money. Much of the world's cocoa comes from West Africa, which provides 70% of total output. The two main suppliers are the Cote d'Ivoire and Ghana (BCCCA case study 2013). The world cocoa market includes exports valued at more than \$1.2 billion from Côte d'Ivoire, the world's top-producing country; \$840 million from Indonesia, the number two producer; and \$650 million from Ghana, the number three producer. The industry also serves as a significant economic

engine in Europe and the United States. As the leading importing country, the Netherlands imports approximately \$2 billion worth of cocoa beans, with the United States following with an estimated \$1.2 billion worth of beans. The seeds of the cacao tree have an intense bitter taste that's why it is fermented to develop the flavor. After fermentation, the beans are dried, cleaned, and roasted. The shell is removed to produce cacao nibs, which are then ground to cocoa mass, pure chocolate in rough form. Because the cocoa mass is usually liquefied before being molded with or without other ingredients, it is called chocolate liquor. The liquor also may be processed into two components: cocoa solids and cocoa butter. Unsweetened baking chocolate (bitter chocolate) contains primarily cocoa solids and cocoa butter in varying proportions. Much of the chocolate consumed today is in the form of sweet chocolate, a combination of cocoa solids, cocoa butter or other fat, and sugar. Milk chocolate is sweet chocolate that additionally contains milk powder or condensed milk. White chocolate contains cocoa butter, sugar, and milk but no cocoa solids. The U.S. cocoa and chocolate industry is composed of approximately 650 companies that directly employ nearly 70,000 Americans. More than 2,000 companies in the European Union are part of the chocolate and confectionery products industry (Holly Houston, 2012). Most of the people of these countries are dependent on the production of cocoa and its related product thus provides livelihood and income to these peoples. Unlike larger industrialized agribusinesses, the vast majority of cocoa still originates on family-run small farms that have limited access to resources and organized markets. From the producer point of view, it is globalized cash crop as the demand of cocoa and its related products are increasing day by day in the world market especially in the countries like Brazil, China, Eastern Europe and India because the consumption is increasing in these countries. Chocolate is loved in all over world which is made by many companies in different size, flavor, design, etc. Many chocolate lovers consume and enjoy chocolate without ever thinking about where it comes from or how it was produced. The chocolate industry is steadily growing at \$50 billion-a-year worldwide business. Europe accounts for 45% of the world's chocolate revenue (Jones & Sarah 2009). Following table provide the overview of top 10 global confectionery companies based on their net sales in 2013 (Candy Industry, 2014). These companies manufacture some form of chocolate including non-confectionery items.

TABLE 1: Global Producers of Chocolate

Company	Net Sales 2013 (US\$ millions)
Mars Inc (USA)	17,640
Mondelēz International Inc (USA)	14,862
Nestlé SA (Switzerland)	11,760
Meiji Holdings Co Ltd (Japan)	11,742*
Ferrero Group (Italy)	10,900
Hershey Foods Corp (USA)	7,043
Arcor (Argentina)	3,700
Chocoladenfabriken Lindt & Sprüngli AG (Switzerland)	3,149
Ezaki Glico Co Ltd (Japan)	3,018*
Yildiz Holding (Turkey)	2,500

Source: Candy Industry, January 2014

*Include non-confectionery items

A report “Global Chocolate, Cocoa Beans, Lecithin, Sugar and Vanilla Market by Market Share, Trade, Prices, Geography Trend and Forecasts (2011-2016)” was conducted by Markets and Markets (M&M) which predicts that global chocolate market will grow to \$98.3 billion in 2016 from the \$83.2 billion as it was in 2010 (M&M 2011). The factors like health benefits of chocolate, seasonal and festive sales, use of chocolate as functional food, etc. play an important role in increasing the demand of cocoa. It is made in the form of a liquid, paste or in a block or used as a flavoring ingredient in other sweet foods. As consumption continues to increase on an annual basis, it becomes more difficult for the industry to keep up with demand. It is estimated that an additional 1 million tons will be needed by 2020 (Mark, Rob 2013).

The expected additional demand of cocoa and its related products raise few question about how to increase the production, how to improve the quality of cocoa beans, etc. On the other hand there is growing demand for guaranteed sustainably produced cocoa. With the increasing global demand for sustainable cocoa the sector has been pressured to use certification as a guarantee for sustainable cocoa production. Since there is not yet sufficient certified cocoa in the system, this pose another concern for whole supply system. At the same time, many cocoa farmers have few resources to improve the cocoa production as they have little earning with it. That’s why there is demand to address the issues related to increase the sustainable production of cocoa and its related products.

II. A ROAD AHEAD: FULL OF CHALLENGES

Although many chocolate manufactures are performing very well in the market, there are continual challenges that the firm must address such as:

- § Millions of smallholder farmers who cultivate small plot size
- § Low productivity and disposable income
- § Little financial help available for agro-inputs and rehabilitation.
- § Unorganized Market
- § In organized market, limited number of traders and manufacturers
- § Less investments by coco farmers as they are not financial sound
- § Underdeveloped supply chain
- § Increased demand for sustainable, certified cocoa
- § Demand for new planting materials
- § Requirement of long-term fund at low interest rate
- § Gradual process of sustainable cocoa production which takes time
- § Requirement of latest technology to increased sustainable cocoa production
- § Replacement of aging trees
- § Quality control before and after delivery
- § Requirement of more land for planting the cocoa trees
- § Demand to increase plant density
- § Increase the production of special high-flavor cocoa
- § Production of disease resistant cocoa and its related products
- § Increase productivity and deployment of improved materials
- § Requirement of practical plant breeding programs
- § Growing demand for organic cocoa products

- § No good access of improved planting material by most of the farmers
- § Continuous requirement of good quality planting material in the farming system of every country
- § Issue related to child labor and slavery in this industry
- § Demand for Fair Trade certified producer
- § More research requirement in total supply chain of cocoa production
- § New product demand from consumers in new markets located in China, Brazil, Russia and India.
- § Reducing incident rates and operational challenges.
- § Improving safety metrics.
- § Increase firms' capacities through partner organizations.
- § Global supply chain expansion into competitors' markets.
- § Benchmark international environmental data.
- § Requirement to act on above issues on priority basis

III. STRATEGIES ADOPTED AT GLOBAL LEVEL

We require continuous formulation and implementation of strategies as there is no single method which can solve the above issues. Now days, most of the companies started to act to solve these issues and they are formulating and implementing many strategies especially related to sustainable cocoa production and certification. Many facilities and incentives are provided by them which creating the opportunities for different categories of farmers. They started to invest in capacity building of farmers which open the way for improve productivity and high income for the farmers. To address the above issues and challenges facing by cocoa producers and farmers, public and private-sector are partnering with each other. The main purpose of this alliance is providing financial help and expertise to improve sustainable cocoa farming. World Cocoa Foundation (WCF) is playing an important role as it promotes a sustainable cocoa economy through economic and social development and environmental conservation in cocoa-growing communities. At global level International Cocoa Initiatives were also taken in which partnership between NGOs, labor unions, cocoa processors and the major chocolate brands is taken place to change the way cocoa is grown. At the same time, International Cocoa Organization is formed by cocoa-producing and cocoa-consuming countries and National Confectioners Association which fosters industry growth by advancing and promoting the interests of the confectionery industry and its consumers. An alliance is also formed among Cocoa Producers which is Inter-governmental organization to promote the research in cocoa farming.

3.1 Sustainability Priority Issues

Some examples of prioritized specific issues that are of concern to stakeholders within an economic, financial, environmental or social point of views as this could substantially impact a firm's capacity to implement and direct a company's business strategy. Generally shared priority issues are as follows: Consumer Health and Talent Management, Global Competitiveness, Carbon Emissions, Sustainable Agriculture, Operations and Clients, Transparency, Public Policy, Supply Chain, Access to Health care, Ethics, Compliance, Food Safety, Child Labor, Governance, and Ethical Sourcing. Many firms' strategic approach to managing issues is strategic and driven by top management. However, it is a very challenging and complex process to embed social and natural environmental concerns into a company's daily decision making throughout the company. Therefore, many companies are adopting the following strategies to meet the challenges:

3.1.1 Improve Farmer Incomes and Farming Communities

In order for companies to make a transition towards a fully certified cocoa supply, many firms have created and implemented a Cocoa Sustainability Strategy. These strategies attempt to increase incomes for farmers through modernization of cocoa farming, evoke new farmers, and improve cocoa farming communities. Some companies are utilizing mobile phone technology to give access to crucial information and training for farmers to increase income and cocoa yields in Cote d'Ivoire, and Ghana, Africa. This will help to foster capacity building and progress in literacy, shared information and learning of cocoa growing, production and marketing for farmers and local communities (Reuters Edition, U.S., 2012). World Education oversees monitoring and evaluation of cocoa programs such as the CocoaLink program. The impact of the program includes:

- § In 2013, CocoaLink farmers increased incomes and cocoa yields with increases of 10 percent cocoa output than the control cocoa farming communities that were studied. The farmers improved cocoa yields over three years resulting in 45.6 percent from 2.5 cocoa bags per acre in 2011 to 3.64 in 2013.
- § Household expenditures, a proxy for incomes, increased 78 percent in test communities
- § Conservation training was administered to 88 percent of CocoaLink farmers compared with 68 percent of farmers not associated with CocoaLink.
- § Basic Literacy training was received by 65 percent of CocoaLink farmers compared resulting in 35 percent higher than farmers not associated with CocoaLink.
- § Bookkeeping training was taught to 65 percent of CocoaLink farmers resulting in 25 percent higher than farmers not associated with non-CocoaLink.
- § One-third of farmers using CocoaLink are women

Barrientos (2011) suggests that recent estimates for demand of cocoa in growing markets will surpass supply by 2020. Therefore, chocolate manufacturers are creating socio-economic sustainability initiatives to sustain their cocoa value chains. The World Cocoa Foundation and key members of the cocoa industry formed a new cocoa strategy entitled, CocoaAction. This initiative aims to increase the social, economic and environmental impact for a sustainable supply of cocoa growing and production for farmers and local communities in Ghana and Cote d'Ivoire, Africa by 2020 (Hershey Press Release, May 20, 2014). The key aims of Cocoa Action are listed as follows:

- § Strengthening interventions between productivity-enhancing and community development.
- § Creating and committing to holistic methods in the shape of a productivity and community development proposal, which portrays how chocolate manufactures can make a substantial and novel contribution.
- § Customized field-level delivery based on local circumstances.
- § A platform to drive national public-private partnerships and interventions within the framework of chocolate manufacturers' programs.

Many chocolate manufacturers are collaborating with the World Bank and NGOs to ensure that all chocolate products are 100 percent certified cocoa worldwide and are verified by independent auditors to make certain the most significant international standards are sustained for environmental, labor, and farming practices. Companies attempt to beat goals of sourcing by at least 10 percent of its cocoa from certified farms and to remain on track to a 100 percent certified supply by 2015 – 2020 and beyond. Chocolate manufacturers are increasingly ensuring that all chocolate products use cocoa that is Rainforest Alliance Certified resulting from a firm's strategy to use cocoa from certified farms (Pasolini, 2014). For example, many chocolate manufacturers' source cocoa from the most recognized cocoa certifying organizations in the world: Fairtrade USA, UTZ, and

Rainforest Alliance, and continues to collaborate with other prominent certification organizations increase certification of more cocoa from cocoa farmers worldwide. In fact there are lots of challenges involved in it. Many chocolate manufacturers understand the crucial capabilities required to modernize cocoa farming and consequently create entrepreneurial sustainability programs, and public/private initiatives.

In a globally competitive environment, labor is more easily mobile, but the communities are “less mobile than the job themselves” (Jinha, 2009, p. 101). Sourcing cocoa from countries that lack a strong knowledge economy provides many social, economic and environmental challenges for global companies, international supply chains, farmers and communities. Many chocolate manufacturers are working to transform its global supply chain for multiple needs and demands from diverse customers in the US and Canada and in emerging global markets. As a result, firms expect progressive growth for innovative product development, customer service and global sourcing improvement that will lower operating costs while maintaining 100 percent tractability and sustainably sourced. Overall, as chocolate manufacturers continue to implement changes into its global supply chain, suppliers will be required to maintain high levels of sustainability practices and conduct such as:

- § Protecting natural resources beyond local environmental laws and regulations.
- § Country regulations and local law compliance.
- § Strict monitoring of sourcing practices with sourcing partners.
- § Protect proprietary and confidential information.
- § Follow the Organization for Economic and Cooperation Development (OECD) Multinational Guidelines on antitrust laws.
- § Risk and Self-Assessment.
- § Independent Auditors.

3.1.2 Strategic Initiatives for Social and Economic Well-being

In order to sustain positive change, many chocolate manufacturers recognize that farming communities must acknowledge the company’s initiative are creating daily value for farmers and their communities. For this reason, firms are making significant efforts to improve socio-economic conditions in West Africa through continuous measurement and innovation for over 10 million people that are dependent upon cocoa farming for securing the necessities of life. Currently, several chocolate manufacturers are focusing the company’s initiatives in the West African regions of Côte d’Ivoire and Ghana, due to cocoa farmers desire to increase farmer incomes and improve the conditions and livelihoods of cocoa farmers and farming communities and in other countries through continuous measurement and innovation projects.

There are many other programs that are initiated by chocolate manufacturers to promote social and economic opportunities for farmers and local communities. However, fluctuations of cocoa prices and cocoa production drive farmer poverty (Marshall, et al., 2013). Furthermore, it is difficult to produce and maintain the highest cocoa quality and to provide equal opportunities to all the farmers every time. Nevertheless, firms are creating new Corporate Social Responsibility (CSR) models for farmers and local communities by providing a better future for farmers and local communities will help to sustain cocoa production and competitive advantage for farmers, local communities and for the company itself from increasing market demands and price fluctuations. A new CSR model can work as a filter to analyze current commitments and explore new opportunities for increasing the wellbeing of the company’s stakeholders such as consumers, employees, investors, business partners, communities and local governments, policy makers and non-governmental organizations for improving

performance that leads to global competitive and comparative advantage for farmers and chocolate manufacturers. In addition, many companies develop initiatives in the form of hosting sports and other activities to promote national consumer education for healthy lifestyles. Another unique and innovative initiative by some chocolate manufacturers is creating shared value between business schools and MBA students to lead private-public coalitions in farming communities for increasing social impact (Financial Times, 2014). Understanding the role of business and management in society is becoming an important strategy for sustaining responsible business strategies. Overall, new business models are needed to create new opportunities for global competition. Many chocolate manufacturers have also taken many steps to protect the natural environment which include sustainable product design, sustainable sourcing of raw materials, etc. Some initiatives taken by firms to:

- Purchase sustainable paper from those suppliers who are certified by Forest Stewardship Council or Sustainable Forestry Initiative and use sustainable forestry practices.
- Focus the company's initiatives towards recyclable packaging, including foil, boxes, syrup bottles, and paper wrappers. Waste reduction assisted the company in saving lots of money for its future operations.
- Develop zero-waste-to-landfill facility. The waste, which is generated from its operation, is not used for land filling. Most of the waste is recycled and the waste which is not able to recycle; goes into energy incinerator and is used as a fuel. Many firms have established 2015 waste reduction goals.
- Purchased palm oil from suppliers who are the members of Roundtable of Sustainable Palm Oil (RSPO) due to the highly controversial impact on ecosystems. Some firms are also members of RSPO.

IV. CONCLUSION

As the expectations of markets and stakeholders evolve, chocolate manufacturers started to refine its approach by managing environmental, social and governance issues. The overall focus is given to engage with its various stakeholder groups, including cocoa farming families, its business partners, consumers and investors. In particular, firms create initiatives for consumer well-being and health, product safety and quality and local community programs in various countries to improve cocoa farming and social conditions. It may be said that chocolate manufacturers various initiatives will yield fruitful results, which will support and advance its business in global markets. Furthermore, we have to understand that these companies can make substantial efforts to increase social, environmental and economic sustainability. Consequently, the capacities of chocolate manufacturers to foster positive social and environmental change in farming communities provides continual challenges and opportunities for farmers and local communities to drive sustainability together and increase the competitiveness of the firm and farming communities.

REFERENCES

- [1] 21st Century Cocoa Sustainability Strategy, The Hershey Company Corporate Social Responsibility, www.thehersheycompany.com, retrieved: April 22, 2014
- [2] Barrientos, S. (2011). Beyond Fair Trade: Why are Mainstream Companies Pursuing Social and Economic Sustainability in Cocoa Sourcing? Paper to ILO/IFC Better Work Conference, October 2011.
- [3] Retrieved from betterwork.com/global/wp-content/.../Session-1-Beyond-Fair-Trade.pdf on May 24, 2014.

- [4] BCCCA Case Study (2013) Creating a sustainable chocolate industry, <http://businesscasestudies.co.uk/bccca/creating-a-sustainable-chocolate-industry/the-world-market-for-cocoa>, retrieved: July 22, 2014.
- [5] Candy Industry (January 2014), <http://www.icco.org/about-cocoa/chocolate-industry.html> retrieved July 22, 2014.
- [6] Financial Times. (April 22, 2014). The MBA blind spot, www.ft.com Retrieved on September 2, 2014.
- [7] Holly Houston (2012) World Cocoa Foundation, The Center for Strategic and International Studies, <http://csis.org/publication/why-sustainable-cocoa-farming-matters-rural-development>, retrieved July 23, 2014.
- [8] Hershey's 2013 Corporate Social Responsibility Report. Retrieved from www.thehersheycompany.com/social-responsibility/.../2013_THC_CSR.pdf on May 24, 2014.
- [9] Hershey's Facts: The Hershey Company, Investor Relations Department, 100 Crystal A Drive, P.O. Box 810, Hershey, PA 17033-0810 Retrieved :www.thehersheycompany.com dated on March 23, 2014
- [10] Hershey India. (2014). <http://www.hersheyindia.com/about/history/>, Retrieved: March 30, 2014
- [11] Hershey's News. (May 20, 2014). Hershey Joins With World's Largest Cocoa And Chocolate Companies in Cocoa Action Initiative. Retrieved from www.thehersheycompany.com on May 24, 2014.
- [12] Hershey's Responsible Sourcing. (2014). Retrieved from www.thehersheycompany.com on May 24, 2014.
- [13] Jones, Sarah (2009). "U.K. Stocks Fluctuate as Mining Shares Rally; Cadbury Declines". Bloomberg, http://en.wikipedia.org/wiki/chocolate#cite_note_45 Retrieved July 24, 2014. Jinha, A. E. (2009). Smiths Falls In The World: A Study of Globalization In A Rural Canadian Town. *Just Labour: A Canadian Journal of Work and Society, Volume 14*. Autumn 2009.
- [14] Kowalchuk & Kristine (2008) "Cuckoo for Cocoa". Westworld Alberta, http://en.wikipedia.org/wiki/chocolate#cite_note_45, Retrieved July 24 February 2014.
- [15] Mark Guiltinan, Rob Lockwood, Siela Maximova, A. Roberto Sena Gomes and Georges Sodr  (2013), Review of Propagation Methodologies to Supply New Cocoa Planting Material to Farmers, Brigitte Lalibert  Bioversity International WCF Partnership Meeting, Washington DC, USA.
- [16] Markets and Markets (M&M), "Global Chocolate, Cocoa Beans, Lecithin, Sugar and Vanilla Market by Market Share, Trade, Prices, Geography Trend and Forecasts (2011-2016)", <http://www.candyindustry.com/articles/global-chocolate-market-worth-98-3-billion-by-2016>, Retrieved July 23, 2014
- [17] Marshall, Scott; Brown, Darrell; Sakarias, Bex; and Cai, Min, "Mad casse: Competing with a 4x Fairtrade business model" (2013).
- [18] Business Administration Faculty Publications and Presentations. Paper 18. Retrieved on March 24, 2014 from http://pdxscholar.library.pdx.edu/busadmin_fac/18
- [19] Meta Efficient (2008), "Criollo Chocolate: Efficient Food of the Gods", www.metaefficient.com/food-and-drink/criollo-chocolate-efficeint-foods-of-the-goods.html, Retrieved July 24, 2014.
- [20] Pasolini, Antonio. (Feb, 2014), Chocolate gets sweeter with CSR in the mix, Just means, <http://www.justmeans.com/blogs/%E2%80%8Bchocolate-gets-sweeter-with-csr-in-the-mix>, Retrieved: May 4, 2014

- [21] Reese, Andrew (2008). REESE'S Peanut Butter Cups: The Untold Story. iUniverse. ISBN 978-0-595-48707-3.
- [22] Reuters Edition, U.S. (August 6, 2012). Hershey's CocoaLink Mobile Phone Program Delivers 100,000 Farmer and Family Messages During First Year in Ghana. Retrieved from <http://www.reuters.com/article/2012/08/06/idUS137424+06-Aug,2012+BW20120806> on May 24, 2014.
- [23] The Hershey Company 2011–2012 Corporate Social Responsibility Disclosure Index www.thehersheycompany.com, Retrieved: May 24, 2014.
- [24] The Hershey Company News. Hershey Announces Global Supply Chain Transformation. www.thehersheycompany.com, Retrieved August 17, 2014.
- [25] World Cocoa Foundation (March 2012) "Cocoa Market Update", <http://worldcocoafoundation.org/wp-content/uploads/Cocoa-Market-Update-as-of-3.20.2012.pdf> retrieved July 22, 2014.

ROLE OF META-HEURISTIC ALGORITHMS IN CLOUD COMPUTING

Ritu Kapur

ME Student, Computer Science Department NITTTR, Chandigarh (India)

ABSTRACT

Efficient Resource Scheduling in cloud has become a challenge for Cloud Service Providers. Resource Scheduling should be such that it minimizes the overall resource cost, minimizes the overall execution time, increases throughput, fails less frequently, balances the load on server and delivers the best possible QoS. The algorithms that help in achieving these aims while doing an efficient resource scheduling come under the category of meta-heuristic algorithms. Some of the examples are Genetic Algorithms, Ant Colony Optimization, and Particle Swarm Optimization etc.

Keywords: *Cloud, Load Balancing, Meta-Heuristic Techniques, QOS, Self- Learning Algorithms*

I. INTRODUCTION

Cloud Computing has emerged as a popular area of research and development in the past few years. Although no unique definition of Cloud Computing exists many standard organizations continue to give various definitions for it [1]. According to National Institute of Standards and Technology (NIST) definition in September 2011 in [2], Cloud computing is defined as “a model for enabling ubiquitous, convenient, on-demand network access to a shared pool of configurable computing resources (e.g., networks, servers, storage, applications, and services) that can be rapidly provisioned and released with minimal management effort or service provider interaction”. Cloud computing as utility provides pay-per use and pay-as-you-go service [3] i.e. a client/user has to only pay for the amount of services used by him [4].

According to [5] and [6], International Standards Organization (ISO) on 24th October 2014 defined cloud computing as “an evolving paradigm” and identified and described its “key characteristics” including broad network access, measured service, multi-tenancy, on-demand self-service, rapid elasticity and scalability, and resource pooling. Cloud computing basically provides three service models: Software as a Service (SaaS), Platform as a Service (PaaS) and Infrastructure as a Service (IaaS) as shown in [2] and [7]. According to [8], [9] and [3], IaaS provides the access to various resources which provide processing, storage, networks, operating systems and various other capabilities of scaling up and down the infrastructure dynamically. The services or resources required by a particular user are listed in the Service Level Agreement (SLA) established as a contract between the cloud service provider and the cloud consumer respectively [10].

According to D. Linthium in [11], Amazon is providing lowest priced instances and thus most of the researchers in [14-17] have deployed Amazon Cloud in [12] and Azure Cloud in [13] for their simulations. CloudSim, being an open source tool can also be used for simulations as used in [18]. The detailed implementation and basic design of CloudSim is explained in [19].

The authors in [20-39] discuss the concept of various meta-heuristic algorithms like Genetic Algorithms (GAs), Ant Colony Optimization (ACO) algorithms, Particle Swarm Optimization (PSO) algorithms etc. Meta-

Heuristic Algorithms [39] are inspired from the natural phenomena and may provide a sufficiently good solution to an optimization problem, especially with incomplete or imperfect information or limited computation capacity. The authors in [20-23, 37, 38] discuss various genetic algorithms. GA provide a solution to complex combinational optimization problems [26], which come under the category of NP-Hard problems and thus their solution is hard to find.

The authors in [24-32, 38] discuss various Ant Colony Optimization (ACO) algorithms. ACO uses a colony of artificial ants which behave as cooperative agents in a mathematical space where they are allowed to search and reinforce pathways (solutions) in order to find the optimal solution [32]. K. Li et al. [24] presents a Load Balanced version of basic ACO proposed by M. Dorigo et al. [28-29]. The authors in [23] also give a load balancing factor for the same. The authors in [31] describe an optimized version of basic PSO algorithm shown by [32]. PSO is similar to GA [32], but there is no direct operation on the individuals of the population. Instead, PSO relies on the social behavior of the particles. In every generation, each particle adjusts its path based on its best position (local best) and the best position among its neighbors.

Meta-Heuristic Algorithms [32] inspired by evolution programs, assume that the solutions to be passed on to the next generations are selected by a particular mechanism. Thus the meta-heuristic algorithms are also called evolutionary or self-learning.

II. ARCHITECTURE

2.1 Cloud Computing Architecture [40]

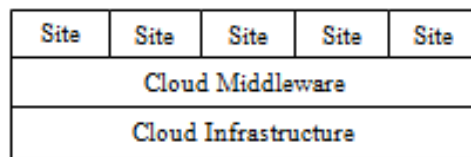


Fig. 1 Cloud Computing Architecture [40]

Cloud Service Providers or Site owners provide various services to the Cloud Consumers through the Middleware Layer from the actually executing Infrastructure Layer below which has the actual hardware resources like processors etc.

2.2 Algorithms

2.2.1 Genetic Algorithm [20-23, 37]

Jingyi Ma [20] proposes a genetic algorithm named as a heuristic genetic load balancing algorithm (HGLBA) which helps in reducing the overall response time of the tasks through its load balancing phenomenon. The algorithm executes in the following manner:-

- A) **Generate:** The first step is to generate the initial population, P(0). This initial population is basically some initial solutions coded in the form of chromosomes. The maximum iteration named as *MaxSize* is initialized to zero i.e. k=0;
- B) **Evaluate:** In the evaluation step, the Fitness value of the Initial Population, P(k), is evaluated on the basis of some function. e.g. the evaluation function in [44] is shown below in equation 1.

$$T_j = \sum_{i=1}^m (w_{ij} * Q_{ij}) \text{ for } \varphi=1, 2, \dots, n \quad (1)$$

where w_{ij} represents the weight listed to various QoS parameters (according to the user preferences), Q_{ij} represents the expected values of QoS parameters, T_j is the fitness function of the task j , m represents the total no. of parameters and n represents the total no. of resource types.

C) Improve: In this improve step, various operations like mutation and crossover etc. are applied in order to generate the next generation, $P(k+1)$.

D) Termination: If the iteration $k > \text{MaxSize}$, we take the best solution and terminate the process otherwise we increment k , i.e. $k=k+1$, and continue the process from step B.

As this algorithm provides optimal allocation of resources, it serves the aim of the load balancing i.e. the minimization of overall execution time. The authors in [53] present a variation of genetic algorithm in an unreliable cloud scenario.

2.2.2 Ant Colony Optimization (ACO) Algorithm [24-31]

M. Dorigo et al. [28-29] present the basic ACO algorithm. K. Li et al. [24] embeds the load balancing parameter into it and thus presents a Load Balanced ACO i.e. LBACO algorithm. According to the authors in [23-28] ants have a general property of locating their path to food. In this phenomenon of locating their food, ants keep on depositing a chemical substance known as pheromone. This pheromone in turn helps new ants on their path to find the shortest route to the food. The path having largest amount of pheromone represents the shortest route. So this process thus leads the new ants to their location in minimum time through the shortest path.

The LBACO follows the following steps:

A) Initialization

The ants i.e. resources are randomly distributed onto various VMs initially. The pheromone is initialized as follows:

$$\tau_j(0) = pe_num_j * pe_mips_j + vm_bw_j \quad (2)$$

where pe_num , pe_mips_j and vm_bw_j represent the no. of available VM processors, MIPS (Million Instructions Per Second) and the bandwidth capacity of the processor VM_j respectively.

B) Choosing the next task

Every k^{th} ant chooses the next task with the probability $p_j^k(t)$ defined as:

$$p_j^k(t) = \frac{(\tau_j)^\alpha * (EV_j)^\beta * (LB_j)^\gamma}{\sum (\tau_j)^\alpha * (EV_j)^\beta * (LB_j)^\gamma} \text{ if } j \in 1 \dots n \quad (3)$$

else $p_j^k(t) = 0$

where $\tau_j(t)$ represents the pheromone value at time t , EV_j represents the computing capacity of j^{th} VM defined as follows:

$$EV_j = pe_num_j * pe_mips_j + vm_bw_j \quad (4)$$

LB_j represents the Load balancing factor for the j^{th} VM represented as follows:

$$LB_j = 1 - \frac{res_j - lastAver_res}{res_j + lastAver_res} \quad (5)$$

where $lastAver_res$ represents the average execution time of all the VMs and res_j represents the current expected execution time, defined as follows:

$$res_j = \frac{total_tasklength}{EV_j} + \frac{InputFilesize}{vm_bw_j} \quad (6)$$

where $total_tasklength$ is the total length of all the tasks submitted to the VM_j and $InputFilesize$ is the length of the task before execution and α, β, γ represent the parameters to control the relative weight of pheromone laid, the computing capacity and the load balancing factor of various VMS.

C. Pheromone Updating

$$\tau_j(t+1) = (1-\rho) * \tau_j(t) + \Delta\tau_j \quad (7)$$

where ρ represents the pheromone decay coefficient,

$$\Delta\tau_j = \frac{1}{r_{ik}} \quad (8)$$

where T_{ik} represents the shortest path searched by k^{th} ant in the i^{th} iteration and once an optimal solution is found, the global pheromone updating is done as follows:

$$\Delta\tau_j = \frac{D}{r_{op}} \quad (9)$$

where D represents the encouragement coefficient and T_{op} represents the found optimal solution.

D. Terminating Step

If all the ants end their search i.e. the solution converges to an optimal value, current optimal solution is saved and the value of makespan variable, N_c , is incremented. If this makespan value proves to be the best value, the process ends else the ants continue to search for a better optimal solution.

Authors in [30-31] give a variation of ACO algorithm in which the workload is distributed uniformly among all the VMs.

2.2.3 Particle Swarm Optimization (PSO) Algorithm [32-36]

Particle Swarm Optimization (PSO) [35] is a population based stochastic optimization technique developed by Dr. Eberhart and Dr. Kennedy in 1995 inspired by social behavior of bird flocking or fish schooling. PSO is similar to GA in the sense that the system is initialized with a population of random solutions and searches for optimal solution by updating generations. However, as compared to GA, PSO does not perform any crossover and mutation operations. In PSO, the potential solutions, called particles fly through the problem space by following the current optimum particles. Each particle keeps track of its coordinates in the problem space, which are associated with the best solution (fitness), it has achieved so far. The fitness value stored is called pbest. Another best value found by the PSO optimizer by examining the particle and its neighbors is lbest. The global best value found by examining the global population is gbest.

The PSO works by varying the velocity per unit time, i.e. acceleration, of each particle towards its pbest and lbest locations. The change known as acceleration is brought about by generating random numbers by the random number generation method. The two basic equations used in PSO for calculation purpose are:

$$V_{i+1} = w * V_i + c_1 r_1 (X_{lb} - X_i) + c_2 r_2 (X_{gb} - X_i) \quad (10)$$

$$X_{i+1} = X_i + V_{i+1} \quad (11)$$

where V_{i+1} is new calculated velocity, w is inertia weight, V_i is current velocity of particle, c_1 is first acceleration coefficient, r_1 is first random variable, X_{lb} is lbest, X_i is current position, c_2 is second acceleration coefficient, r_2 is second random variable, X_{gb} is gbest, X_{i+1} is next calculated position value of variable.

The algorithm proposed by [31] has the following steps:

- A) **Initialize:** The population of particles, i.e. tasks, is initialized by initializing candidate solution, Inertia weight, pbest, lbest, gbest and other PSO variables.
- B) **Generate:** Particle mapping are generated with machines using smallest position value heuristic.
- C) **Evaluate:** Next, the fitness parameter is evaluated by using the make span parameter. If the current candidate solution has best fitness value, the new mapping is updated with its value; else the previous candidate solution is retained.
- D) **Update:** On the basis of the previous evaluate step, pbest and gbest value is evaluated

- E) Calculate:** New velocity value and new particle position is calculated based on the equation 10 and 11.
- F) Termination:** If the maximum no. of iterations are reached, candidate mapping's expected time to complete matrix is calculated and the control is passed onto the load balancing component else the process iterates to step B.
- G) Load Balancing:** Next we check if load balancing is required or not. If it is required, an appropriate max-max or min-min algorithm concept is chosen for shuffling the task mappings. Tasks are shuffled and reordered and mapping is reevaluated and the load balancing is rechecked. If the new mapping is found to be load balanced the process is terminated and the final task machine is ready for execution. If the load is not found to be balanced, the tasks are reshuffled and the process continues till a perfectly load balanced mapping is found.

The simulations by the authors in [31] prove that the proposed algorithm outperforms the basic algorithm.

III. CONCLUSION

The paper starts by introducing the concept of cloud computing and the importance of efficient resource scheduling in it. Then the importance of Meta-Heuristic algorithms like GA, ACO, LBACO, PSO etc. is explained. Meta-Heuristic algorithms help in balancing the workload. Thus a more balanced workload helps in reducing the load on server and thus decreasing the possibility of server failure and delivering a better QoS.

REFERENCES

- [1] D. Linthincum (2014), "It's pointless to define cloud computing", <http://www.infoworld.com>
- [2] "Cloud Computing Bible", by Barrie Sosinsky, Chapter 2
- [3] A. Aggarwal and S. Jain, "Efficient Optimal Algorithm and Task Scheduling in Cloud Computing Environment", International Journal of Computer Trends and Technology (IJCTT), vol. 9, pp. 344-349, Mar 2014
- [4] D. Jensen, C. D. Locke, and H. Toluca (1985), A time-driven scheduling model for real-time systems, In IEEE Real-Time Systems Symposium.
- [5] J. Borne (20th October 2014), "ISO publishes new cloud computing standards and definitions", www.cloudcomputing-news.net
- [6] T. Roughton (17th October 2014), "Cloud Computing terms defined in new ISO standard", www.out-law.com
- [7] "Cloud Computing, A Practical Approach" by Anthony T. Velte, Toby J. Velte and Robert Elsenpeter, 2010 edition, Chapter 2.
- [8] "Real time task scheduling", last chapter, Version 2, IIT Kharagpur.
- [9] Casati and M. Shan (2001)., Definition, execution, analysis and optimization of composite e-service, IEEE Data Engineering.
- [10] R Buyya, C. S. Yeo and Venugopal, "Market oriented cloud computing: Vision, hype, and reality for delivering IT services as computing utilities" in *Proc. of the 10th IEEE International Conference on the High Performance Computing and Communications*, 2008.
- [11] D. Linthincum, "Faster and Cheaper: The cloud is becoming harder to resist", <http://www.infoworld.com>
- [12] Amazon elastic compute cloud [Online]. Available: <http://aws.amazon.com/ec2>
- [13] Microsoft windows azure. [Online]. Available: <http://code.google.com/windowsazure/>

- [14] X. Nan, Y. He, and L. Guan, "Optimization of Workload Scheduling for Multimedia Cloud Computing," in *Proc. IEEE International Symposium on Circuits and Systems (ISCAS)*, pp. 1–4, 2013.
- [15] X. Nan, Y. He, and L. Guan, "Towards Optimal Resource Allocation For Differentiated Multimedia Services in Cloud Computing Environment," in *Proc. IEEE International Conference on Acoustic, Speech and Signal Processing (ICASSP)*, pp. 1–5, 2014.
- [16] X. Nan, Y. He, and L. Guan, "Optimal resource allocation for multimedia cloud based on queuing model," in *Proc. IEEE International Workshop on Multimedia Signal Processing (MMSP)*, pp. 1–6, 2011.
- [17] X. Nan, Y. He, and L. Guan, "Optimal resource allocation for multimedia cloud in Priority Service Scheme," in *Proc. IEEE International Symposium on Circuits and Systems (ISCAS)*, pp. 1–4, 2012.
- [18] Aggarwal and S. Jain, "Efficient Optimal Algorithm and Task Scheduling in Cloud Computing Environment", *International Journal of Computer Trends and Technology (IJCTT)*, vol. 9, pp. 344-349, Mar 2014.
- [19] R. Raman, R. Calheiros, R.N.(2009), "Modeling and Simulation of Scalable Cloud Environment and the CloudSim Toolkit: Challenges and Opportunities", IEEE publication , pp1-11, 2009.
- [20] J. Ma, "A Novel Heuristic Genetic Load Balancing Algorithm in Grid Computing", in *Proc. of IEEE International Conference on Intelligent Human-Machine Systems and Cybernetics*, pp. 166-169, 2010.
- [21] J. Alcaraz and C. Maroto, "A robust genetic algorithm for resource allocation in project scheduling", *Annals of Operations Research* 102 (2001) pp. 83–109.
- [22] S. Hartmann, "A competitive genetic algorithm for the resource-constrained project scheduling", *Naval Research Logistics* 456 (1998) pp. 733–750.
- [23] U. Kohlmorgen, H. Schmeck and K. Haase, "Experiences with fine-grained parallel genetic algorithms", *Annals of Operations Research* 90 (1999) pp. 203–219.
- [24] K. Li, G. Xu, G. Zhao, Y. Dong and D. Wang, "Cloud Task scheduling on Load Balancing Ant Colony Optimization", in the *Proc. of IEEE Sixth Annual ChinaGrid Conference*, 2011, pp. 3-9
- [25] Merkle, M. Middendorf and H. Schmeck, "Ant Colony Optimization for Resource-Constrained Project Scheduling", in the *Proc. of IEEE transactions on Evolutionary Computation*, Vol. 6, NO. 4, August 2002, pp. 333-346
- [26] B. Tierney, W. Johnston, J. Lee and M. Thompson, "A data intensive distributed computing architecture for grid applications", *Future Generation Computing System* 2000, 16(5): pp. 473-481, 2000.
- [27] G. Guo-Ning and H. Ting-Lei, "Genetic Simulated Annealing Algorithm for Task Scheduling based on Cloud Computing Environment", in *Proc. of International Conference on Intelligent Computing and Integrated Systems*, pp. 60-63, 2010.
- [28] M. Dorigo and C. Blum, "Ant colony optimization theory: A survey in Theoretical Computer Science", 344 (2–3) (2005), DOI: 10.1016/j.tcs.2005.05.020, pp.243–278, 2005.
- [29] M. Dorigo and L.M. Gambardella, "Ant colony system: A cooperative learning approach to the traveling salesman problem", in *IEEE Transactions on Evolutionary Computation* (1997), pp. 53–66, 1997.
- [30] Bagherzadeh, J., MadadyarAdeh, M., "An Improved Ant Algorithm for Grid Scheduling Problem" in 14th International CSI Computer Conference (CSICC), pp.323-328, 2009.
- [31] Lorpunmanee, S., Sap, M.N, Abdul Hanan Abdullah, A.H., "An Ant Colony Optimization for Dynamic Job Scheduling in Grid Environment" in *Proceedings of World Academy of Science, English and Technology* Volume 23 august 2007, ISSN 1307-6884, 2007.

- [32] Anupinder Singh and Mala Kalra, "PSO Based Load Balancing Algorithm for Cloud Environment", M.E. diss., NITTTR, Chandigarh, 2014.
- [33] M. Clerc, "The Swarm and the Queen: Towards a Deterministic and Adaptive Particle Swarm Optimization", in *IEEE Proc. of the 1999 Congress on Evolutionary Computation, Washington, DC, vol. 3*, pp. 19-24, 1999.
- [34] Y. Shi and R. C. Eberhart, "Parameter selection in particle swarm optimization", in *7th International Conference on Evolutionary Programming, San Diego, California, USA*, pp. 591-600, Springer 1998.
- [35] R. C. Eberhart and Y. Shi, "Particle Swarm Optimization: Developments, Applications and Resources", in *IEEE Proc. of the 2001 Congress on Evolutionary Computation, Seoul, vol. 1*, pp. 81-86, 2001.
- [36] J. Kennedy and R. Eberhart, "Particle Swarm Optimization", in *IEEE Proc. of International Conference on Neural Networks, vol. 4*, pp. 1942-1948, 1999.
- [37] Lovejit Singh and Sarbjeet Singh, "A Genetic Algorithm for Scheduling Workflow Applications in Unreliable Cloud Environment", *Second International Conference on Security in Computer Networks and Distributed Systems (SNDS-2014)*, Springer Berlin Heidelberg, pp. 139-150, 2014.
- [38] Ritu Kapur and Maitreyee Dutta, "Review of various Load Balancing and Green Computing Techniques in Cloud", in the *Proc. of 7th International Conference on Advances in Computing Sciences, Software Solutions, E-Learning, Information and Communication Technology (ACSEICT-2015)*, *Journal of Basic and Applied Engineering Research (JBAER)*, Print ISSN: 2350-0077, Online ISSN: 2350-0255; Vol 2, No. 2; pp. 122-127, 2015.
- [39] C.W. Tsai and J.J. Rodrigues, "Metaheuristic Scheduling for Cloud: A survey," *IEEE Systems Journal*, vol. PP, no. pp, pp. 279-291, 16 May 2013.
- [40] Verma, G. Dasgupta, T. K. Nayak, P. De, and R. Kothari, "Server workload analysis for power minimization using consolidation," in *USENIX'09*. Berkeley, CA, USA: USENIX Association, pp. 28-28, 2009.

EMBEDDED Z- SOURCE INVERTER H –BRIDGE

ArchanaMishra¹, K.M.Tripath²

¹Department of Electrical and Electronics, K.I.E.T, Ghaziabad, (India)

²Associate Professor & Head of Electrical and Electronics Department,
I.T.M GIDA, Gorakhpur (India)

ABSTRACT

The present work deals with an Embedded Z-source inverter in which various voltage and current circuitries is represented as a single unit and inverter follows buck –boost energy conversion technique. The shoot through state by which two semiconductor switches of the same phase leg can be turned ON simultaneously is a unique feature of EZ source inverter. This feature gives an advantage of improved reliability and reduced output distortion as no dead time is needed. These inverter remove the drawback of traditional voltage source and current source inverters. The loads demanding a high voltage gain to match the input source voltage differences such as power conditioning unit for renewable energy sources fuel, solar cell and motor drives etc. require EZ source inverters. These EZ inverters are safe to use and complexity is also greatly reduced. The designing of EZ-source inverters can be made by using only passive elements excluding additional active semiconductor. These latter features are attained without using any additional passive filter which surely is a favorable advantage since an added filter will raise the system cost and, at certain time can complicate the dynamic tuning and resonant consideration of the inverters. Removal of additional passive filter cheap and low harmonic distortion produce a smaller current or voltage maintained across the dc input source. To demonstrate these features analysis, simulation, and experimental results were carried out.

Keyword: Embedded Z-Source Inverters, Motor Drives, Buck-Boost, Z-Source Inverters.

I. INTRODUCTION

Power Converters are used for electrical power processing. To overcome the problems of the traditional V-source and I-source converters, an impedance-source (or impedance-fed) power converter (abbreviated as Z-source converter) and its control method for implementing dc-to-ac, ac-to-dc, ac-to-ac, and dc-to-dc power conversion. It employs a unique impedance network (or circuit) to couple the converter main circuit to the power source, load, or another converter, for providing unique features that cannot be observed in the traditional V- and I-source converters where a capacitor and inductor are used, respectively. In Z-source inverter there is a two-port network that consists of a split-inductor and capacitors and connected in X shape is employed to provide an impedance source (Z-source) coupling the converter (or inverter) to the dc source, load, or another converter. The dc source/or load can be either a voltage or a current source/or load. Therefore, the dc source can be a battery, diode-rectifier, thyristor converter, fuel cell, an inductor, a capacitor, or a combination of those. Switches used in the converter can be a combination of switching devices and diodes. The Z-source converter (ZSC) topology [1] in power conversion, which has unique features that can overcome the limitations of VSI and CSI, fig (1) shows the ZSC implemented as a 3-phase DC/AC converter (inverter). Although DC/AC conversion

is the most common application of the Z-source topology, it can also be applied to AC/DC and AC/AC power conversions [3]. The X shape impedance is the Z-source network which is composed of two split inductors and two capacitors to provide a coupling between the DC source and the inverter bridge. The Z-source inverter (ZSI) has the unique buck-boost capability which ideally gives an output voltage range from zero to infinity regardless of the input voltage. This is achieved by using a switching state that is not permitted in the VSI which is called the -shoot-through state. This is the state when both upper and lower switches of a phase leg are turned on. In a conventional VSI switching pattern, there are eight permissible switching states. Six of those switching states are called the - active states where the load sees the input voltage and the remaining two states are called the - zero states where either the entire upper or all the lower. The idea behind this is that when we look from the Z-source network point of view, in the shoot-through, the Z-source network is shorted and in the active state, the Z-source network sees the load. In this circuit fig (1) when the parallel switch S2 is on, the Z-source impedance network is shorted and the load sees zero voltage. Similarly, when S2 is off the Z-source network sees the load and active state occurs. It can be observed that the dc-link voltage has a pulsating nature. For simplification purposes, Z-source network parameters are selected as; $L_1=L_2$ and $C_1=C_2$ which makes the Z-source network symmetrical [2],-[5]. Accordingly, the capacitor and inductor voltages of the Z-source network become,

$$V_{C1} = V_{C2} = V_C \tag{1}$$

$$V_{L1} = V_{L2} = V_L$$

Given that the converter is in the shoot-through state for an interval of T_0 during a switching cycle, from the equivalent circuit in fig (1) we have,

$$V_L = V_C \quad \text{and} \quad V_{dc} = 0 \tag{2}$$

Similarly, if the converter is in the active state for an interval of T_1 during the switching cycle T , from the equivalent circuit in fig(1) we have [6],

$$V_L = V_g - V_C \quad \text{and}$$

$$V_{dc} = V_C - V_L = 2V_C - V_g \tag{3}$$

Where V_g is the DC source voltage and $T_0 = T_1 + T_2$

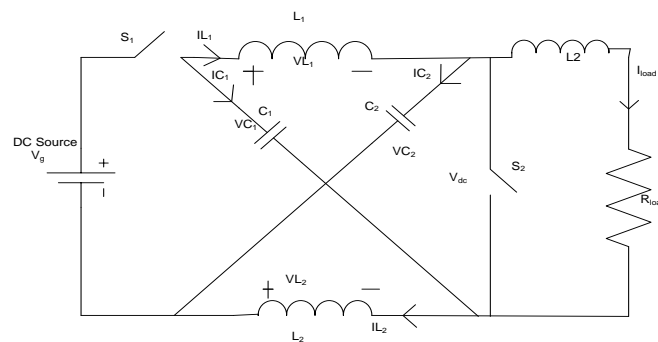


Fig. 1: Simplified ZSC

The average value of the voltage across an inductor for a switching period (T) is zero in steady state, so from Eq. (2) and Eq. (3) we have [3],

$$\frac{1}{T} \int_0^T V_L(t) dt = \frac{T_0 V_C + T_1 (V_g - V_C)}{T} = 0 \tag{4}$$

Or

$$\frac{V_C}{V_g} = \frac{T_1}{T_1 - T_0} = \frac{1-D}{1-2D} \frac{V_g}{V_g} \frac{T_1}{T_0} \tag{5}$$

Where $D=T_0/T$ is the shoot-through duty cycle, V_c is the steady state (DC) value of the capacitor voltage and V_g is the steady state value of the input voltage. The peak value (V_{DCR}) of the pulsating dc-link voltage (V_{dc}) is expressed in Eq. (3) and it can be rewritten in steady state as [3],

$$V_{den}=2V_c - V_g = \frac{T_1}{T_1-T_0} V_g = \frac{1}{1-2D} V_g = B V_g \quad (6)$$

Where B is known as the boosting factor based on, and is the steady state value of the peak dc-link voltage. Eq. (6) gives the voltage conversion ratio of the ZSC. Since D is between zero and 0.5, can take any value between one and

$$V_{ac} = M \frac{V_{den}}{2} \quad (7)$$

Where, M is the modulation index of the inverter. Using Eq. (6), Eq. (7) can be rewritten as

$$V_{ac} = MB \frac{V_g}{2} \quad (8)$$

Eq.(8) has an additional multiplication factor of compared to the VSI voltage conversion ratio which gives the boosting capability to the Z-source inverter. Consider the H-bridge Z-source inverter in fig(2), the active and null states in which the two switches of a phase-leg are switched complementary, are common to both conventional VSI and the H-bridge Z-source inverter. However, the remaining three shoot-through states in which one phase-leg (H1 and H2) or two phase-legs (H3) are short-circuited, are unique to the H-bridge Z-source inverter [4]. When in a shoot-through state, the Z-source inductor currents are boosted but the inverter output voltage is kept at 0V, similar to that of a null state where the AC load is short-circuited. Therefore, for a fixed frequency, inserting of shoot-through states within the null intervals with the active state intervals maintained constant will not alter the normalized volt-sec average per switching cycle. This feature allows all existing volt-sec PWM methods to be used for controlling a Z-source inverter with only minor modifications added to insert the shoot-through states [4].

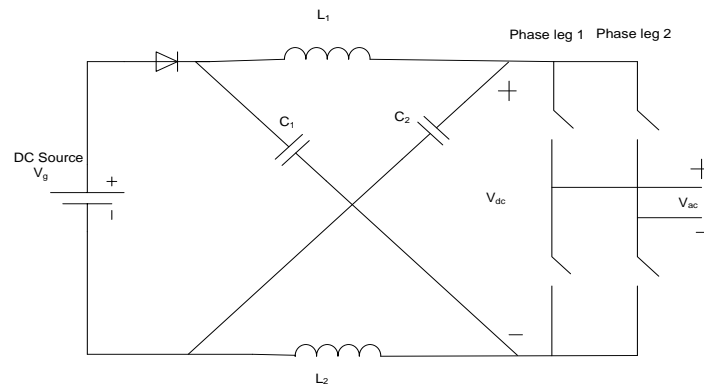


Fig. 2: H bridge (single phase) Z source inverter

The formulation of modulating reference signals are needed for carrier-based Z-source inverter modulation. For a conventional VSI, the reference signals used are $V_a = M \cos(\omega t)$ for modulating phase-leg $\{S1, S4\}$, and $-V_a$ for phase-leg $\{S3, S6\}$. In general, the first state transition during the falling carrier edge occurs when the maximum of the two signals $V_{max} = \max(V_a, -V_a)$ crosses the falling slope of the carrier at time t_{H1} . In order to insert a shoot-through state adjacent to this transition from $t_{H1} - 0.5t_0$ to t_{H1} , the upper (odd-numbered) and lower (even-numbered) switches of the relevant phase-leg should therefore be modulated using

$$V_{max(sx)} = V_{max(sy)} + \frac{T_0}{T} \quad (9)$$

$$V_{max(sy)} = V_{max} \quad (10)$$

Where V_{\max} causes the upper switch to turn ON at $t_{H1} - 0.5t_o$ and $V_{\max(xy)}$ causes the lower switch to turn OFF at t_{H1} . Obviously, these switching actions insert the desired shoot-through state H1. Following through similar analysis, the second shoot-through state H2 can be inserted from at t_{H2to} at $t_{H1} + 0.5t_o$ by using the following modified reference signals for controlling the other two switches

$$V_{\min(sy)} = V_{\min} - \frac{TO}{T} \quad (11)$$

$$V_{\min(sy)} = V_{\min} \quad (12)$$

Where $V_{\min} = \min(V_a, -V_a)$ represents the minimum of V_a and $-V_a$. Without modification, the same derived equations (12) and (14) can also be used for ensuring the correct insertion of shoot-through states during the rising carrier edge. The voltage stress under simple boosting modulation method can be calculated by,

$$V_S = BV_g = (2G-1) V_g \quad (13)$$

The voltage stress for the maximum boosting method is derived

$$V_S = B_g = \left(\frac{3\sqrt{3}G}{\pi} - 1\right) V_g \quad (14)$$

II. MODELLING OF EMBEDDED ZSE

The voltage-type EZ-source inverter shown in fig(3) has its dc sources embedded within the X- shaped LC impedance network with its inductive elements $L1$ and $L2$ now, respectively, used for filtering the currents drawn from the two dc sources without using any external LC filter[13]. The impedance network used buck or boost the input voltage depends upon the boosting factor. This network also act as a second order filter. This network should require less inductance and smaller in size. Similarly capacitors required less capacitance and smaller in size. The output voltage from impedance network is fed to the three phase inverter main circuit. The inverter main circuit consists of six switches. Gating signals are generated from the driving circuit. Depends upon the Gating signal inverter operates and the output of inverter is fed to the R-L load. When the two inductors (L_1 and L_2) are small and approach zero, the Impedance source network reduces to two capacitors (C_1 and C_2) in parallel and becomes traditional voltage source. Similarly, when the two capacitors (C_1 and C_2) are small and approach zero, the Impedance Source Network reduces to two inductors (L_1 and L_2) in series and becomes a traditional current source. Therefore considering additional filtering and energy storage by the capacitors, the impedance source network should require less inductance and smaller size compared with the traditional current source inverters.

III. MATHEMATICAL ANALYSIS OF EMBEDDED IMPEDANCE NETWORK

The switches that are from the same phase-leg can be turned on simultaneously to introduce a shoot-through state without damaging semiconductor devices. When the inverter bridge is in shot-through mode, the front-end diode D is reverse biased with its blocking-voltage expression and other state equations written as follows[6]-[13].

Shoot through ($S_X = S_X$, X=A, B, OR; C, D=OFF)

$$V_L = V_C + V_{dc}/2, V_i = 0$$

$$V_d = V_D = -2V_C \quad (14)$$

$$I_L = -I_C, I_i = I_L - I_C, I_{dc} = 0$$

Alternatively, when in non-shoot-through active or null state current flows from Z-Source network through the inverter topology to connect ac load during time interval T_1 . The expression for non-shoot through is written as,

Non shoot-through ($S_{X \neq X}$, $X=A, B, OR C$; $D=ON$)

$$V_L = V_{dc}/2 - V_C V_i = 2V_C$$

$$V_d = V_D = 0 \tag{15}$$

$$I_{dc} = I_L + I_C$$

$$I_{dc} \neq 0 \tag{16}$$

Performing state-space averaging on (14) and (15) then results obtained from the following expressions which are derived for the calculation of capacitive voltage V_C , peak dc-link voltage V_P , and peak ac output voltage V_a .

$$V_C = \frac{V_{dc}/2}{1 - 2T_0/T} \tag{17}$$

$$V_P = \frac{V_{dc}}{1 - T_0/T} \tag{18}$$

$$V_{ac} = M \frac{V_P}{2} \tag{19}$$

Where T_0/T refers to the shoot-through ratio ($T_0/T < 0.5$) for a single switching period, M denotes the modulation index that is used for traditional inverter control, and $B = 1/(1 - 2T_0/T)$ is the boost factor. Clearly, the term in the expression for V_{ac} represents the output amplitude produced by a traditional VSI, which can be boosted by raising B above unity and adjusting M accordingly [13]. Embedded Z source inverter produce the same gain even though the Embedded Source inverter has dc source embedded within the impedance network for achieving inherent filtering. Observing carefully, a second advantage is also noted in when comparing its capacitive voltage V_C with Z source inverter [8]-[6]. Inferring that second advantage introduced by embedding the source is a significant reduction of the capacitor sizing (voltage rating). The reduction is as much as 50% under nominal condition during which M is set close to unity. Although the Embedded Z-source inverter shown in fig (3) uses two independent dc sources to produce balanced front-end impedance in the network but in practice, it is not required for both the sources to be balanced at all. In extreme cases, one or more sources can be omitted. The elimination of one source is a very favorable aspect to the industry, where locating a single source is definitely much easier. The omission of one source is in principle favorable to the industry, where locating a single source is definitely much easier. Relevant mathematical analysis and experimental testing for the case of only a single source powering the EZ-source inverter have already been presented by the authors in [10], where it is generally concluded that a single source is sufficient, if unbalanced voltage drops across the front-end passive LC elements are acceptable. In addition to [10], the same analysis can also be found in [11] and [12], which in principle are independent research papers reporting on the same topic and printed at about the same time in the same conferences. The extent of compensation achieved by the described technique is likely to be affected by parasitic components found in a real design, which is beyond the scope of this paper and therefore left for a future investigation.

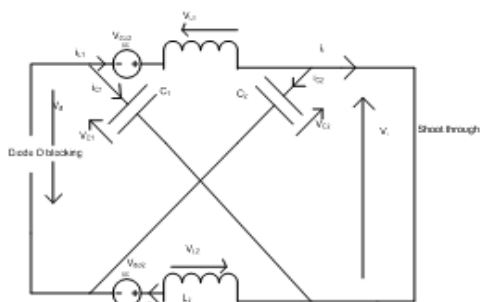


Fig.3 (a)

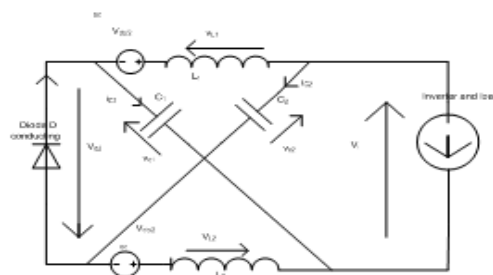


Fig.3 (b)

Fig.3: Equivalent circuit of Embedded Source inverter (a) shoot through state (b) nonshoot-through state.

IV. RESULTS AND DICSSSIONS

This circuit also provides reduced line current harmonics With an EZ-source network constructed using $L = 3.3\text{mH}$, $C = 2800 \mu\text{F}$, and $V_{dc} \approx 100 \text{ V}$ and connected to inverter the relevant waveforms obtained by setting the relevant control parameters to $M = 1.15 \times 0.7$ and $T_0/T = 0$ for no shoot-through state insertion .From the fig 4, it is obvious that the output current is sinusoidal, and the measured line-voltage pulse height produced by the inverter, which corresponds to its dc-link voltage of v_i , matches the unboosted theoretical value of $\approx 100 \text{ V}$ calculated using (4). Next, with M kept constant and a shoot-through duration of $T_0/T = 0.3$ added to the inverter-state

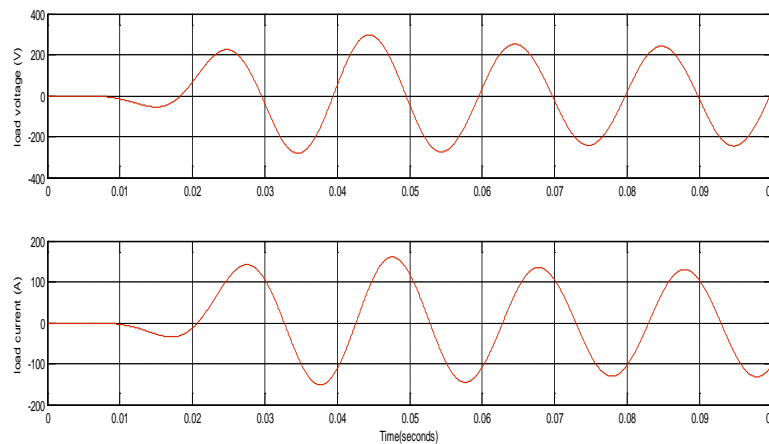


Fig.4: Load voltage and load current

Here sinusoidal waveform of voltage across the load is obtained, peak values being 300V. The current through load is Sinusoidal and the peak value of current is 150 A, as demanded by the load. Due to unexcited EZ-network components, (L1, L2, C1 and C2) in theZ-source inverter took 0.5 seconds to reach at steady state.

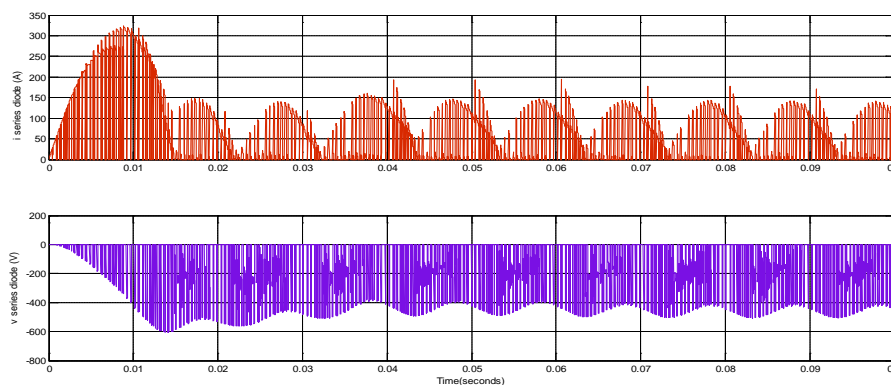


Fig.5: Current and voltage through series diode

The input current passing through the series diode and input voltage that appears across the series diode is shown in fig (5).

V. CONCLUSION

The analysis and simulation of embedded z source H Bridge has been done.The graphplotted in experimental results verified that the boosting of output voltage can be done upto to any value irrespective of input voltage by using E- Sourceinverter. By doing slight modification in the circuitan alternative family of dc-link EZ-source inverters can also be implemented with an even lower network capacitive voltage attained at the expense of no

inherent inductive filtering, a noisier source current waveform even under no voltage boosting condition, and the presence of a small negative capacitive voltage. These advantages are obtained with no degradation in gain, diode blocking voltage, and other characteristic properties of the X-shaped impedance network for the same specified shoot-through duration. The practicality of the new Embedded Z-source inverters has been proved by performing and experimentally testing the inverter. Needless to say, in current type inverter also we can apply this embedded concepts.

REFERENCES

- [1] Ali,U,andShajith and Kamaraj, “A modified space vector PWM for Bi- directional Z-source inverter”, International Conference on Emerging Trends in Electrical and Computer Technology pp. 342-34,(2011).
- [2] B. Farhangi and S. Farhangi, “Comparison of Z-Source Inverter and Boost-Buck Inverter Topologies as a single phase transformer-less Photovoltaic Grid- Connected Power Conditioner”,IEEE Power Electronics Specialist Conference pp. 74-792006.(2006).
- [3] Bakar, M. S., Rahim, N. A. and Ghazali, K. H, “Analysis of various PWM controls on single-phase Z-source inverter”.), IEEE Student Conference on Research and Development (SCOReD) pp. 448-451, (2010).
- [4] P. Loh, D. M. Vilathgamuwa, Y. S. Lai, G. T. Chua and Y. Li,“Pulse-Width Modulation of Z-Source Inverters”. IEEE Transactions on Power Electronics vol. 20, no. 6, pp. 1346-1355(2005).
- [5] Chandrasekhar, T. and Veerachary, M. “Control of single-phase Z-source inverter for a grid connected system”, International Conference on Power Systems pp. 1-6. (2009).
- [6] Poh Chiang Loh, Feng Gao,andFredeBlaabjerg, “Embedded EZ-Source Inverter” Industry Applications Society Annual Meeting, Edmonton, AB, Canada, October 5–9, and approved for publication in the IEEE TRANSACTIONS ON INDUSTRY APPLICATIONS(2008).
- [7] F. Z. Peng, M. Shen, and K. Holland, “Application of Z-source inverter for traction drive of fuel cell— Battery hybrid electric vehicles,IEEE Transactions on Power Electronics vol. 22, no. 3, pp. 1054–1061, (2007).
- [8] Zhiqiang Gao, Ke Shen, Jianze Wang and Qichao Chen, “An Improved Control Method for Inductive Load of Z-Source Inverter”, pp.1-4, March 28-31, Asia-Pacific Power and Energy Engineering Conference (APPEEC)(2010).
- [9] Y. H. Kim, H. W. Moon, S. H. Kim, E. J. Cheong, and C. Y. Won, “A fuel cell system with Z-source inverters and ultra-capacitors”,in Proc. IPEMC, pp. 1587–1591(2004).
- [10] F.Gao, P. C. Loh, F. Blaabjerg, and C. J. Gajanayake, “Operational analysis and comparative evaluation of embedded Z-source inverters,” in *Proc. IEEE PESC*, 2008, pp. 2757–2763.
- [11] J Anderson and F. Z. Peng, “Four quasi-Z-source inverters,” in *Proc. IEEE PESC*, 2008, pp. 2743–2749.
- [12] J. Anderson and F. Z. Peng, “A class of quasi-Z-source inverters,” in *Conf. Rec. IEEE IAS Annu. Meeting*, 2008, pp. 1–7.
- [13] P.Kannan,“Harmonics Analysis and Design of Embedded Z Source inverter for Induction Motor Drive” in January 30(2014).

DEMOGRAPHIC CLUSTERING OF PEPTIDE FRAGMENTS USING PARALLEL PROGRAMMING APPROACH

Aman Sharma

Project Student, Indian Institute of Science, Bangalore, Supercomputer Education and Research Centre

M. Tech Scholar CSE Student, School of Computing Science & Engineering, Vellore Institute of Technology, Vellore, Tamilnadu, (India)

ABSTRACT

An existing algorithm that is demographic clustering of peptide fragments that work in serial manner. Parallel programming approach used to reduce the delay and increased the efficiency of the algorithm. We thus show that the parallel programming can provide better results. Because serial processing works on single core that's why it takes more time if we have large amount of data and files at that time parallel cores can easily split the load among the processors and provide high efficiency. In this paper, our concept representing hash table modification and clustering using parallel programming. As the domain, a perl implementation dealing with increase the efficiency of the algorithm and reducing the time delay. The proposed work shows the efficiency difference between disk and RAM.

Keyword: Demographic Clustering, Peptide Fragments and Parallel Programming.

BACKGROUND

Program is some set of instructions. Process is program is in execution. During last year's performance is becoming the major issue. Today, almost everything is our life has a connection with how to reduce delay and increase high performance of the system. The performance has become one of the most important platforms for research in computer science field. The parallel programming plays the major role in terms of efficiency and performance.

Parallel programming is one major area to increase the performance by split the workload among all the threads. Parallel programming is running program for utilizing all the core and try to divide equal workload among all the processes.

In case of threads of execution is the smallest sequence of programmed instructions that can be managed independently by an OSS. OSS stands for operating system scheduler. Some regions behind for using threads like increase performance which is easy method to take advantage of multi-core, better utilization which means reduce latency and efficient data sharing which is sharing data through memory more efficient than message-passing. There is risks increase complexity of application, difficult to debug (data races, deadlocks etc.). Modern operating system load programs as process like resource holder and execution. A process starts executing at its entry point as a thread. Threads can create other threads within the process.

Concurrency means two or more threads are in progress at the same time. Parallelism means two or more threads are executing at same time.

I. INTRODUCTION

Demographic clustering using peptide fragment problem based on the bioinformatics and computer science field with parallel programming language. The existing work of demographic clustering using peptide fragment was based on the serial manner. So that is why that was not giving the satisfactory performance. This work was taking more time and delay that was major problem for those people who are working in demographic clustering using peptide fragment topic. The problem behind demographic clustering using peptide fragment was based on serial manner. We have proposed the parallel version demographic clustering using peptide fragment that is more efficient than existing serial manner. The proposed work increased the efficiency of demographic clustering using peptide fragments with parallel programming so more fragment will be work fast and provide better results compare to serial version.

II. PARALLEL PROGRAMMING APPROACH

The Demographic clustering using peptide fragments with parallel programming needed because increasing the efficiency of running fragments. Parent process forks child processes. Each child process reads a set of files and creates local hash tables. Then each child picks ($\$FR/\text{Number of child processes}$) random fragments from local hash tables and sends to parent process. The parent adds the fragments received from the child processes and creates a final hash table which will have $\$FR$ entries finally.

III. SEQUENTIAL VS. PARALLEL APPROACH

3.1 Sequential Algorithm for Demographic Clustering Of Peptide Fragments

The sequential algorithm for demographic clustering of peptide fragments has four inputs like a sequence of pairs of angles (ϕ_1, ψ_1), (ϕ_2 , and ψ_2) and so on, fragment length FL , distance threshold R and angle difference ANG .

Firstly, a sequence of overlapping fragments, of length FL , is created from the sequence of pairs of angles: F_1, F_1 .

Then, in two phases, the algorithm clusters these fragments such that each fragment in a cluster is within a distance R and angle ANG from the center or average of the cluster.

In the first phase, the algorithm picks each fragment F_k and checks each existing cluster center C_L as to whether they satisfy the distance and angle conditions, and if yes, the algorithm adds the fragment to the cluster and computes the new center, otherwise a new cluster is created with F_k as its first member.

In the second phase, the algorithm checks each fragment F_k as to whether it still satisfies the conditions with respect to the center of its cluster. If it does not, then F_k is removed from its cluster, and center of that cluster is recomputed. Then, a search is performed over the rest of the clusters to see if F_k can be accommodated within any of them. If such a cluster is found, then F_k is put in that cluster and its center is recomputed. Otherwise, a new cluster is created with F_k as its first member.

The second phase of the algorithm is repeated until the number of rejects in a round is less than or equal to the number of rejects in the previous round.

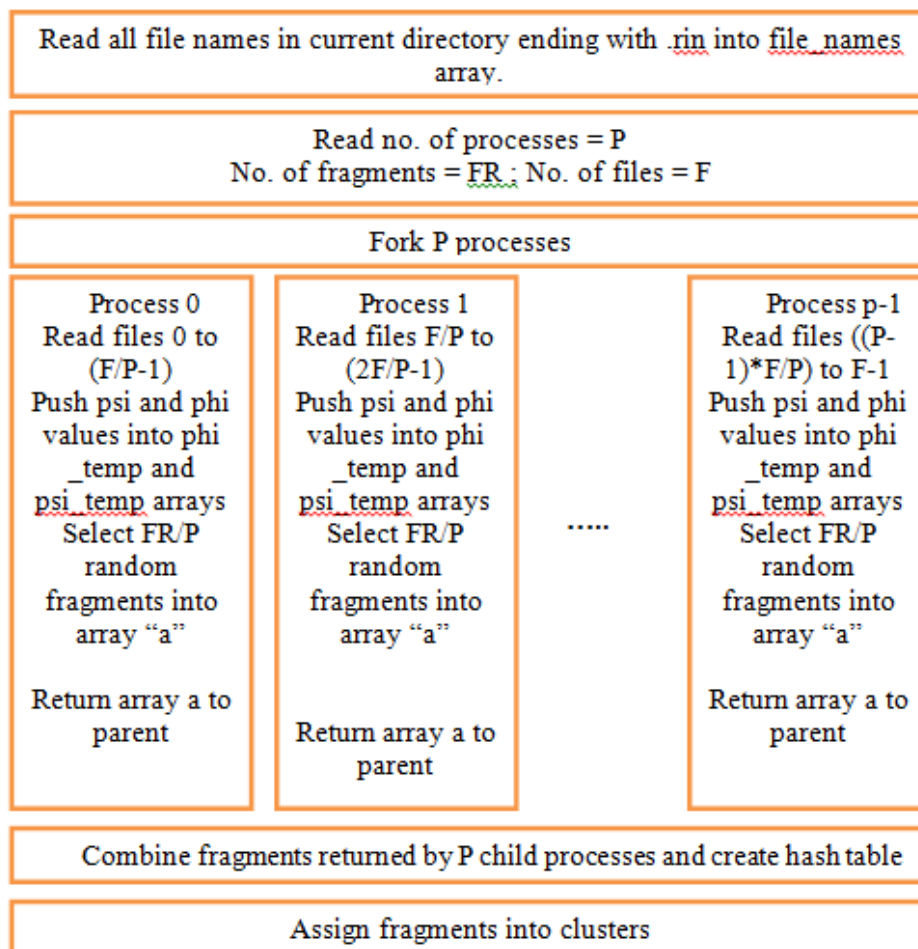
3.2 Parallel Algorithm for Demographic Clustering Of Peptide Fragments

Similarly the parallel algorithm for demographic clustering of peptide fragments has four inputs like a sequence of pairs of angles (ϕ_1, ψ_1), (ϕ_2, ψ_2) and so on, fragment length FL, distance threshold R and angle difference ANG. In parallel algorithm for demographic clustering of peptide fragments has component's read all file names in current directory ending with .rin into file_names array, Read no. of processes = P, fork P processes, for starting process process 0 read files 0 to (F/P-1), push ψ and ϕ values into ϕ_temp and ψ_temp arrays, select FR/P random fragments into array "a", return array a to parent, same apply for all the process. Combine fragments returned by P child processes and create hash table and Assign fragments into clusters. Parent process forks child processes. Each child process reads a set of files and creates local hash tables. Then each child picks ($FR/Number$ of child processes) random fragments from local hash tables and sends to parent process. The parent adds the fragments received from the child processes and creates a final hash table which will have \$FR entries finally.

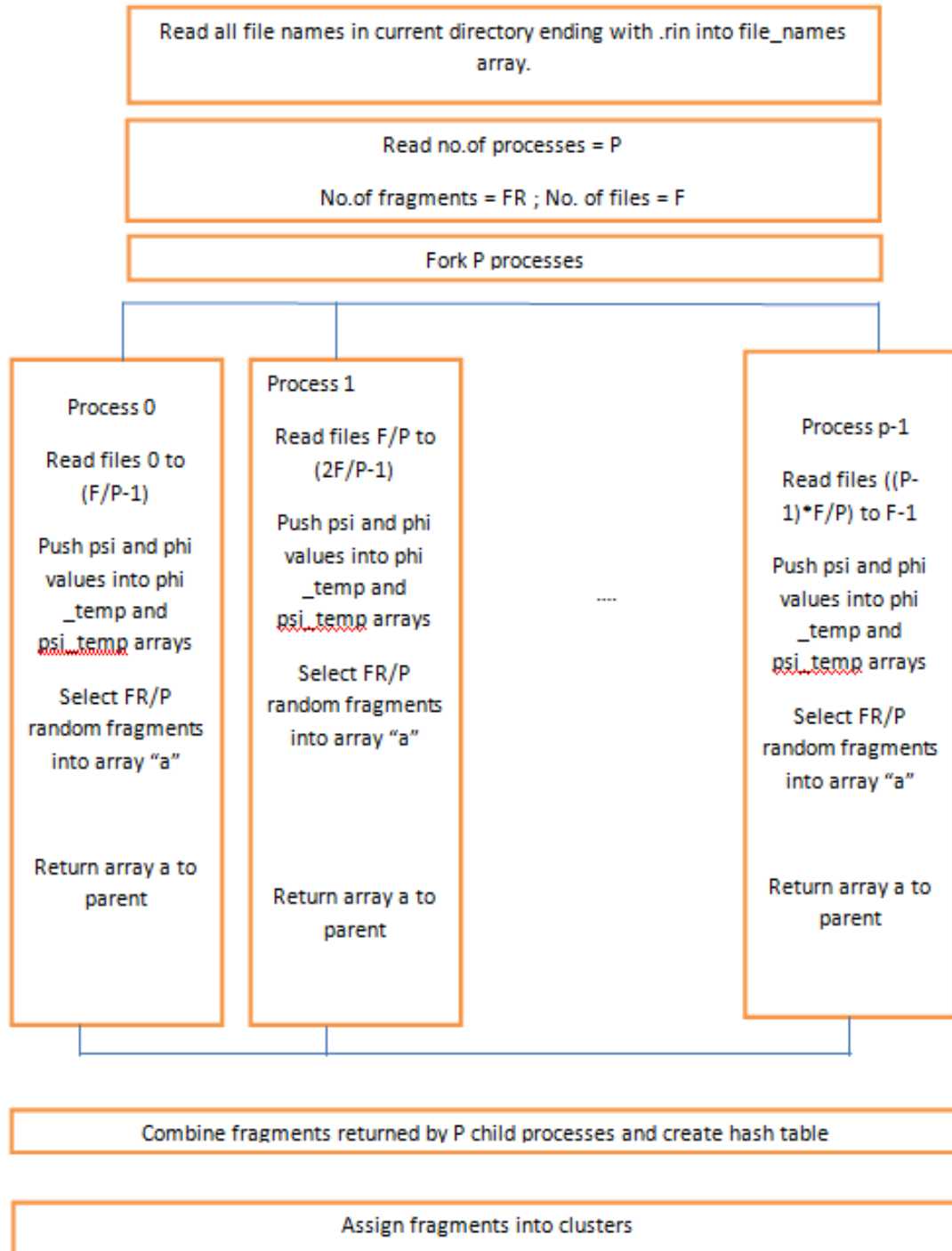
All clusters should be visible to all processes. Otherwise, each process would have its own set of clusters some of which would overlap partially with clusters present in other processes. After parallel clustering, the parent process should do additional processing to merge clusters formed by the child processes and reassign fragments.

3.3 Design of Parallel Architecture

Parallel algorithm architecture is a conceptual model that defines the structure, behavior and more views of the system.



The above represents read all file names in current directory ending with .rin into file_names array, read no. of processes = P, No. of fragments = FR ; No. of files = F, Fork P processes, Process 0 read files 0 to (F/P-1), Push psi and phi values into phi _temp and psi_temp arrays, select FR/P random fragments into array “a”, return array a to parent, combine fragments returned by P child processes and create hash table and assign fragments into clusters.



Reading files to create fragment list is the most time consuming step in the serial code. Serial fragment list creation takes around 6seconds compared to around 1 second taken by clustering step. So by parallelizing fragment list creation step, the most time consuming part of the code has been parallelized. Also fragment list creation step is readily parallelizable compared to clustering since there is no synchronization needed between processes for fragment list creation. When clustering step is parallelized, the parent processes has to do additional work in combining the clusters returned by child processes in addition to combining the fragment list. Clusters returned by the child processes might overlap and hence the parent has to do additional work to reassign fragments to correct clusters. Clustering has less parallelism and more overhead. So parallelizing it doesn't improve the overall time.

IV. RESULT ANALYSIS

The following results are based on hash table modification that shows the difference between disk time and RAM time. The parallel hash table code is also available based on the request

4.1 Disk Results Table

Cores	total time	Hash time
1	8.7	5.88
2	5.62	2.94
3	4.36	2.06
4	3.81	1.61
5	4.06	1.83
6	3.44	1.55
7	3.62	1.57
8	3.68	1.4

4.2 Ram Results Table

Cores	Total time	Hash time
1	7.34	5.79
2	4.99	2.95
3	4.34	2.05
4	4.06	1.82
5	3.52	1.84
6	3.36	1.56
7	3.27	1.49
8	3.42	1.4

4.3 Disk Results with Different Cores

Table 1. core 2	Fragment length						
Number of Fragments	8	10	12	14	16	18	20
1000	4.76	6.85	6.34	8.06	8.96	9.57	10.32
2000	11.39	14.04	15.53	15.14	25.59	23.37	25.6
4000	23.71	54.83	56.02	93.64	68.37	90.85	85.09
6000	43.48	110.2	160.01	118.07	171.95	199.57	176.13
8000	102.34	170.45	188.97	238.95	351.92	212.38	309.43

Table 2. core 4	Fragment length						
Number of Fragments	8	10	12	14	16	18	20
1000	3.53	4.88	5.45	6.17	6.75	7.66	8.33
2000	8.41	11.25	14.58	16.59	21.31	22.82	22.38
4000	26.31	47.61	67.42	68.64	79.81	107.98	61.64
6000	53.21	77.022	91.18	118.48	175.32	196.152	173.55
8000	83.23	127.99	182.67	373.29	343.02	334.91	376.26

Table 3. core 8	Fragment length						
Number of Fragments	8	10	12	14	16	18	20
1000	3.26	4.37	5.22	5.94	6.45	7.17	7.68
2000	8.28	13.09	13.53	13.3	18.69	25.22	22.28
4000	1	45.8	43.7	55.69	77.09	85.62	96.41
6000	39.63	86.14	107.9	169.04	167.97	119.03	165.4

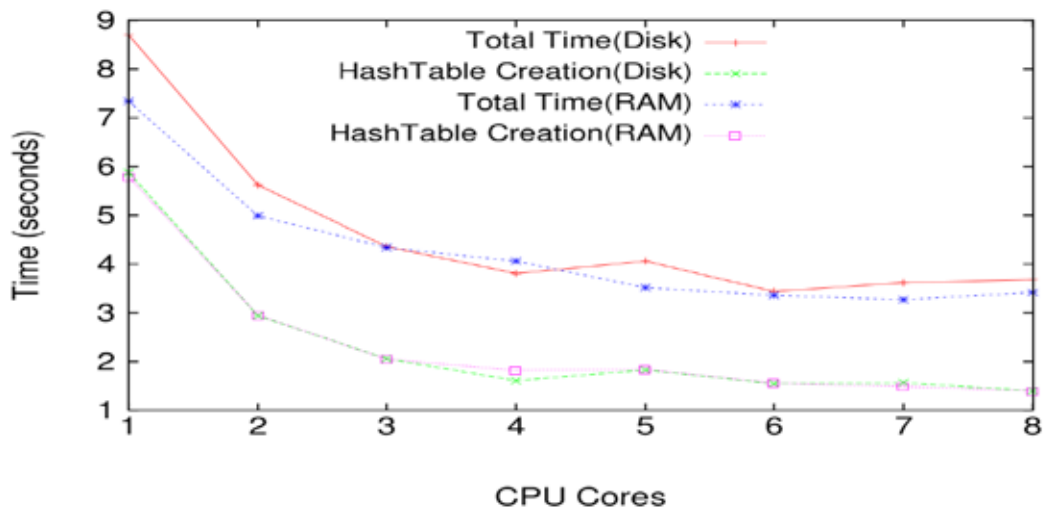
4.4 Ram Results with Different Cores

Table 4. core 8		Fragment length					
Number of Fragments	8	10	12	14	16	18	20
1000	5.91	6.7	6.97	7.96	8.85	9.48	10.31
2000	10.62	14.58	21.03	15.55	17.43	23.17	20.33
4000	24.93	60.28	55.47	69.18	65.34	77.73	100
6000	40.48	107.11	115.44	140.3	170.8	233.25	213.59
8000	85.86	167.09	224.19	250.67	297.24	332.38	369.3

Table 5. core 8		Fragment length					
Number of Fragments	8	10	12	14	16	18	20
1000	3.85	5.1	5.42	6.15	7.02	7.39	7.7
2000	8.26	10.97	22.76	20.12	22.7	22.7	23.06
4000	21.82	38.77	54.23	56.03	63.44	88.72	77.94
6000	55.68	101.94	155.62	190.47	197.46	189.85	212.02
8000	81.07	163.78	217.54	195.5	281.05	389.88	516.04

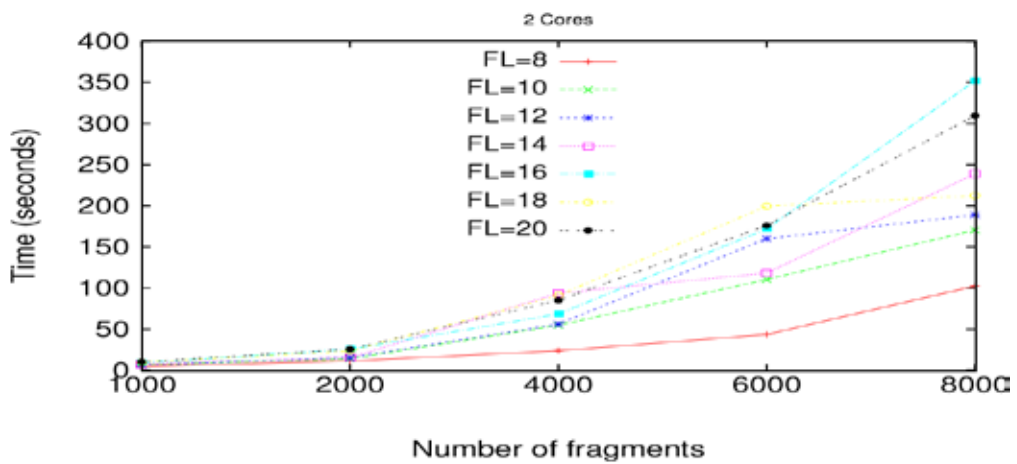
Table 5. core 8		Fragment length					
Number of Fragments	8	10	12	14	16	18	20
1000	3.62	5.08	5.29	5.96	6.54	7.14	7.54
2000	8.43	14.85	19.63	12.9	15.55	25.18	18.1
4000	28.75	53.11	43.55	94.32	79.56	55.67	97.63
6000	53.64	87.12	112.31	139.11	165.13	154.78	207.66
8000	64.35	118.03	183	332.11	397.41	202.18	289.7

4.5 Total Results Representation with Ram and Disk

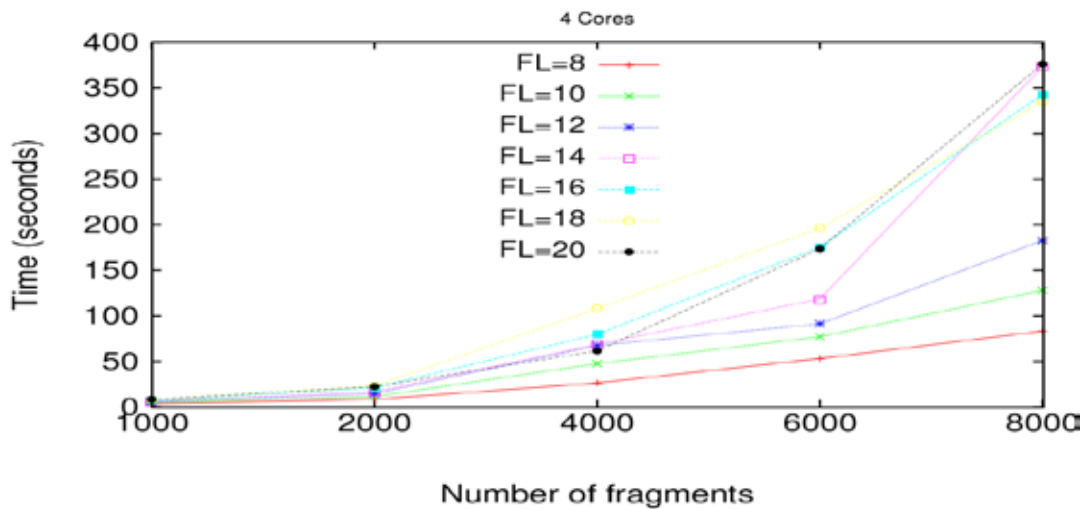


GRAPH 1: DISK & RAM RESULTS TABLE

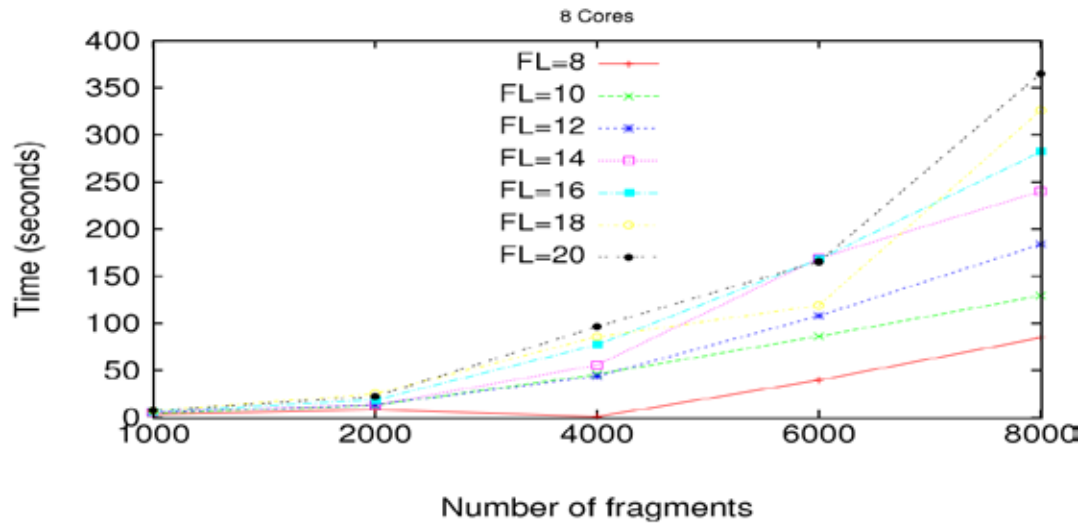
4.6 Disk Results with Different Cores and Graph



GRAPH 2: DISK RESULTS TABLE WITH 2 CORES

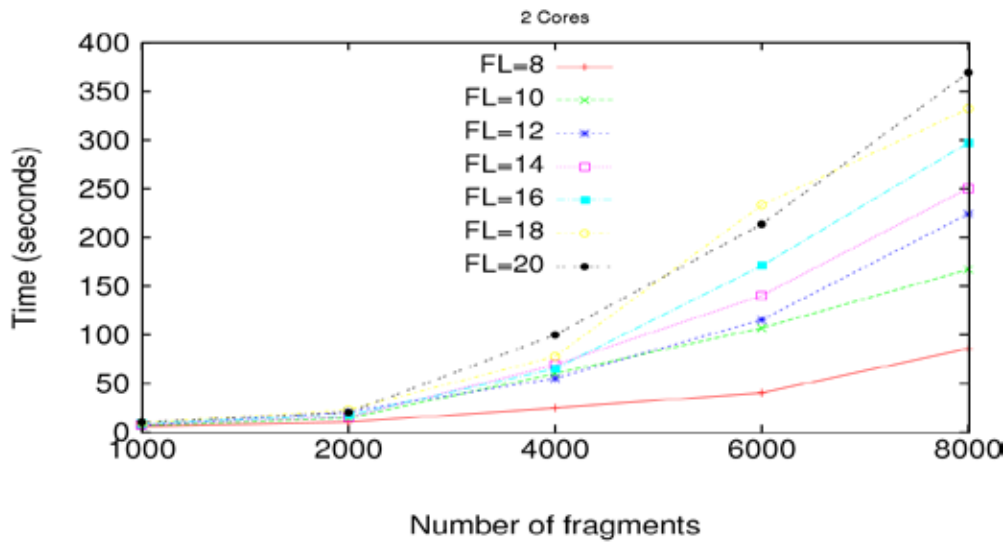


GRAPH 3: DISK RESULTS TABLE WITH 4 CORES

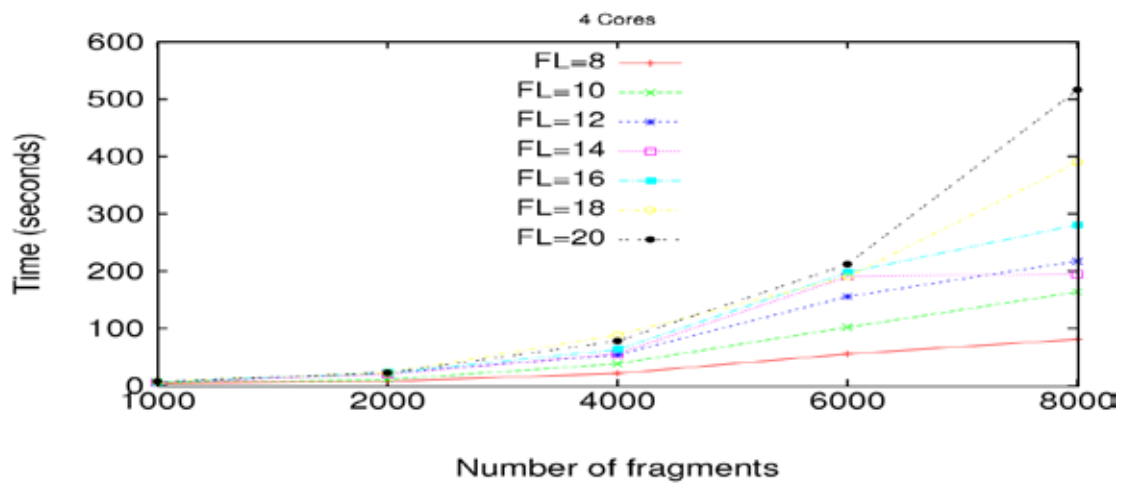


GRAPH 4: DISK RESULTS TABLE WITH 8 CORES

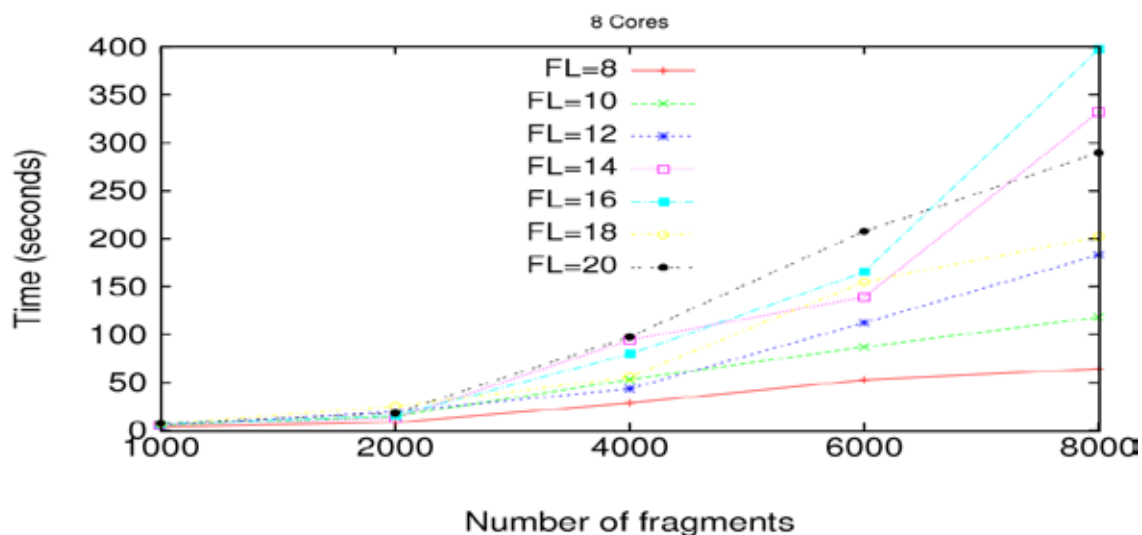
4.7 Ram Results with Different Cores and Graph



GRAPH 5: RAM RESULTS TABLE WITH 2 CORES



GRAPH 6: RAM RESULTS TABLE WITH 4 CORES



GRAPH 7: RAM RESULTS TABLE WITH 8 CORES

4.8 Snapshots

```

user@gisvm: ~/Desktop/upgrade
File Edit View Search Terminal Help
user@gisvm:~/Desktop/upgrade$ perl demo_clust.pl
Usage: ./demo_clust.pl -i <inputlist> -f <fragment length> -t <torsion diff> -d
<minimum distance> -c <min cluster to print> -b <bfactor less than X angstroms**2> -o
<occupancy> -l <loop # iterations> -s <read first # fragments from input> -r <
randomly read # fragments from input>
user@gisvm:~/Desktop/upgrade$ perl.exe demo_clust.pl -i list -f 12 -c 2
bash: perl.exe: command not found
user@gisvm:~/Desktop/upgrade$ perl.exe demo_clust.pl -i list -f 12 -c 2
bash: perl.exe: command not found
user@gisvm:~/Desktop/upgrade$ perl.exe demo_clust.pl -i list -f 12 -c 2
bash: perl.exe: command not found
user@gisvm:~/Desktop/upgrade$ perl demo_clust.pl -i list -f 12 -c 2
Program: demo_clust.pl
Output: RESULT
Inputlist:list
Fragment length:12
Torsion diff (degrees):60
Distance Threshold (degrees):360
Print Clusters with minimum number of points:2
B-Factor screen (<= Angstroms**2):60
Occupancy Threshold (>=):1
Number of iterations to refine (0=automatic):0
Number of Fragments serially read from Input List PDB Files for Calculation (0=automatic):0

user@gisvm: ~/Desktop/upgrade
File Edit View Search Terminal Help
Number of iterations to refine (0=automatic):0
Number of Fragments serially read from Input List PDB Files for Calculation (0=automatic):0
Number of Fragments randomly read from Input List PDB Files for Calculation (0=automatic):0
Note: Serial reading is done prior to random selection in case you specified both options

End making Rin files. Elapsed: 0.000406, User: 0.05, System=0.02
End making Hash Table. Elapsed: 0.500968, User: 0.27, System=0.1
End Assigning 1903 Clusters to 2460+1 records. Elapsed: 30.925351, User: 30.19, System=0.15
Loop 0: 43 reassigned. Time Elapsed: 59.206334, User: 57.93, System=0.18
Loop 1: 28 reassigned. Time Elapsed: 87.454491, User: 85.72, System=0.18
Loop 2: 21 reassigned. Time Elapsed: 122.861663, User: 116.27, System=0.28
Loop 3: 23 reassigned. Time Elapsed: 151.363564, User: 144.28, System=0.3
End of job. Elapsed: 152.315491, User: 145.11, System=0.32
user@gisvm:~/Desktop/upgrade$ time demo_clust.pl

```

V. CONCLUSION

We proposed one approach to parallelizing the demographic clustering of peptide algorithm. The approach is suitable for multi core computations and the computation we have modified based on serial manner of algorithm. The demographic clustering of peptide algorithm work based on reduction. Parallelization technique applied on sequence method for improving the efficiency of the algorithm. In proposed parallelization work we have modified demographic clustering of peptide fragments by parallel programming approach. All the existing methods are implemented in proper way both serial and parallel way. Finally after analyzing the algorithm performance and comparing the result or the algorithm in both parallel and serial approach we can come to a conclusion that our system is computationally efficient in parallel manner. The system should consider more on the CPU and memory usage as they are the main factor that should be reduced during parallel execution of the system by utilizing all the four cores of the processor.

VI. FUTURE WORK

The future work in this work is to take million or billions of fragments and try to utilize more than four cores. After Parallelism these steps more efficiency will come if each cluster or for X clusters, fork/spawn X processes, In each process compute distance of fragment from fragment center, Unlabeled fragments that are out of cluster based on distance threshold from center.

REFERENCES

- [1] Karuppasmy Manikandan, DebnathPal, Suryanarayanarao Ramkumar, Nathan E Brener, Sitharama S Iyengar and Guna Seetharaman, "Functionally important segments in proteins dissected using gene ontology and geometric clustering of peptide fragments", Genome biology, 2008.
- [2] http://en.wikipedia.org/wiki/Parallel_programming_model
- [3] [http://en.wikipedia.org/wiki/Thread_\(computing\)](http://en.wikipedia.org/wiki/Thread_(computing))
- [4] http://en.wikipedia.org/wiki/Cluster_analysis
- [5] http://en.wikipedia.org/wiki/Multi-core_processor
- [6] <https://metacpan.org/pod/Parallel::ForkManager>
- [7] <http://search.cpan.org/~dlux/Parallel-ForkManager-0.7.5/ForkManager.pm>
- [8] http://aaroncrane.co.uk/talks/multicore_for_mortals/paper.html
- [9] http://aaroncrane.co.uk/talks/multicore_for_mortals/paper.html
- [10] <http://www.go4expert.com/articles/parallel-processing-faster-perl-scripts-t9083/>
- [11] <http://perltricks.com/article/61/2014/1/21/Make-your-code-run-faster-with-Perl-s-secret-turbo-module>
- [12] <http://act.yapc.eu/ye2013/talk/4946>
- [13] <https://sandeepnamburi.wordpress.com/2011/07/31/parallel-processing-with-perl-for-bioinformatics/>

EFFICACY & TOLERABILITY OF BETA INTERFERON IN A COHORT OF INDIA PATIENT AT A QUATERNARY CARE HOSPITAL: A PILOT STUDY

Dubey Ashwani¹, Singh Abhishek Pratap², Mishra Vertika³,
Das Saumya⁴, Dwivedee Shamsheer⁵

^{1,2,3,4} Institute of Pharmacy, Noida Institute of Engineering & Technology, Greater Noida, U.P., (India)

⁵ Department of Neurology, Fortis Memorial Research Institute, Gurgaon, Haryana, (India)

ABSTRACT

This study focuses on Beta Interferon mechanisms of action, evidence of efficacy, safety, and tolerability in a cohort of Indian patient at a quaternary care hospital: A Pilot Study. I have given a brief idea about the multiple sclerosis as Beta Interferon had shown effective decrease in relapse of multiple sclerosis. We will enroll those patient in our study to whom Beta Interferon will be prescribe by the physician. In this synopsis I had did extensive literature review of previous research performed related to Beta Interferon. I have reviewed that Beta Interferon have been extensively used for Multiple Sclerosis, Rheumatoid Arthritis or any autoimmune related diseases. In Japan a study had shown safety profile in cancer patient treating with Beta Interferon.

I. INTRODUCTION

1.1 Beta Interferon

GENERIC NAME	BRAND NAME
Beta Interferon	Avonex, Betaseron, Extavia and Rabif

1.1.2 Mechansim of Action

IFN β was first tested for treatment of MS due to its antiviral property, as it was thought that the cause of the disease lay in a viral infection. Today, although viral infections are still considered and studied, at least as contributory factors, IFN β is regarded more as an immunomodulatory and antiproliferative treatment. Laboratory and clinical studies have in fact shown that it inhibits MS activity, acting on a variety of processes and molecular mediators within the immune system. IFN β modifies the cytokine production in favor of the antiinflammatory subset, such as Il-10 and Il-4, inhibiting the release of proinflammatory cytokines such as IFN β and tumor necrosis factor (Rothuizen et al 1999; Yong et al 1998). Other pharmacodinamic properties of IFN β include inhibition of T-cell activation, block of production of oxygen free radicals by mononuclear phagocytes, and reduced expression of major histocompatibility complex class II molecules, which in turn reduces self-antigen presentation in the CNS (Dhib-Jalbut 2002). A recent ex vivo and in vitro longitudinal study demonstrated that IFN β in its 1a form enhances CD4⁺ regulatory T cells activity (de Andres et al 2007). Beneficial effects of IFN β may also be due to to a protective role exerted at the level of the blood-brain barrier (BBB), by reducing the activity of metalloproteases that are responsible for BBB disruption, and/or by preventing adhesion and subsequent migration of T-cells into the CNS (Galboiz et al 2001). In particular, it was demonstrated that IFN β 1a regulates the expression of serum and membrane-associated intercellular adhesion

molecules (Giorelli et al 2002), and it is associated with up-regulation of vinculin and N-cadherin expression in brain endothelial cells (Harzheim et al 2004) restoring BBB disruption IFN β action-related.

Most of these pharmacodynamic properties depend on the interaction of IFN β with cell surface receptors (Wagstaff and Goa 1998). This interaction induces an intracellular signal cascade leading to the expression of IFN-stimulated genes, whose products such as neopterin, myxovirus resistance protein A, β 2 microglobulin, and 2',5'-oligoadenylate synthetase, besides carrying out the effect of IFN, have also been studied and proposed as a tool to monitor the drug activity, and potentially the biological response to treatment (Bertolotto et al 2001). However controversial the definition of IFNs β as disease-modifying drugs may be, recent experimental studies have proposed a novel and neuroprotective mechanism of action for IFN β . The survival of retinal ganglion cells in the animal model MS, the experimental autoimmune encephalomyelitis, was enhanced by treatment with IFN β 1a (Sättler et al 2006). In addition, another study proved that IFN β stimulates the secretion of nerve growth factors by endothelial cells (Biernacki et al 2005). This axon protective effect was related to the antiinflammatory properties of the drug.

1.2 Background Study

1.2.1 Over the last 15 years, pivotal randomized, multicenter, double-blind, placebo-controlled studies have led to the market licence of interferons beta (IFNs β) for the treatment of RR MS (The IFNB Multiple Sclerosis Study Group 1993; Jacobs et al 1996; PRISMS Study Group 1998) and to its worldwide use in clinical settings.

1.2.2 Additional studies have then assessed efficacy of IFNs β in clinically isolated syndromes (CIS) likely to develop MS (Jacobs et al 2001; Comi et al 2001), and in SP forms of the disease with superimposing relapses (European Study Group on Interferon beta-1b in Secondary Progressive MS 1998; Secondary Progressive Efficacy Clinical Trial of Recombinant Interferon-beta-1a in MS(SPECTRIMS) Study Group 2001)

II. AIM AND OBJECTIVE OF STUDY

2.1 AIM

"Efficacy & Tolerability of Beta Interferon in a cohort of Indian patient at a quaternary care hospital: A Pilot Study"

2.2 Plan of work

- Ø A detailed literature review had been performed regarding efficacy and tolerability of Beta Interferon in various tertiary & quaternary care hospitals.
- Ø On the basis of literature review we have decided to study the efficacy and tolerability of Beta Interferon in various quaternary & tertiary care hospital.
- Ø The study will be conducted after approval from the Institutional ethic committee and Institutional Scientific Committee
- Ø Informed consent form for participation will be collected from patient prior to data collection.
- Ø A drug monitoring Performa will be use to collect study specific data after approval.
- Ø The data will be collected using various data sources and analysis will be made on efficacy and tolerability of Beta Interferon.
- Ø Patients will be selected on the basis of inclusion and exclusion criteria.
- Ø Sample size of patient 20 + 2 treating with Beta interferon will be included.

2.3 Study Criteria

2.3.1 Inclusion Criteria

All patients treating with Beta Interferon (In-patients as well as out patients) with co-morbidity in Fortis Memorial Research Institute, Gurgaon, Haryana.

2.3.2 Exclusion Criteria

- Critically ill patients in ICU or Critical care setting
- History or presence of malignancy.

2.4 Duration of Study

October 2014 to January 2015

2.5 Sample Size

20+2

2.6 Data Elements

The following details will be entered:

- Demographic profile of the patient will be noted.
- The diagnosis will be noted.
- Prescribed beta interferon drug and its dose/frequency/duration will be noted.
- Any co-morbid condition will be noted.

2.7 Source of Data

- Patient's Medical Records.

III. RESULT & DISCUSSION

We will report here the study titled "**Efficacy & Tolerability of Beta Interferon in a cohort of Indian patient in a quaternary care hospital: A Pilot Study**".

This is a Pilot study which will be carrying out from October 2014 in IPD and OPD of Fortis Memorial Research Institute, Sector-44 Opposite Huda city Metro Station, Gurgaon, Haryana (India).

The study of efficacy and tolerability of Beta Interferon is component of clinical research which will seeks monitoring & evaluation as it is necessary to identify safety assessment and adverse event occur in Indian patient treating with Beta Interferon.

3.1 Result

In Results we will monitor these aspects

3.1.1 Demographic Profile of the Study Population

- a. Age
- b. Gender
- c. Stage of multiple sclerosis among patients
- d. Co-morbidities

3.1.2 Diagnostic Parameter

3.2 Discussion

This study will evaluate and discuss the efficacy and tolerability of beta interferon in a cohort Indian patient at a quaternary care hospital: A Pilot study.

IV. REFERENCES

- [1] Calabresi PA. Diagnosis and management of multiple sclerosis. *Am Fam Physician*. 2004;70: Page no. 1935–1944.
- [2] Hauser SL, Goodwin DS. Multiple sclerosis and other demyelinating diseases. In: Fauci AS, Braunwald E, Kasper DL, Hauser SL, editors. *Harrison's Principles of Internal Medicine*. 17th ed. II. New York: McGraw-Hill Medical; 2008. Page no. 2611–2621.
- [3] Weinschenker BC. Epidemiology of multiple sclerosis. *Neurol Clin*. 1996;142: Page no. 1–308.
- [4] Olek MJ. Epidemiology, risk factors and clinical features of multiple sclerosis in adults. Available at: www.uptodate.com/contents/epidemiology-and-clinical-features-of-multiple-sclerosis-in-adults.
- [5] X plain patient education multiple sclerosis pdf. www.X-Plain.com.
- [6] <http://www.mayoclinic.org/diseases-conditions/multiple-sclerosis/in-depth/multiple-sclerosis-risk-factors/art-20094645>.
www.webmd.com/multiple-sclerosis/default.html.
- [8] [Anthony](#) T. *Reeder clinical neuroscience*, Vol 1, Page no. 404-405.
- [9] Houtchens MK, Lublin FD, Miller AE, Khoury SJ. Multiple sclerosis and other inflammatory demyelinating diseases of the central nervous system. In: Daroff RB, Fenichel GM, Jankovic J, Mazziotta JC, eds. *Bradley's Neurology in Clinical Practice* . 6th ed. Philadelphia, Pa: Elsevier Saunders; 2012: Chapter 54.
- [10] Cree BAC. Multiple sclerosis. In: Brust JCM, editor. *Current Diagnosis and Treatment in Neurology*. New York: Lange Medical Books/McGraw-Hill Medical; 2007.
- [11] McDonald WI, Compston A, Edan G, et al. Recommended diagnostic criteria for multiple sclerosis: Guidelines from the International Panel on the diagnosis of multiple sclerosis. *Ann Neurol*. 2001;50 Page no:121–127.
- [12] Brunton LL. Immunomodulators. In: Lazo JS, Parker KL, editors. *Goodman & Gilman's The Pharmacological Basis of Therapeutics*. 11th ed. New York: McGraw-Hill Medical; 2005. Page no. 1424–1427. Beck RW, Cleary PA, Trobe JD, et al. The effect of corticosteroids for acute optic neuritis on the subsequent development of multiple sclerosis. *N Engl J Med*. 1993;329: Page no. 1764–1769.
- [13] La Mantia L, Eoli M, Milanese C, et al. Double-blind trial of dexamethasone versus methylprednisolone in multiple sclerosis acute relapses. *Eur Neurol*. 1994;34:199–203.
- [14] Milligan NM, Newcombe R, Compston DA. A double-blind controlled trial of high dose methylprednisolone in patients with multiple sclerosis: 1. Clinical effects. *J Neurol Neurosurg Psychiatry*. 1987;50: Page no.511–516.
- [15] Dhib-Jalbut S, Marks S. Interferon-beta mechanisms of action in multiple sclerosis. *Neurology*. 2010;74 (Suppl 1):S17–S24.
- [16] PRISMS Study Group and the University of British Columbia MS/MRI Analysis Group PRISMS-4: Long-term efficacy of interferon beta-1a in relapsing MS. *Neurology*. 2001;56: Page no.1628–1636.
- [17] Paty DW, Li DK. Interferon beta-1b is effective in relapsing–remitting multiple sclerosis: II. MRI analysis results of a multi-center, randomized, double-blind, placebo-controlled trial. *Neurology*. 1993;43: Page no.662–667.
- [18] Simon JH, Jacobs LD, Campion M, et al. Magnetic resonance studies of intramuscular interferon beta-1a for relapsing multiple sclerosis. *Ann Neurol*. 1998;43: Page no.79–87.

- [19] Li DK, Paty DW. Magnetic resonance imaging results of the PRISMS trial: A randomized, double-blind, placebo-controlled study of interferon beta-1a in relapsing–remitting multiple sclerosis. Prevention of relapses and disability by interferon beta-1a subcutaneously in multiple sclerosis. *Ann Neurol.* 1999;46: Page no.197–206.
- [20] Rice GP, Oger J, Duquette P, et al. Treatment with interferon beta-1b improves quality of life in multiple sclerosis. *Can J Neurol Sci.* 1999;26: Page no.276–282.
- [21] Fischer JS, Priore RL, Jacobs LD, et al. Neuropsychological effects of interferon beta-1a in relapsing multiple sclerosis. *Ann Neurol.* 2000;48: Page no.885–892.
- [22] Panitch H, Goodin DS, Francis G, et al. Randomized, comparative study of interferon beta-1a treatment regimens in MS: The EVIDENCE trial. *Neurology.* 2002;59: Page no.1496–1506.
- [23] Bertolotto A, Malucchi S, Sala A, et al. Differential effects of three interferon betas on neutralizing antibodies in patients with multiple sclerosis: A follow-up study in an independent laboratory. *J Neurol Neurosurg Psychiatry.* 2002;73: Page no.148–153.
- [24] Ekstein D, Linetsky E, Abramsky O, et al. Polyneuropathy associated with interferon beta treatment in patients with multiple sclerosis. *Neurology.* 2005;65:456–458.
- [25] Ford CC, Goodman AD, Johnson K, et al. Continuous long-term immunomodulatory therapy in relapsing multiple sclerosis: Results from the 15-year analysis of the U.S. prospective open-label study of glatiramer acetate. *Mult Scler.* 2010;16: Page no.342–350.
- [26] North Wales, Pa: Teva; Feb, 2009. Copaxone[®] (glatiramer acetate injection), prescribing information. Available at: www.shared-solutions.com/pdfs/PrescribingInformation.aspx. Accessed October 3, 2011.
- [27] Johnson KP, Brooks BR, Cohen JA, et al. Extended use of glatiramer acetate (Copaxone) is well tolerated and maintains its clinical effect on multiple sclerosis relapse rate and degree of disability. *Neurology.* 1998;50: Page no.701–708.
- [28] Comi G, Filippi M, Wolinsky JS. European/Canadian multicenter, double-blind, randomized, placebo-controlled study of the effects of glatiramer acetate on magnetic resonance imaging: Measured disease activity and burden in patients with relapsing multiple sclerosis. *Ann Neurol.* 2001;49: Page no.290–297.
- [29] Johnson KP, Brooks BR, Cohen JA, et al. Copolymer 1 reduces relapse rate and improves disability in relapsing–remitting multiple sclerosis: Results of a phase III multicenter, double-blind placebo-controlled trial. *Neurology.* 1995;45: Page no.1268–1276.
- [30] Copaxone: Monitoring more than 2,100 patients. Available at: www.mediguard.org/medication/side-effects/copaxone. Accessed May 18, 2011. Rockland, Mass: EMD Serono, Inc; Aug, 2008. Novantrone[®] (mitoxantrone for injection concentrate), prescribing information. Available at: www.accessdata.fda.gov/drugsatfda_docs/label/2009/019297s030s0311bl.pdf. Accessed October 3, 2011.

A COMPLETE ANALYSIS AND DYNAMIC SIMULATIONS OF SUPERCONDUCTING LOGIC GATES

Dr. Kurapati Srinivas

Department of Physics, GMR Institute of Technology, Rajam, A.P., (India)

ABSTRACT

A thorough investigation has been made to obtain SQUID device parameters and properties, and the optimization of the latter for the application of logics gates. SQUID OR, AND gates have been designed theoretically using the optimized techniques. Our concept of turn-on delay has been applied for critically ascertaining the switching speed of these logic gates. The dynamic response of the logics gates have been obtained by computer-simulation. This paper will help for the scientists to have a complete understanding of SQUID logic gates before they are fabricated experimentally to obtain better results. Further, in this paper a thorough investigation of resistive logic gates such as JAWS, DCI and RCJL has been made. The current equations of each gate at each stage have been deduced. The dynamic response of these gates have been obtained by the computer-simulation. The concept of turn-on delay has been introduced. The effect of overdrive current on turn-on delay for resistive logic gates has been shown. This will provide a better understanding of switching dynamics of the logic gates. Further, we have shown the effect of overdrive current on these logic gates. This paper will help scientists and researchers to have complete understanding of superconducting logic gates before they are fabricated experimentally to obtain optimum results.

Keywords: *Josephson Junction, Superconducting Logic Gates, Computer-Simulation*

I. INTRODUCTION

Josephson junction alone cannot be used as a logic gate since it lacks isolation, i.e., the output signal can propagate in the input as well as in the output branches, whereas for logic operation the signal must propagate only in the output branches. The other problem with this circuit is that the output current is not sufficient to switch more than one load. High-gain Josephson logic devices are desired for many reasons: first, they provide higher fan-out capability (fan-out means the number of loads). Second, high-gain to some extent can be traded off to improve the circuit tolerances from variations in processing parameters such as critical currents.

Finally, high-gain would result in shorter gate delays because of the shorter turn-on delays [1]-[4] and the shorter time required for signal currents to reach the device threshold. In practice, a gain of 3 is found to be optimum for Josephson logic circuits. At gains much larger than 3, there is no significant improvements in the gate delay but, on the other hand, the noise margins for the "0" state degrades considerably.

The Superconducting Quantum Interference Device (SQUID) is a device which can be used for both logic and memory applications. It consists of two Josephson junctions coupled by two inductors. The two most attractive features of SQUID devices for logic applications are isolation and serially connected fan-out. The isolation is provided by the transformer coupling between the SQUID and the input. The other advantage of

SQUID is the serial fan-out capability whereby the control lines of many load devices can be connected in series with a single output line.

Before fabricating DC SQUID as a logic and memory device, it is very much necessary to have a thorough understanding and optimization of the device for better results. Earlier I have made an attempt to design DC SQUID as a memory device using computer -simulation method [5].

Since the present paper deals with the design of logic gates using the SQUID, it is necessary to have a detailed information regarding the parameters, properties and their optimization for the application of logic and memory cell. In fact, in the present paper we have made an attempt on this line.

Two attractive features of SQUID devices for logic applications are isolation and serially connected fan-out. The isolation is provided by the transformer coupling between the SQUID and the input. The isolation is not perfect in the sense that a noise pulse (typically 5 percent) is fed back into the control line when the SQUID switches to the non-zero voltage. The other advantage is the serial fan-out capability by which the control lines of many load devices can be connected in series with a single output line.

The main drawbacks of SQUID devices for logic application are relatively large device area and high sensitivity to stray magnetic fields. In SQUID 80% of the area is occupied by the transformer [1]. Further, the high sensitivity to stray magnetic field requires that the SQUID based logic circuits be well shielded from the stray magnetic fields.

The resistive logic gates such as JAWS (Josephson Auto-Weber System) [6], DCI (Direct Coupled Isolation) [7] and RCJL (Resistor Coupled Josephson Logic) [8] are chosen because the gate logic delay in this case would consist of the turn-on delay, switching delay and propagation delay, but not the crossing delay as in the case of magnetically coupled logic gates. Further, these resistive logic gates do not have a factor of limiting the size very seriously. So, the gate propagation delay can be made sufficiently small. Therefore, the small time constant of the Josephson junction can be directly attained to these gates. It has been considered by the earlier workers that the turn-on delay of a logic gate is the time taken for the logic gate to obtain 2% of the output current to the load. This consideration seems to be arbitrary.

Due to this fact, in the present paper we have made a thorough investigation of the resistive logic gates. Our concept of turn-on delay has been introduced which will be able to remove the confusion in critically ascertaining the switching speed of these logic gates. Further, the effect of overdrive current on these resistive logic gates has been studied.

II. BRIEF THEORY OF DC SQUID

The Superconducting Quantum Interference Device (SQUID) is a device which can be used for both logic and memory applications. It consists of two Josephson junctions coupled by two inductors as shown in Fig.1a. The two most attractive features of SQUID devices for logic applications are isolation and serially connected fan-out. The isolation is provided by the transformer coupling between the SQUID and the input. The other advantage of SQUID is the serial fan-out capability whereby the control lines of many load devices can be connected in series with a single output line.

An equivalent circuit of SQUID [9] is shown in Fig.2a. When the Josephson junction A and B are assumed to be point junctions, the maximum Josephson current ratio of the junctions A and B is $a = I_a/I_b > 1$. The total inductance between the junctions is $L = L_1 + L_2$. The insertion point of the gate current I_g is given by the tap

ratio, $p = L_1/L$. The control current I_c represents a transformed control current I_c' of a separate control line. The total flux in the interferometer is an integer multiple N of one flux quantum $\phi_0 = 2.07$ mVps. Flux quantum states (FQS) exist within limited range in the current plane I_g, I_c . Their threshold curves are as functions of phase differences across the junctions q_a and q_b :

$$I_g = (a \cdot \sin q_a + \sin q_b) \cdot I_b \text{ ----- (1a)}$$

$$I_c = [(q_a - q_b + 2pN) / l - (1-p) \cdot \sin q_b + p \cdot a \sin q_a] \cdot I_b \text{ ... (1b)}$$

$$q_b = \arccos\left(\frac{-a \cos q_a}{1 + a \cos q_a}\right); a = I_a / I_b; L = L_1 + L_2$$

$$p = L_1 / L; l = 2pL \cdot I_b / \phi_0$$

The curves depend on five magnitude parameters

The characteristic phase $l = 2pL I_b / \phi_0$. The maximum Josephson current of the smaller junction I_0

The current ratio, a

The tap ratio, p

The number of flux quanta N .

An example of two FQS in the normalized current plane with $i_g = I_g/I_0$ and $i_c = I_c/I_0$ is given in Fig.3b, for $l = p, a=8, p=0.25$ and $N=0, 1$ [9].

For $N = 0$ mode, the points A and C are point symmetric with respect to the origin. The same is true for the points B and D. The currents at the points are given analytically [9].

$$A) I_{gA} = (a+1) I_0$$

$$I_{cA} = (p \cdot (a+1) - 1) \cdot I_0$$

$$B) I_{gB} = (a-1) I_0$$

$$I_{cB} = (p/l + p \cdot (a-1) + 1) I_0$$

The control current shift is given by [9]

$$\Delta I_c = \phi_0 / (L_1 + L_2)$$

which can also can be written as

$$\Delta I_c = 2p I_0 / l$$

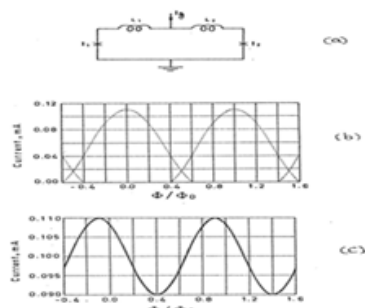


Fig. 1 (a) Diagram of a dc SQUID with bias current. The inductances and junctions on the two sides may be different. The crosses represent the junctions, including resistances and capacitances. **(b)** The positive half of the threshold characteristic of a symmetric dc SQUID having $L_1 = L_2 = 2.0$ pH and $I_1 = I_2 = 55 \mu A$. **(c)** The positive portion of the threshold characteristic of an asymmetric dc SQUID with $L_1 = L_2 = 2.0$ pH and $I_1 = 100 \mu A; I_2 = 10 \mu A$.

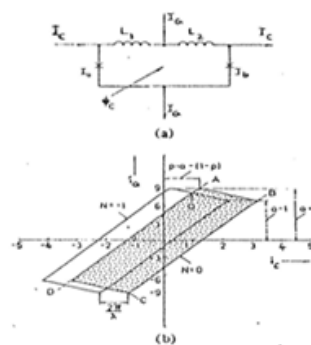


Fig. 2 dc SQUID with two Josephson junctions A and B the total inductance $L = L_1 + L_2$ **(a)** Equivalent circuit with gate current I_g and the control current I_c . **(b)** Threshold curves of flux quantum states $I_c = I_g / I_b$ versus $I_c = I_c / I_b$ for $a = 8.0, \lambda = 2\pi, p = L_1 / L = 0.25$ and $N = -1, 0$.

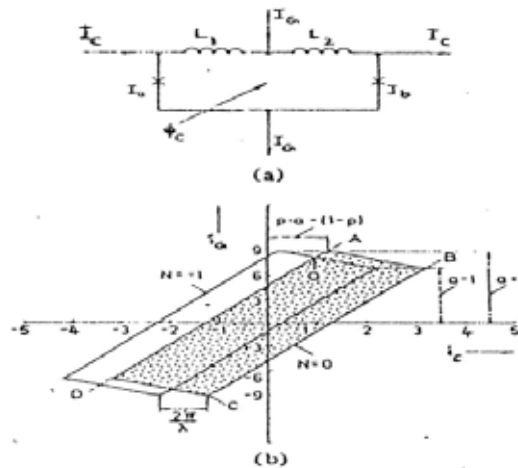


Fig. 3 dc SQUID with two Josephson junctions A and B the total inductance $L = L_1 + L_2$ (a) Equivalent circuit with gate current I_G and the control current I_C . (b) Threshold curves of flux quantum states $I_G = I_C / I_b$ versus $I_C = I_C / I_b$ for $a = 8.0$, $l = 2p$, $p = L_1 / L = 0.25$ and $N = -1, 0$.

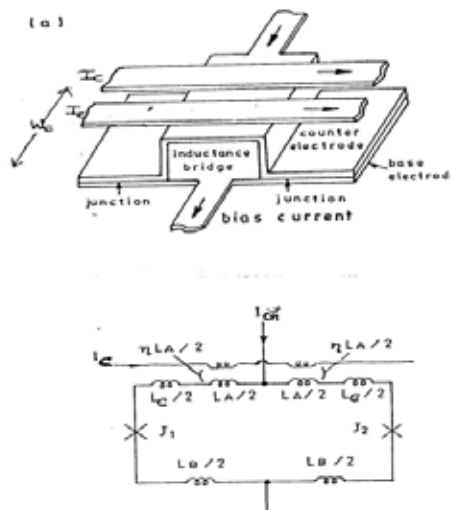


Fig. 3 SQUID and its Equivalent circuit of as a SQUID OR gate

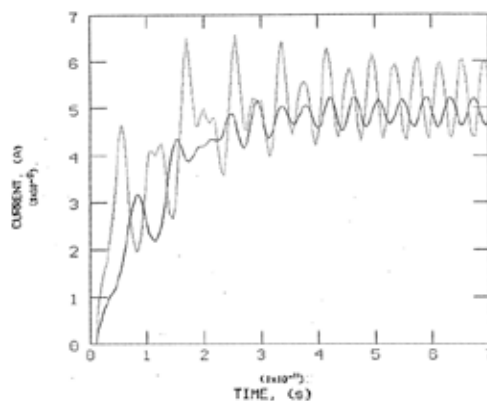


Fig. 4 Dynamic response of a SQUID OR gate using two different technologies. The solid curve shows the output current of Pb-alloy based OR gate with time, whereas the dotted curve indicates the output current variation with time for Nb/A10x/Nb based OR gate

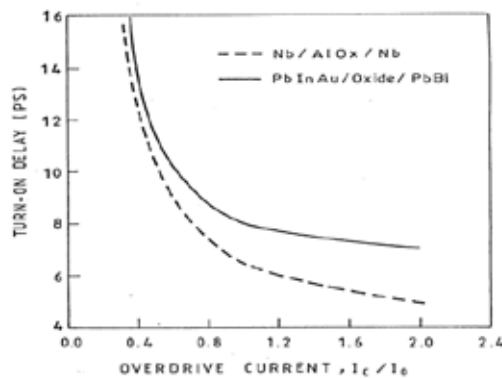


Fig. 5 The turn-on delay of a SQUID OR gate depends on overdrive current. The solid curve indicates the turn-on delay vs overdrive for a Pb-alloy based OR gate, whereas the dotted curve shows the turn-on delay vs overdrive for a Nb/AlOx/Nb based OR gate.

2.1 Dynamic Response of the SQUID

In designing Josephson digital circuits, computer simulations of the static as well as of the dynamic device behaviour play an essential role because of the lack of sufficiently accurate analytical approximations.

The dynamic description of the superconducting networks, containing Josephson tunnel junctions, self- and mutual inductances, capacitances and resistors, results in a set of equations for the current continuity and zero-voltage sum and the particular current-voltage integral equations of the junctions. IBM and Bell Labs have been adopting the standard electrical network

analysis programs (for examples ASTAP [10], SPICE [11], etc) in order to obtain the circuit static as well as the dynamic response [9].

In the present case we have adopted a more general approach to obtain the dynamic response of SQUID. The dynamic equations of the SQUID have been taken and solved numerically by the Runge-Kutta method. In the switching dynamics of a logic gate, the high-frequency oscillation present in the load current with oscillation periods of a few ps stems from the oscillating supercurrent in the interferometer junctions. The frequency of these oscillations is related by to the actual junction voltage. Because these oscillations are still slow enough and can have sufficient energy to switch the following gate, they have to be modelled accurately although the overall switching transient is in the tenths of ps. For an accurate computation of this oscillation, a minimum time-step size in the simulation of about 0.01 has to be used [12].

From Eqns.(10a) and (10b) we can have,

$$(1 - P)I_G + I_C = [(q_a - q_b + 2pN)I_o / l + a I_o \sin q_a]$$

In the dynamic case the above equation modifies to:

$$(1 - P)I_G + I_C = (q_a - q_b + 2pN) I_o / l + a I_o \sin q_a + a \frac{f_o}{2p} C_j \frac{d^2 q_a}{dt^2} + a \frac{f_o}{2p R_a} \frac{dq_a}{dt}$$

$$\text{or } \frac{d^2 q_a}{dt^2} = \frac{2p}{f_o C_j a} [(1 - p)I_G + I_C + (\frac{q_a - q_b - 2pN}{l}) I_o - a I_o \sin q_a - \frac{a f_o}{2p R_a} \frac{dq_a}{dt}] \text{----- (2)}$$

Similarly,

$$\frac{d^2 q_b}{dt^2} = \frac{2p}{f_o C_j b} [pI_G - I_C + (\frac{q_a - q_b + 2pN}{l}) I_o + b I_o \sin q_b - \frac{b f_o}{2p R_b} \frac{dq_b}{dt}] \text{----- (3)}$$

Eqns. (2) and (3) are in the form of the second order differential equation. These equations can be solved by fourth – order Runge-Kutta method on a computer to obtain the dynamic response of the SQUID.

III. SQUID AS AN OR GATE

The basic structure of SQUID OR gate is shown in Fig. 6a and its equivalent circuit is given in Fig. 6b. The SQUID OR gate consists of a 2-junction bridge. In designing the SQUID OR gate, it is necessary to obtain threshold characteristic as a function of various device dimensions. The threshold characteristic is calculated by solving equations derived from the equivalent circuits (shown Fig.6b).

In the calculation, estimated values of inductances in the equivalent circuit play a key role. According to Suzuki [13] the inductances L_A , L_B and L_C are given by

$$\begin{aligned} L_A &= \mu_0 [(d_{12} + l_{eff})^2 + l_{eff}^2 l_J] / K W_c \\ L_B &= \mu_0 l_B (1 + l_J) / [K W_c \sinh(d_B/l_B)] \\ L_C &= \mu_0 l_C (1 + l_J) / [K W_c \sinh(d_C/l_C)] \end{aligned} \quad (4)$$

where l is the bridge length, l_J is the junction length, W_c is the counter electrode width, d_{12} is the thickness of the insulating layer, K is the fringing factor calculated by given [10], d and d_C are the base and counter electrode respectively, and μ_0 is the permeability.

Here l_{eff} is the sum of the effective London penetration depth of both electrodes, and is given by

$$l_{eff} = l_B \tanh(d_B/2 l_B) + l_C \tanh(d_C/2 l_C)$$

The loop inductance L_{loop} is the sum of L_A , L_B and L_C , and is given by

$$\begin{aligned} L_{loop} &= L_A + L_B + L_C = \mu_0 [(d_{12} + l_{loop})^2 + l_{loop}^2 l_J] / K W_c \text{ and} \\ l_{loop} &= l_B \coth(d_B/l_B) + l_C \coth(d_C/l_C) \end{aligned}$$

(K , fringing factor, approximately equal to $(1 + 4 d_{12}/W)$ where $W \gg d_{12}$) For a 2.5 mm Josephson junction technology, the material parameters used for designing the SQUID OR gate .

Further, the SQUID OR gate is designed under the following conditions:

Line width and line spacing = 2mm

Layer-to-Layer registration = 1.5mm.

With $W_c = 7.0\text{mm}$ the device area of the SQUID OR gate is 7mm x 16.5mm.
 $p = L_J/L = 0.5$ and $l = 1.01 p$ (approximately).

Dynamic response:

The dynamic response of the designed SQUID OR gate is obtained by substituting the values of device parameters in Eqns. (2) and (3) and solving them by using the fourth-order Runge-Kutta method on a computer.

In Fig.4 the dynamic response of the designed SQUID OR gate has been obtained for two different technologies. The solid curve shows the output current (load) variation of the SQUID OR gate with time using Pb-alloy technology whereas the dotted curve is obtained from Nb/A10x/Nb Josephson junction base SQUID OR gate. It is apparent from the simulation that the Nb/A10x/Nb base SQUID OR gate has better features over Pb-alloy based OR gate.

Using our concept of the turn-on delay of the Josephson junction [14], the turn-on delay of the SQUID OR gate has been obtained. We have considered the turn-on delay of the SQUID as the time needed for the output phase of the SQUID to reach its phase $p/2$.

In Fig.5, we have shown the turn-on delay of a SQUID logic gate dependence on the overdrive current. The solid curve indicates the turn-on delay vs overdrive curve for a Pb-ally based SQUID OR gate, whereas the dotted curve is the turn-on delay vs time one for a Nb/A10x/Nb based SQUID OR gate. It can be observed from the figure that the turn-on delay for a Pb-alloy based SQUID OR gate is higher than the Nb/A10 x/Nb based OR gate. This because of the low junction capacitance (0.37pF) in the case of Nb/A10x/Nb based OR gate.

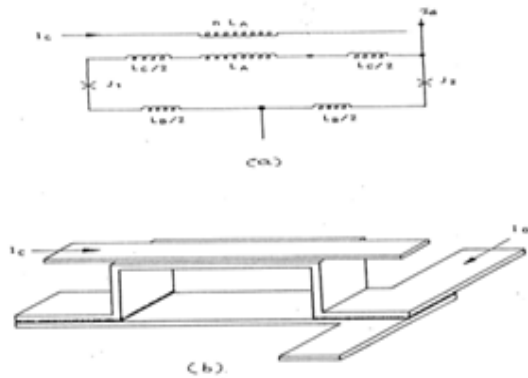


Fig. 7 (a) Equivalent circuit of a SQUID AND gate. b) Static characteristic of the SQUID AND gate. The parameters used for plotting are $a = 1.0$, $b = 3.0$, $\lambda = 0.87\pi$ and $p = L_1 / L = 1.0$

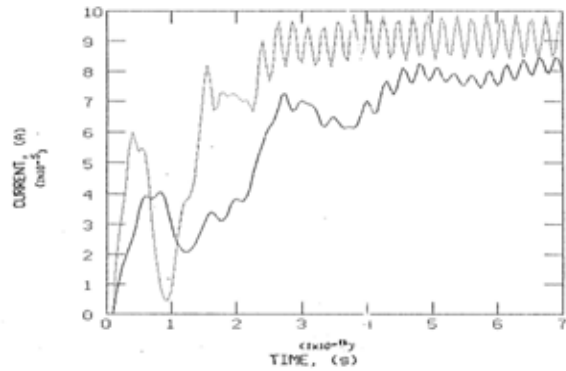


Fig.8 Dynamic response of a SQUID AND gate using two different technologies. The solid curve shows the output current of Pb-alloy based AND gate with time, whereas the dotted curve indicates the output current variation with time for a Nb/A10x/Nb based AND gate

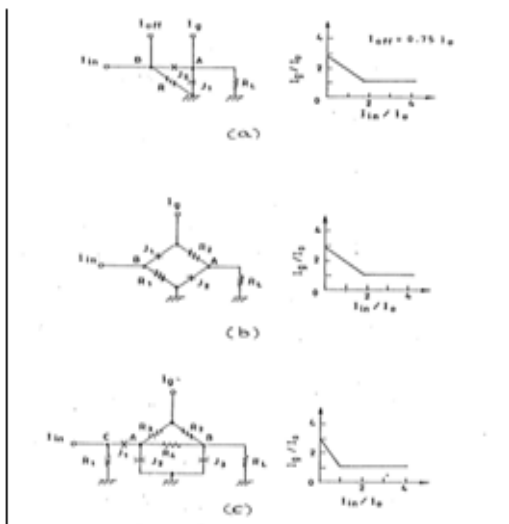


Fig.9 Circuit configuration of the resistive logic gates with threshold characteristics. (a) JAWS (b) DCI and (c) RCJL

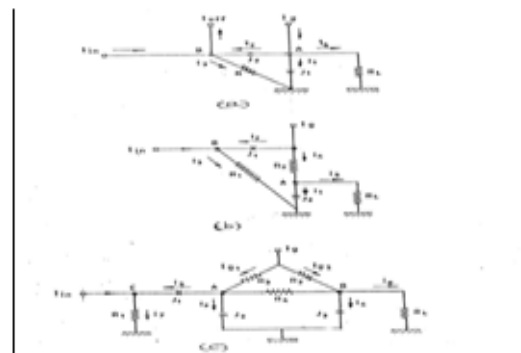


Fig.10 Circuit configuration of the resistive logic gates with current indication at each stage of the logic gate. (a) JAWS (b) DCI and (c) RCJL.

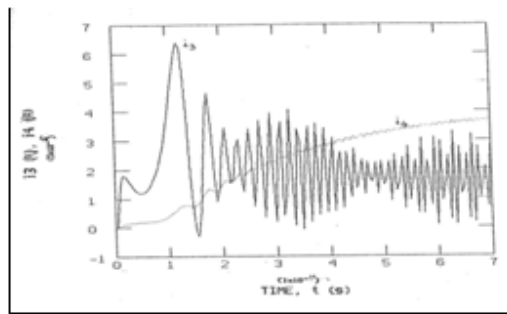


Fig. 11 Simulated switching dynamics of the JAWS gate. Circuit parameters used in the simulation are $I_0 = 0.1 \text{ mA}$, $C_j = 0.8 \text{ pF}$, $r = 0.8\Omega$, $r_L = 10\Omega$.

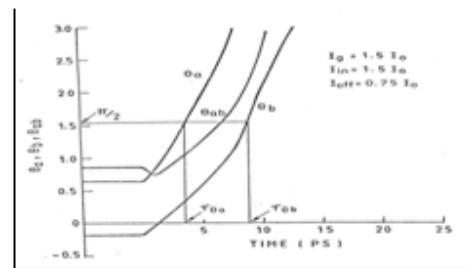


Fig. 12 Simulated phase evolution vs time for a JAWS gate. θ_a and $\theta_a - \theta_b$ are the phase differences of the junctions J_1 and J_2 .

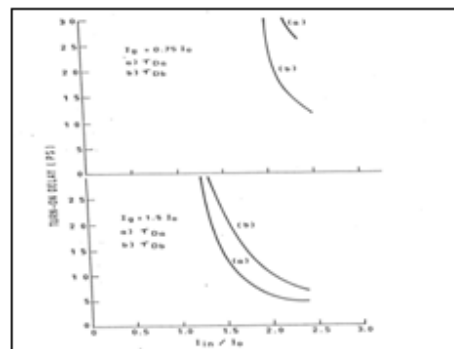


Fig. 13 Turn-on delay of the JAWS gate vs input current. T_{Da} and T_{Db} represent the turn-on delay variation with time at point 'a' and 'b' respectively (as shown in Fig 2a)

IV. SQUID AS AN AND GATE

Asymmetric interferometers with two Josephson junctions or asymmetric dc SQUIDS are very promising devices for digital logic gates. Logic circuits based on these SQUIDS have been investigated [1] [4] . An asymmetric AND interferometer using 3-junctions interferometer have been discussed [15]. In general 3-junction interferometers are used for logic gates whereas 2-junction interferometers are used for the memory application although 3-junction interferometers have better gain tolerances than 2-junction interferometer [16] we have considered 2-junction interferometers for realizing logic gates.

Further, the 2-junction interferometers are simpler and occupy less space compared to 3-junction interferometers. The equivalent circuit of a symmetric two Josephson junction interferometer with nonlinear current injection used for the SQUID AND gate is shown in Fig.6. (according to Beha [9]). The interferometer loop consists of the inductance $L = L_1 + L_2$ and the Josephson junctions A and B with the maximum Josephson currents in zero currents in zero field $I_{ja} = a.I_0$ and $I_{jb} = b.I_0$. A and B are the phases differences of the Josephson Junctions A and B. Analytic expressions for the calculation of the boundaries of flux quantum states-are derived as follows: The flux quantization condition and the Kirchoff law yield for the current i_{CN} and the gate current i_G as follows

$$i_{CN} = \frac{1}{pI} [q_a - q_b - (1-p)/b \sin q_b + 2\rho N] \dots (5a)$$

$$i_G = a \cdot \sin q_a + b \cdot \sin q_b - i_{CN} \dots (5b)$$

$$l = 2\rho LI_o / I_o ; L = L_1 + L_2 ; p = L_1 / L$$

Two interferometer as AND gates to achieve the high gain, large slope and wide tolerances, the device parameters are $p = 1.0$ and $l = 0.87p$ [16]. In the present case we have tried to achieve these parameters. Beha [17] has investigated a high density SQUID structure for NDRO memory cell. We have used the same structure in order to design AND gate.

. Fig. 7a shows the basic structure of the AND gate and Fig.7b shows its equivalent circuit. It can be observed from the two structures (Fig 7a) that there is only one difference in the current injection. Except this the two structures are identical. The device parameters obtained are similar to SQUID OR gate. The device parameters are $p = L_1/L = 1.0$ and $l = 1.0 p$ (approximately) have been obtained .For the SQUID AND gate with $W_c = 3.5\text{mm}$, the area of the gate becomes $3.5\text{mm} \times 16.5\text{mm}$. This is a very small dimension of the AND gate.

In Fig.8 the dynamic response of the designed SQUID AND gate has been obtained for two different technologies. The solid curve shows the output current (load) variation of the SQUID AND gate with time using Pb-alloy technology whereas the dotted curve is obtained from Nb/A10x/Nb Josephson junction based SQUID AND gate. It is apparent from the simulation that the Nb/A10 x/Nb base SQUID AND gate has better features over Pb-alloy based AND gate.

V. JAWS (JOSEPHSON AUTO-WEBER SYSTEM)

A gate of this kind has been reported by Fulton, et al [6] and is called JAWS. The basic gate employs two junctions and a resistor as shown in Fig.9 where J_1 and J_2 represent Josephson junctions with critical currents $2I_o$ and I_o and junction capacitances $2C_j$ and C_j respectively. R_L is the load resistor with a resistance r_L . R is the input resistor with a resistance r .

The JAWS gate is biased in the superconducting state by the gate current I_g and the offset current I_{off} . The current levels in J_1 and J_2 are $I_g - I_{off}$ and I_{off} , respectively. When the input signal I_{in} is directly injected to this JAWS device, it will add to the bias current in junction J_1 and subtract from the bias current in junction J_2 . The junction J_1 is a current-summing junction which switches first in the gate. This makes J_1 highly resistive, steering most of the signal and the gate current leads to ground through the resistor R . The gate current I_g is selected to be sufficient to then switch J_2 to the non-zero voltage state. With both J_1 and J_2 in the high resistance state, the gate current is steered to the load R and the signal current to ground via the resistor R . The high-resistance of J_2 prevents gate current from feeding back into the input signal line and thus provides isolation.

Fig.10 we have shown the current equations at each stage of the logic gate mentioned. According to Fig.2a, the current equation at each stage can be written as:

$$i_1 = 2 I_o \sin q_a + 2 C_j \frac{dV_a}{dt} \quad (1.1)$$

$$i_2 = I_o \sin(q_a - q_b) + C_j \frac{d}{dt} (V_a - V_b) \quad (6.2)$$

$$i_3 = V_b / r \quad (1.3)$$

$$i_4 = V_a / r_L \quad (1.4)$$

$$V_a = \frac{f_o}{2\rho} \frac{dq_a}{dt}, V_b = \frac{f_o}{2\rho} \frac{dq_b}{dt} \quad (6.5)$$

$$I_g = i_1 + i_2 + i_4 \quad (6.6)$$

$$\text{and } I_{in} + i_2 = i_{off} + i_3 \quad (5.7)$$

(Note: Here the effect of subgap quasiparticle resistance R_j has been neglected since $R_j \gg r, r_L$).

Dynamic case:

Eqn. (6.1) can be written as

$$i_1 = 2 I_o \sin q_a + 2 C_j \frac{d^2 q_a}{dt^2} \frac{I_o}{2\rho}$$

$$\text{or } \frac{d^2 q_a}{dt^2} = \frac{\rho}{f_o C_j} [i_1 - 2 I_o \sin q_a] \quad (6.8)$$

Similarly, Eqn.(1.2) can be written as

$$\frac{d^2 q_b}{dt^2} = \frac{2\rho}{f_o C_j} \left[\frac{i_1}{2} - i_2 - 2 I_o \sin q_a + I_o \sin (q_a - q_b) \right] \quad (1.9)$$

Further, from Eqns. (6.6) and (6.7) we get, $i_1 = I_g + I_{in} - I_{off} - (i_3 + i_4)$

$$i_2 = I_{off} - I_{in} + i_3$$

Substituting the above values i_1 and i_2 in Eqns.(6.8) and (6.9), we obtain,

$$\frac{d^2 q_a}{dt^2} = \frac{\rho}{f_o C_j} [i_g + I_{in} - I_{off}$$

$$- 2 I_o \sin q_a \frac{f_o}{2\rho r} \frac{dq_b}{dt}$$

$$- \frac{f_o}{2\rho r_L} \frac{dq_a}{dt}] \quad (6.II)$$

$$\text{and } \frac{d^2 q_b}{dt^2} = \frac{2\rho}{f_o C_j} \left[\frac{i_g}{2} + \frac{3}{2} I_{off} + \frac{3}{2} I_{in}$$

$$+ 2 I_o \sin q_a + I_o \sin (q_a - q_b) \right]$$

$$- \frac{3 f_o}{4\rho r} \frac{dq_b}{dt} - \frac{f_o}{4\rho r_L} \frac{dq_a}{dt} \quad (6.III)$$

Computer-simulated pulse response of the JAWS gate can be obtained by solving the Eqns.(6.II)and(6.III) for an input current I_{in} applied as a step function at $t=0$ with amplitude $1.5 I_{th}$ (threshold current).

In Fig.11 the current variations with time at different stages of the JAWS gate (shown in Fig.10a) have been plotted. The parameters chosen for plotting are $I_o = 0.1\text{mA}$ and $C_j = 0.8\text{pF}$. These curves are almost similar to

those obtained by Josephson [5] using computer simulation. This gives confidence to our simulation approach that we have adopted in the present case in order to investigate the switching dynamics of logic gates. Since Nb/A10 x/Nb Josephson technology has better qualities over Pb-alloy technology, we have used Nb/A10 x/Nb Josephson junction parameters for the simulation of the resistive logic gates such as JAW, DCI and RCJL. The parameters are $I_0 = 87\text{mA}$ and $C_j = 0.37\text{pF}$. It may be pointed out that in estimating the turn-on delay of a logic gate, Sone [5] has considered the time that is needed to reach 2% of the output current to the load.

This consideration seems to be arbitrary. In the present case we have defined turn-on delay of a logic gate in a more critical way using the concept of the turn-on delay of Josephson junction discussed in paper[6]. It is the time taken by the output phase to reach to a value $\pi/2$

The solid curve indicates the current variation (i_3) with time at stage 'b' as shown in Fig.10a and the dotted curve indicates the current i_4 (output current) with time at a stage 'A'. Further, in Fig.12 we have shown the phase variations with time at different stages of the JAWS gate. The biasing and overdrive current conditions are as follows: $I_g = 1.5 I_0$; $I_{in} = 1.5 I_0$ and $I_{off} = 0.75I_0$. Using our concept of turn-on delay[6], the turn-on delay at each stage of the JAWS gate has been indicated. This will give an exact physical understanding of switching dynamics of the JAWS gate[7].

Also we have plotted (Fig-13) the effect of overdrive current on the turn-on delay of a JAWS gate under different biasing conditions, $I_g = 0.75 I_0$, $1.5 I_0$ and $2.25 I_0$. In. It can be observed from Fig.7 that the turn-on delay of a JAWS gate decreases with the increase of overdrive current. Also, the turn-on delay decreases with the increase of biasing rate. So by choosing large biasing and overdrive currents we can minimize the turn-on delay of the JAWS gate.

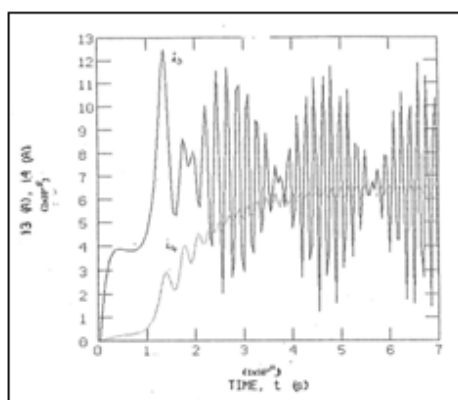


Fig.14 Simulated switching dynamics of the DCI gate. Circuit parameters used in the simulation are from Nb/A10x/Nb Josephson technology and are given as $I_0 = 0.087 \text{ mA}$, $C_j = 0.37 \text{ pF}$, $R_1 = R_2 = 0.8\Omega$, $r_L = 10\Omega$. The switching waveforms current flowing in the input resistor R and the output current respectively.

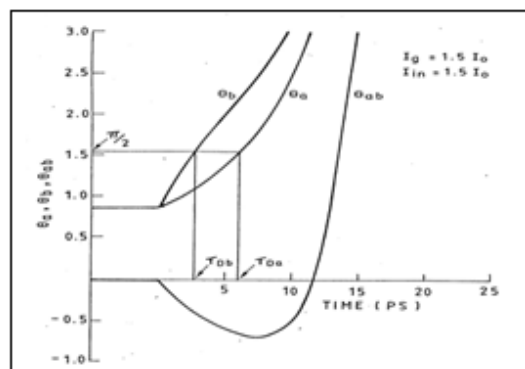


Fig.15 Simulated phase evolution vs time for a DCI gate. θ_a and θ_{ab} are the phase differences of the junctions J_1 and J_2 , respectively. $I_0 = 0.087 \text{ mA}$, $C_j = 0.37 \text{ pF}$, $R_1 = R_2 = 0.8 \Omega$ and $r_L = 10 \Omega$.

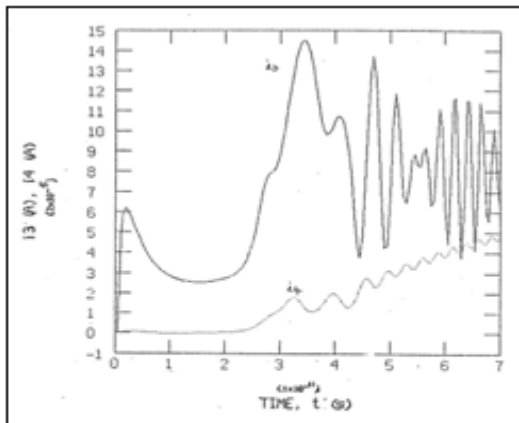


Fig.16 Simulated switching dynamics of the RCJL gate. Circuit parameters used in the simulation are from Nb/AlOx/Nb Josephson technology and are given as $I_0 = 0.087 \text{ mA}$, $C_j = 0.37 \text{ pF}$, $R_1 = R_2 = R_3 = 0.8 \text{ } \Omega$, $rL = 10 \text{ } \Omega$.

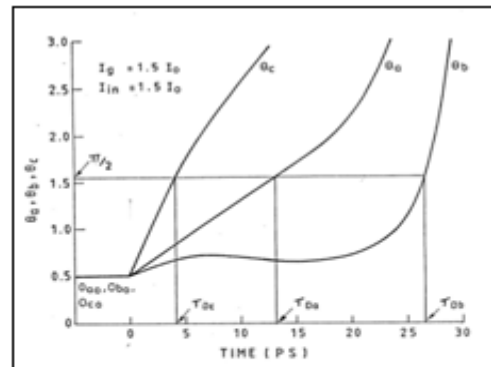


Fig. 17 Simulated phase evolution vs time for a RCJL gate. θ_a , θ_b and θ_c are the phase variations at points c_a , 'b' and 'c' respectively. Circuit parameters used in the simulation are $I_0 = 0.087 \text{ Ma}$, $C_j = 0.37 \text{ pF}$, $R_1 = R_2 = R_3 = 0.8$ and $rL = 10 \text{ } \Omega$

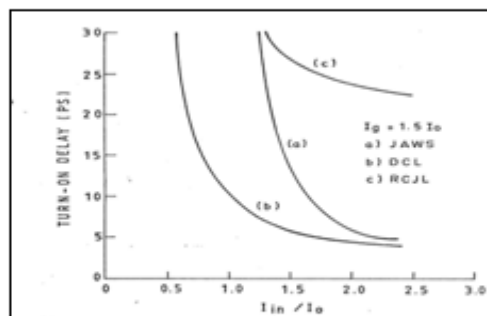


Fig. 18 Turn on delay vs input current of JAWS, DCI and RCJL gate under same biasing condition, $I_g = 1.5I_0$.

VI. DCI (DIRECT COUPLED ISOLATION)

This was proposed by Gheewala et al [7]. Here the Josephson junction is used just a so called "diode" junction - connecting the input signal to logic device to provide isolation.

It consists of two Josephson junctions J_1 and J_2 as shown in Fig.10b. The junctions J_1 has a critical current I_0 and junction capacitance C_j , and the junction J_2 has a critical current $2 I_0$ and the junction capacitance $2C_j$. The resistances of R_1 and R_2 are r and $r/2$ respectively. The DCI gate is biased in the superconducting state by the injection of the input current I_{in} . The junction J_2 plays the role of the current-summing junction in this gate.

When the input signal I_{in} is directly injected to this DCI gate, it will add to the bias current in junction J_2 and subtract from the bias in junction J_1 . The junction J_2 is a current-summing junction which switches first to non-zero voltage state. This makes J_2 highly resistive, steering most of the signal and the gate current to ground through the resistor R_1 ($R_L \gg R_1$). The gate current I_g is selected to be sufficient to then switch J_1 to the non-zero voltage state. With both J_1 and J_2 in the high-resistance state, the gate current is steered to the R_L and signal current to ground via the resistor R_1 . The high-resistance of J_1 prevents gate current from feeding back into the input signal line and thus provides isolation. However, the isolation is not perfect and a small amount of current (typically 3-5 percent) is fed back into the input line.

The above DCI gate can be modified or converted to a JAWS gate (as shown Fig.10b). Here two differences are there between DCI and JAWS gates, one is the I_{off} current is absent for DCI gate and the other one is that the extra resistor R_2 is connected in series with the junction J_2 .

According to Fig.10b the current equations at each stage of the DCI gate can be written as similar to JAWS gate Dynamic case: By modifying equations 6.1 to 6.6 we can obtain similar type Eqns.(6.II)and(6.III) for an input current I_{in} applied as a step function at $t=0$ with amplitude $1.5 I_{th}$ (threshold current

The dynamic response of the DCI gate at each stage (shown in Fig.14) have been obtained from computer simulation. The DCI logic gate characteristics are similar to JAWS gate, and have advantages over JAWS in the better margin and gains due to the lack of I_{off} (offset) current In Fig.15 we have shown the phase variations with time at different stages of the DCI gate (shown in Fig.10b). The biasing and overdrive current conditions are as follows: $I_g = 1.5 I_0$ and $I_{in} = 1.5 I_0$

VII. RCJL (RESISTOR COUPLED JOSEPHSON LOGIC)

The circuit configuration and the threshold curve for the RCJL gate are shown in Fig.10c. The junctions J_1 , J_2 and J_3 have critical currents I_0 , $3/2 I_0$, and $3/2 I_0$, and junction capacitances of C_j , $3/2 C_j$, and $3/2 C_j$, respectively. The resistor R_2 , R_3 and R_4 have the same values of the resistance r' and the resistance of R_1 is r . The RCJL gate is biased in the superconducting state by the injection of the input current I_{in} . The junction J_2 plays a role of the current-summing junction in this gate. The operation of the RCJL gate is as follows:

Initially the gate current I_g splits into I_{g1} and I_{g2} in the inverse ratio of resistors r_2 and r_3 . When the input current I_{in} (I_c) is applied at the node C, the I_{in} goes through the junction J_1 and is injected into the junction J_2 . The junction J_2 subsequently switches from the superconducting state to the resistive state. A fraction of the Josephson current having shown in J_2 , swings over the junction J_3 through r_2 , r_3 , r_4 , and causes J_3 to switch. Consequently, the gate current I_g is steered towards the junction J_1 , and J_1 switching results. After J_1 switching, I_g is steered into the load R_1 and I_{in} is terminated through R_1 . Gate switching with input-output isolation is completed. In the RCJL gate, total I_{in} current contributes to initialization of the switching sequence, while only a fraction of I_g contributes to it. This results in a high input sensitivity.

According to Fig.2c, the current equations at each stage of the RCJL gate can be written as as similar to JAWS gate:

(b) Dynamic case: By modifying current equations we can obtain similar type Eqns.(6.II)and(6.III) for an input current I_{in} applied as a step function at $t=0$ with amplitude $1.5 I_{th}$ (threshold current

Computer-simulated pulse response of the RCJL gate can be obtained by solving the for an input current I_{in} applied as a step function at $t=0$ with amplitude $1.5 I_{th}$

The current variations with time for a RCJL gate at each stage have been plotted in Fig.16 using computer simulation. The parameters used are the same that have been used for JAWS and DCI gates. The solid curve shows the current variation with time at point 'A' (as shown in Fig.10c) and the dotted curve shows the output current variation with time.

In Fig.17 we have shown the phase variations with time at different stages of the RCJL gate using computer simulation. The biasing and overdrive current conditions are as follows: $I_g = 1.5 I_0$ and $I_{in} 1.5 I_0$. Using our concept of turn-on delay[6], the turn-on delay at each stage of the RCJL gate has been indicated. This will give an exact physical understanding of switching dynamics of the RCJL logic gate[7].

Finally in Fig.18 we have compared the effect of turn-on delay vs overdrive for JAWS, DCI and RCJL gates under the same biasing condition, $I_g = 1.5I_0$. It is observed for the low fan-out (here fan-out is one) the DCI logic gate seems to be a better choice for the logic circuit application because of its low turn-on delay and high-speed performance.

VIII. CONCLUSIONS

In the present paper we have made an attempt to obtain the optimized parameters, properties and optimizations techniques of SQUID to be useful for the design of logics and memory cells. For logic and memory applications, it is found that the optimized device parameters are $p = 0.5$ and $l = p$. However, for the SQUID used as an AND gate, the device parameters are obtained as $p = 1.0$ and $l = p$, so that it provides large gain and operating margins. The logic and memory cell have been designed using these optimized techniques and the dynamic response of these have been obtained by computer-simulation. It is apparent from the simulation that the speed of the designed logic and memory cell is extremely high compared to earlier investigations. Further, the circuit dimension of the logic and memory cell is very low.

A thorough investigation of JAWS, DCI and RCJL logic gates have been made [6][7][8]. The dynamic response of these logic gates are obtained by computer-simulation. The concept of our turn-on delay [14] has been introduced which has helped us in critically ascertaining the switching speed of the logic gates. The effect of turn-on delay on overdrive current has been studied. It is observed that for low fan-outs, the DCI logic gate seems to be a better choice for logic circuit application. It is expected that the concept of turn-on delay will be able to remove confusions which are lying in the earlier investigations.

IX. ACKNOWLEDGEMENTS

I would like to acknowledge Prof.C.L.R.S.V. Prasad, Principal and Professor Nagendar Parashar Director (Academic) of GMR Institute of Technology, Rajam, A.P,India for their constant encouragement to finish this work

REFERENCES

- [1] T. R. Gheewala, " Josephson logic devices and circuits," IEEE Trans. Electron Devices vol. ED- 27, no.10, October 1980, pp. 1857-1869.
- [2] P. Gueret " Experimental observation of switching transients resulting from single flux-quantum transitions in superconducting. Josephson devices," Appl. Phys. Lett. vol.25, 1974, p.426.
- [3] P. Gueret "Storage and detection of a single flux quantum in Josephson-junction devices," IEEE Trans. Magnetics vol. MAG-11, 1975, p.751.
- [4] P. Wolf, " SQUIDS as computer elements," SQUIDS : Superconducting Quantum Interference Devices And Their Applications, H. D. Hahlbohrn and H. Lubbig (Eds.), Walter de Gruyter, Berlin, FRG, 1977, pp. 519-540.
- [5] K. Srinivas, "DYNAMIC SIMULATIONS OF SUPERCONDUCTING QUANTUM INTERFERENCE DEVICE (SQUID) MEMORY CELL" International Journal of Scientific & Engineering Research Volume 4, Issue 1, January-2013 ISSN 2229-5518

- [6] T. A. Fulton, S. S. Pei and L. N. Dunkleberger, " A simple high performance current switched Josephson logic," Appl. Phys. Lett. . vol.34, no.10, May 1979, pp. 709-711.
- [7] R. Gheewala and A. Mukherjee, " Josephson direct coupled logic (DCL)," IEDM Tech. Dig., (Washington DC, December 3-5, 1979), pp. 482-484.
- [8] J. Sone, T. Yoshida and H. Abe, " Resistor coupled Josephson logic," Appl. Phys. Lett. vol.40, 1982, p.741.
- [9] J. Wunch, W. Jutzi and E. Crocoll, " Parameter evaluation of asymmetric interferometers with two Josephson junctions," IEEE Trans. Magnetics vol.MAG-18, no.2, March 1982, pp. 735-737.
- [10] ASTAP, IBM Advanced Statistical Analysis Program, IBM publication No. SH20-1118, available through IBM Branch office.
- [11] SPICE 2 Report, Version 2E0 1978, E. Cohen, A. Vladimirescer and O. D. Pederson, Univ. of California, Dept. of Elect. Engg. and Computer Science.
- [12] H. Jackel, W. Bachtold, " Computer-simulation models for digital Josephson Devices and circuits," CIRCUIT ANALYSIS SIMULATION AND DESIGN, A. E. Rulhi (Ed.), Elsevier Science publishers B. V. (North-Holland), 1986, pp. 179-205.
- [13] H. Suzuki, ' Characteristics of Single Flux Quantum Josephson cells," Fujitsu Sci. Tech. J. vol.19, no.4, December 1983, pp. 475-496.
- [14] K. Srinivas, J. C. Biswas and S. K. Dutta Roy , " Turn-on delay of a Josephson junction," J of Low Temperature Physics" , vol.74, Nos. 5/6 1989 , pp.407-415.
- [15] H. Beha and H. Jackel, " High-Tolerance Three-Josephson junction current-injection logic devices (HTCID)," IEEE Trans. Magnetics, vol.MAG-17, no.6. November 1981, pp. 3423-4325.
- [16] H. Beha, W. Jorger and W. Jutzi, " A four input AND gate with five asymmetric interferometers," IEEE Trans. Magnetics vol.MAG-17, no.1, January 1981, pp. 587-590.
- [17] H. Beha, " High-density NDRO SFQ Josephson interferometer memory cell," IEEE Trans. Magnetics vol.MAG-17, no.1, January 1981, pp.3426-3428.
- [18] T. R. Gheewala, " Josephson logic devices and circuits," IEEE Trans. Electron Devices vol.ED-27, no.10, October 1980, pp.1857-1869.
- [19] T. A. Fulton, S. S. Pei and L. N. Dunkleberger, " A simple high performance current switched Josephson logic," Appl. Phys. Lett. . vol.34, no.10, May 1979, pp. 709-711
- [20] K. Srinivas, "Dynamic response of Josephson resistive logic JAWS gate" International Journal of Scientific and Engineering Research IJSER Volume 2, Issue 10, Oct-2011.
- [21] K. Srinivas, "Dynamic response of Josephson resistive logic DCI gate " International Journal of Scientific and Engineering Research IJSER Volume 2, Issue 10, Oct-2011.
- [22] K. Srinivas, "Dynamic response of Josephson resistive logic RCJL gate International Journal of Scientific and Engineering Research IJSER Volume 2, Issue 10, Oct-2011.

DGLAP EVOLUTION EQUATIONS IN LEADING ORDER AND NEXT-TO-LEADING ORDER AND HADRON STRUCTURE FUNCTIONS AT LOW-X

R Rajkhowa¹, N J Hazarika²

¹Physics Department, T. H. B College, Jamugurihat, Sonitpur, Assam, (India)

²Mathematics Department, T. H. B College, Jamugurihat, Sonitpur, Assam, (India)

ABSTRACT

We present unique solutions of singlet and non-singlet Dokshitzer-Gribov-Lipatov-Altarelli-Parisi (DGLAP) evolution equations in leading order (LO) and next-to-leading order (NLO) at low-x. We obtain t-evolutions of deuteron, proton, neutron and difference and ratio of proton and neutron structure functions and x- evolution of deuteron structure function at low-x from DGLAP evolution equations. The results of t-evolutions are compared with HERA and NMC low-x low-Q² data and x-evolution are compared with NMC low-x low-Q² data. And also we compare our results of t-evolution of proton structure functions with a recent global parameterization.

PACS No.: 12.38.Bx, 12.39-x, 13.60Hb.

Keywords: Altarelli-Parisi Equation, Complete Solution, Low-X Physics, Particular Solution, Structure Function, Unique Solution.

I. INTRODUCTION

In some earlier papers [1-4], particular solutions of the Dokshitzer-Gribov-Lipatov-Altarelli-Parisi (DGLAP) evolution equations [5-8] for t and x-evolutions of singlet and non-singlet structure functions in leading order (LO) and next-to-leading order (NLO) at low-x have been reported, which are non unique solutions. The present paper reports unique solutions of DGLAP evolution equations computed from complete solutions in LO and NLO at low-x and calculation of t and x- evolutions for singlet and non-singlet structure functions, and hence t-evolution of deuteron, proton, neutron, difference and ratio of proton and neutron structure functions, and x- evolution of deuteron structure functions. These results are compared with HERA [9], NMC [10] low-x low Q² data and also with recent global parameterization [11]. Here Section 1, Section 2, and Section 3 will give the introduction, the necessary theory and the results and discussion respectively.

II. THEORY

Though the necessary theory has been discussed elsewhere [2-4], here we have mentioned some essential steps for clarity. The DGLAP evolution equations with splitting functions [12-13] for singlet and non-singlet structure functions are in the standard forms [14 -15]

$$\frac{\partial F_2^S(x, t)}{\partial t} - \frac{\alpha_s(t)}{2p} \left[\frac{2}{3} \{3 + 4 \ln(1-x)\} F_2^S(x, t) + \frac{4}{3} \frac{1}{x(1-x)} \int_x^1 \frac{dw}{1-w} \{ (1+w^2) F_2^S\left(\frac{x}{w}, t\right) - 2F_2^S(x, t) \} \right]$$

$$+ N_f \int_x^1 \{w^2 + (1-w)^2\} G\left(\frac{x}{w}, t\right) dw \} = 0, \quad (1)$$

$$\frac{\partial F_2^{NS}(x, t)}{\partial t} - \frac{a_{s1}(t)}{2p} \left[\frac{2}{3} \{3 + 4 \ln(1-x)\} F_2^{NS}(x, t) + \frac{4}{3} \int_x^1 \frac{dw}{1-w} \{ (1+w^2) F_2^{NS} \frac{\partial^2 x}{\partial w^2}, t \} - 2 F_2^{NS}(x, t) \right] = 0, \quad (2)$$

for LO, and

$$\begin{aligned} & \frac{\partial F_2^S(x, t)}{\partial t} - \frac{a_s(t)}{2p} \left[\frac{2}{3} \{3 + 4 \ln(1-x)\} F_2^S(x, t) + \frac{4}{3} \int_x^1 \frac{dw}{1-w} \{ (1+w^2) F_2^S \frac{\partial^2 x}{\partial w^2}, t \} - 2 F_2^S(x, t) \right] \\ & + N_f \int_x^1 \{w^2 + (1-w)^2\} G\left(\frac{x}{w}, t\right) dw \} - \frac{a_s(t)}{2p} \frac{\partial^2}{\partial x^2} \left[(x-1) F_2^S(x, t) \int_0^1 \frac{df(w)}{dw} dw + \int_x^1 \frac{df(w)}{dx} F_2^S\left(\frac{x}{w}, t\right) dw \right] \\ & + \int_x^1 \frac{\partial F_{qq}^S(w)}{\partial w} F_2^S\left(\frac{x}{w}, t\right) dw + \int_x^1 \frac{\partial F_{qg}^S(w)}{\partial w} G\left(\frac{x}{w}, t\right) dw \} = 0, \end{aligned} \quad (3)$$

$$\begin{aligned} & \frac{\partial F_2^{NS}(x, t)}{\partial t} - \frac{a_s(t)}{2p} \frac{\partial^2}{\partial x^2} \left[\{3 + 4 \ln(1-x)\} F_2^{NS}(x, t) + \frac{4}{3} \int_x^1 \frac{dw}{1-w} \{ (1+w^2) F_2^{NS} \frac{\partial^2 x}{\partial w^2}, t \} - 2 F_2^{NS}(x, t) \right] \\ & - \frac{a_s(t)}{2p} \frac{\partial^2}{\partial x^2} \left[(x-1) F_2^{NS}(x, t) \int_0^1 \frac{df(w)}{dw} dw + \int_x^1 \frac{df(w)}{dx} F_2^{NS} \frac{\partial^2 x}{\partial w^2}, t \} dw \right] = 0, \end{aligned} \quad (4)$$

for NLO, where,

$$t = \ln \frac{Q^2}{L^2}, \quad a_{s1}(t) = \frac{4p}{b_0 t}, \quad a_s(t) = \frac{4p}{b_0 t} \frac{\partial}{\partial t} - \frac{b_1 \ln t}{b_0 t^2} \frac{\partial}{\partial t}, \quad b_0 = \frac{33 - 2n_f}{3} \text{ and } b_1 = \frac{306 - 38n_f}{3},$$

N_f being the number of flavours. Here,

$$f(w) = C_F^2 [P_F(w) - P_A(w)] + \frac{1}{2} C_F C_A [P_G(w) + P_A(w)] + C_F T_R N_f P_{N_F}(w)$$

and

$$F_{qq}^S(w) = 2 C_F T_R N_f F_{qq}(w) \text{ and } F_{qg}^S(w) = C_F T_R N_f F_{qg}^1(w) + C_G T_R N_f F_{qg}^2(w).$$

The explicit forms of higher order kernels are taken from references [12-13]. Here

$$C_A = C_G = N_C = 3, \quad C_F = (N_C^2 - 1) / 2N_C \text{ and } T_R = 1/2.$$

Using Taylor expansion method and neglecting higher order terms of x as discussed in our earlier works [1-4, 17-19], $F_2^S(x/w, t)$ can be approximated for low- x as

$$F_2^S(x/w, t) \approx F_2^S(x, t) + x \sum_{k=1}^{\infty} \frac{\partial^k F_2^S(x, t)}{\partial x^k}.$$

where,

$$u = 1 - w \text{ and } \frac{x}{1-u} = x \sum_{l=0}^{\infty} u^l.$$

Similarly, $G(x/w, t)$ and $F_2^{NS}(x/w, t)$ can be approximated for small- x . Then putting these values of $F_2^S(x/w, t)$, $G(x/w, t)$ and $F_2^{NS}(x/w, t)$ in equation (1) and (3) and performing u -integrations we get,

$$\frac{\partial F_2^S(x, t)}{\partial t} - \frac{a_{s1}(t)}{2p} \frac{\partial}{\partial x} A_1(x) F_2^S(x, t) + A_2(x) G(x, t) + A_3(x) \frac{\partial F_2^S(x, t)}{\partial x} + A_4(x) \frac{\partial G(x, t)}{\partial x} = 0 \quad (5)$$

in LO and

$$\begin{aligned} & \frac{\partial F_2^S(x, t)}{\partial t} - \frac{a_{s1}(t)}{2p} \frac{\partial}{\partial x} A_1(x) F_2^S(x, t) + \frac{a_{s2}(t)}{c} \frac{\partial^2}{\partial x^2} B_1(x) \frac{\partial F_2^S(x, t)}{\partial x} - \frac{a_{s3}(t)}{2p} \frac{\partial}{\partial x} A_2(x) F_2^S(x, t) + \frac{a_{s4}(t)}{c} \frac{\partial^2}{\partial x^2} B_2(x) \frac{\partial G(x, t)}{\partial x} \\ & - \frac{a_{s5}(t)}{2p} \frac{\partial}{\partial x} A_3(x) F_2^S(x, t) + \frac{a_{s6}(t)}{c} \frac{\partial^2}{\partial x^2} B_3(x) \frac{\partial F_2^S(x, t)}{\partial x} - \frac{a_{s7}(t)}{2p} \frac{\partial}{\partial x} A_4(x) G(x, t) + \frac{a_{s8}(t)}{c} \frac{\partial^2}{\partial x^2} B_4(x) \frac{\partial G(x, t)}{\partial x} = 0, \quad (6) \end{aligned}$$

in NLO, where,

$$A_1(x) = \frac{2}{3} \{3 + 4 \ln(1-x) + (x-1)(x+3)\},$$

$$A_2(x) = N_f \left[\frac{1}{3} (1-x)(2-x+2x^2) \right],$$

$$A_3(x) = \frac{2}{3} \{x(1-x^2) + 2x \ln(\frac{1}{x})\},$$

$$A_4(x) = N_f x \left\{ \ln \frac{1}{x} - \frac{1}{3} (1-x)(5-4x+2x^2) \right\}$$

$$B_1(x) = x \int_0^1 f(w) dw - \int_0^x f(w) dw + \frac{4}{3} N_f \int_0^1 F_{qq}(w) dw,$$

$$B_2(x) = \int_x^1 F_{qg}^S(w) dw,$$

$$B_3(x) = x \int_0^1 \left\{ f(w) + \frac{4}{3} N_f F_{qq}(w) \right\} \frac{1-w}{w} dw,$$

$$B_4(x) = x \int_0^1 \frac{1-w}{w} F_{qg}^S(w) dw.$$

Let us assume for simplicity [1-4, 17-19]

$$G(x, t) = K(x) F_2^S(x, t) \quad (7)$$

where $K(x)$ is a function of x . In this connection, earlier we considered [1, 4] $K(x) = k, ax^b, ce^{-dx}$, where k, a, b, c, d are constants. Agreement of the results with experimental data is found to be excellent for $k = 4.5, a = 4.5, b = 0.01, c = 5, d = 1$ for low- x in LO and $a = 10, b = 0.016, c = 0.5, d = -3.8$ for low- x in NLO. Therefore equation (5) and (6) becomes

$$\frac{\partial F_2^S(x, t)}{\partial t} - \frac{a_{s1}(t)}{2p} \frac{\partial}{\partial x} L_1(x) F_2^S(x, t) + L_2(x) \frac{\partial F_2^S(x, t)}{\partial x} = 0, \quad (8)$$

in LO and

$$\frac{\partial F_2^S(x,t)}{\partial t} - \frac{\dot{a}_s(t)}{2p} L_1(x) + \frac{\ddot{a}_s(t)}{2p} M_1(x) \frac{\partial F_2^S(x,t)}{\partial x} - \frac{\dot{a}_s(t)}{2p} L_2(x) + \frac{\ddot{a}_s(t)}{2p} M_2(x) \frac{\partial F_2^S(x,t)}{\partial x} = 0, \quad (9)$$

in NLO.

For simplicity, we can write equation (8) as

$$\frac{\partial F_2^S(x,t)}{\partial t} - \frac{\dot{a}_s(t)}{2p} L_1'(x,t) F_2^S(x,t) + L_2'(x,t) \frac{\partial F_2^S(x,t)}{\partial x} = 0, \quad (10)$$

where,

$$L_1(x) = A_1(x) + K(x)A_2(x) + A_4(x) \frac{\partial K(x)}{\partial x},$$

$$L_2(x) = A_3(x) + K(x)A_4(x),$$

$$M_1(x) = B_1(x) + K(x)B_2(x) + B_4(x) \frac{\partial K(x)}{\partial x},$$

$$M_2(x) = B_3(x) + K(x)B_4(x),$$

$$L_1'(x,t) = \frac{a_{s_1}(t)}{2p} L_1(x), L_2'(x,t) = \frac{a_{s_1}(t)}{2p} L_2(x),$$

For a possible solution of equation (9), we assume [2-4, 15] that

$$\frac{\ddot{a}_s(t)}{2p} = T_0 \frac{\ddot{a}_s(t)}{2p} \quad (11)$$

where, T_0 is a numerical parameter to be obtained from the particular Q^2 -range under study. By a suitable choice of T_0 we can reduce the error to a minimum. Now equation (9) can be recast as

$$\frac{\partial F_2^S(x,t)}{\partial t} - \frac{\dot{a}_s(t)}{2p} P(x,t) F_2^S(x,t) + Q(x,t) \frac{\partial F_2^S(x,t)}{\partial x} = 0, \quad (12)$$

in NLO, where,

$$P(x,t) = \frac{a_s(t)}{2p} [L_1(x) + T_0 M_1(x)] \text{ and } Q(x,t) = \frac{a_s(t)}{2p} [L_2(x) + T_0 M_2(x)]$$

The general solutions [20-21] of equation (10) is $F(U, V) = 0$, where F is an arbitrary function and $U(x, t, F_2^S) = C_1$ and $V(x, t, F_2^S) = C_2$ where, C_1 and C_2 are constants and they form a solutions of equations

$$\frac{dx}{L_2'(x,t)} = \frac{dt}{-1} = \frac{dF_2^S(x,t)}{-L_1'(x,t) F_2^S(x,t)} \quad (13)$$

Solving equation (13) we obtain,

$$U(x, t, F_2^S) = t \exp\left(\frac{1}{A_f} \int \frac{1}{L_2(x)} dx\right) \text{ and } V(x, t, F_2^S) = F_2^S(x, t) \exp\left(\frac{1}{\beta} \int \frac{L_1(x)}{L_2(x)} dx\right)$$

where, $A_f = 4/(33-2N_f)$. Since U , and V are two independent solutions of equation (13) and if α and β are arbitrary constants, then $V = \alpha U + \beta$ may be taken as a complete solution [20-21] of equation (10). We take this

form as this is the simplest form of a complete solution which contains both the arbitrary constants α and β .

Then the complete solution [20-21]

$$F_2^S(x, t) \exp\left\{\int_{\hat{u}}^{\hat{u}'} \frac{L_1(x)}{L_2(x)} dx\right\} = \alpha \exp\left\{\int_{\hat{u}}^{\hat{u}'} \frac{1}{A_f} \frac{L_1(x)}{L_2(x)} dx\right\} + \beta, \quad (14)$$

is a two-parameter family of planes.

Due to conservation of the electromagnetic current, F_2 must vanish as Q^2 goes to zero [22-23]. Also $R \rightarrow 0$ in this limit. Here R indicates ratio of longitudinal and transverse cross-sections of virtual photon in DIS process. This implies that scaling should not be a valid concept in the region of very low Q^2 . The exchanged photon is then almost real and the close similarity of real photonic and hadronic interactions justifies the use of the Vector Meson Dominance (VMD) concept [24-25] for the description of F_2 . In the language of perturbation theory this concept is equivalent to a statement that a physical photon spends part of its time as a “bare”, point-like photon and part as a virtual hadron (s) [23]. The power and beauty of explaining scaling violations with field theoretic methods (i.e., radiative corrections in QCD) remains, however, unchallenged in as much as they provide us with a framework for the whole x -region with essentially only one free parameter A [26]. For Q^2 values much larger than A^2 , the effective coupling is small and a perturbative description in terms of quarks and gluons interacting weakly makes sense. For Q^2 of order A^2 , the effective coupling is infinite and we cannot make such a picture, since quarks and gluons will arrange themselves into strongly bound clusters, namely, hadrons [22] and so the perturbation series breaks down at small- Q^2 [27]. Thus, it can be thought of A as marking the boundary between a world of quasi-free quarks and gluons, and the world of pions, protons, and so on. The value of A is not predicted by the theory; it is a free parameter to be determined from experiment. It should expect that it is of the order of a typical hadronic mass [22]. Since the value of A is so small we can assume at $Q = A$, $F_2^S(x, t) = 0$ due to conservation of the electromagnetic current [22-23]. This dynamical prediction agrees with most ad hoc parameterizations and with the data [26]. Using this boundary condition in equation (14) we get $\beta = 0$ and

$$F_2^S(x, t) = \alpha \exp\left\{\int_{\hat{u}}^{\hat{u}'} \frac{1}{A_f} \frac{L_1(x)}{L_2(x)} dx\right\} - \frac{L_1(x)}{L_2(x)} \frac{\partial}{\partial \hat{u}} \quad (15)$$

Now, defining

$$F_2^S(x, t_0) = \alpha \exp\left\{\int_{\hat{u}}^{\hat{u}'} \frac{1}{A_f} \frac{L_1(x)}{L_2(x)} dx\right\} - \frac{L_1(x)}{L_2(x)} \frac{\partial}{\partial \hat{u}} \quad (15)$$

at $t = t_0$, where, $t_0 = \ln(Q_0^2/\Lambda^2)$ at any lower value $Q = Q_0$, we get from equations (15)

$$F_2^S(x, t) = F_2^S(x_0, t_0) \frac{\partial}{\partial t} \quad (16)$$

which gives the t -evolutions of singlet structure function $F_2^S(x, t)$ in LO. Proceeding in the same way we get

$$F_2^S(x, t) = F_2^S(x, t_0) \frac{\partial}{\partial t} (b/t+1) \exp\left\{\int_{\hat{u}}^{\hat{u}'} \frac{1}{A_f} \frac{L_1(x)}{L_2(x)} dx\right\} - \frac{1}{t_0} \frac{\partial}{\partial \hat{u}} \quad (17)$$

which gives the t -evolutions of singlet structure function $F_2^S(x, t)$ in NLO, where $b = \beta_1/\beta_0^2$

We observed that the Lagrange's auxiliary system of ordinary differential equations (12) occurred in the formalism can not be solved without the additional assumption of linearization (equation 11) and introduction of an adhoc parameter T_0 [2-4, 15]. This parameter does not effect in the results of t- evolution of structure functions.

Proceeding exactly in the same way, we get for non-singlet structure functions

$$F_2^{NS}(x, t) = F_2^{NS}(x, t_0) \exp\left\{ \frac{\beta_0}{\beta_0 - 1} \ln\left(\frac{t}{t_0}\right) \right\} \quad (18)$$

$$F_2^{NS}(x, t) = F_2^{NS}(x, t_0) \exp\left\{ \frac{\beta_0}{\beta_0 - 1} \ln\left(\frac{t}{t_0}\right) \right\} \exp\left\{ -\frac{1}{t_0} \int_{t_0}^t \frac{du}{u} \right\} \quad (19)$$

which gives the t-evolutions of non-singlet structure functions $F_2^{NS}(x, t)$ in LO and NLO respectively.

We observe that if b tends to zero, then equation (17) and (19) tends to equation (16) and (18) respectively, i.e., solution of NLO equations goes to that of LO equations. Physically b tends to zero means number of flavours is high. Again defining,

$$F_2^S(x_0, t) = a t \exp\left\{ \frac{\beta_0}{\beta_0 - 1} \ln\left(\frac{t}{t_0}\right) \right\} \frac{1}{L_2(x)} - \frac{L_1(x)}{L_2(x)} \int_{x_0}^x \frac{dx}{x} \quad (15)$$

we obtain from equation (15)

$$F_2^S(x, t) = F_2^S(x_0, t) \exp\left\{ \frac{\beta_0}{\beta_0 - 1} \ln\left(\frac{t}{t_0}\right) \right\} \frac{1}{L_2(x)} - \frac{L_1(x)}{L_2(x)} \int_{x_0}^x \frac{dx}{x} \quad (20)$$

which gives the x-evolutions of singlet structure function $F_2^S(x, t)$ in LO. Similarly we get

$$F_2^S(x, t) = F_2^S(x_0, t) \exp\left\{ \frac{\beta_0}{\beta_0 - 1} \ln\left(\frac{t}{t_0}\right) \right\} \frac{1}{L_2(x) + T_0 M_2(x)} - \frac{L_1(x) + T_0 M_1(x)}{L_2(x) + T_0 M_2(x)} \int_{x_0}^x \frac{dx}{x}, \quad (21)$$

which gives the x-evolutions of singlet structure function $F_2^S(x, t)$ in NLO, where $a = 2/\beta_0$.

Proceeding in the same way, we get

$$F_2^{NS}(x, t) = F_2^{NS}(x_0, t) \exp\left\{ \frac{\beta_0}{\beta_0 - 1} \ln\left(\frac{t}{t_0}\right) \right\} \frac{1}{A_3(x)} - \frac{A_1(x)}{A_3(x)} \int_{x_0}^x \frac{dx}{x} \quad (22)$$

and

$$F_2^{NS}(x, t) = F_2^{NS}(x_0, t) \exp\left\{ \frac{\beta_0}{\beta_0 - 1} \ln\left(\frac{t}{t_0}\right) \right\} \frac{1}{A_5(x) + T_0 B_5(x)} - \frac{A_6(x) + T_0 B_6(x)}{A_5(x) + T_0 B_5(x)} \int_{x_0}^x \frac{dx}{x} \quad (23)$$

which gives the x-evolution of non-singlet structure functions $F_2^{NS}(x, t)$ in LO and NLO respectively. Here,

$$A_5(x) = \frac{2}{3} \left\{ x(1-x^2) + 2x \ln\left(\frac{1}{x}\right) \right\}, \quad B_5(x) = x \int_0^{1-x} \frac{f(w)dw}{w}$$

$$A_6(x) = \frac{2}{3} \{3 + 4 \ln(1-x) + (x-1)(x+3)\}, \quad B_6(x) = - \int_0^x f(w)dw + x \int_0^1 f(w)dw.$$

In our earlier communications [1-4] we observed that if in the relation $\beta = \alpha^y$, y varies between minimum to a maximum value, the powers of (t/t_0) in LO and powers of $t^{b/t+1}/t_0^{b/t_0+1}$, co-efficient of $b(1/t - 1/t_0)$ of exponential part in NLO in t -evolutions and the numerator of the first term in the integral sign in x -evolution in both LO and NLO varies between 2 to 1. Then it is understood that the particular solutions of DGLAP evolution equations in LO and NLO obtained by that methodology were not unique and so the t - evolutions of deuteron, proton and neutron structure functions, and x - evolution of deuteron structure function obtained by this methodology were not unique. Thus by this methodology, instead of having a single solution we arrive a band of solutions, of course the range for these solutions is reasonably narrow.

Now deuteron, proton and neutron structure functions measured in deep inelastic electro-production can be written in terms of singlet and non-singlet quark distribution functions [22] as

$$F_2^d(x, t) = 5/9 F_2^S(x, t), \tag{24}$$

$$F_2^p(x, t) = 5/18 F_2^S(x, t) + 3/18 F_2^{NS}(x, t), \tag{25}$$

$$F_2^n(x, t) = 5/18 F_2^S(x, t) - 3/18 F_2^{NS}(x, t), \tag{26}$$

$$F_2^p(x, t) - F_2^n(x, t) = 1/3 F_2^{NS}(x, t). \tag{27}$$

Now using equations (16), (17) and (20) and (21) in equation (24) we will get t and x -evolution of deuteron structure function $F_2^d(x, t)$ at low- x as

$$F_2^d(x, t) = F_2^d(x, t_0) \int_{t_0}^t \frac{\partial}{\partial t} \tag{28}$$

in LO

$$F_2^d(x, t) = F_2^d(x, t_0) \int_{t_0}^t \frac{\partial}{\partial t} \exp \left[\frac{b}{t} - \frac{b}{t_0} \right] - \frac{1}{t_0} \int_{t_0}^t \frac{\partial}{\partial t} \tag{29}$$

in NLO and

$$F_2^d(x, t) = F_2^d(x_0, t) \exp \left[\frac{x}{t} \int_{t_0}^t \frac{\partial}{\partial t} \frac{1}{L_2(x)} - \frac{L_1(x)}{L_2(x)} \int_{t_0}^t \frac{\partial}{\partial t} \right] \tag{30}$$

in LO

$$F_2^d(x, t) = F_2^d(x_0, t) \exp \left[\frac{x}{t} \int_{t_0}^t \frac{\partial}{\partial t} \frac{1}{L_2(x) + T_0 M_2(x)} - \frac{L_1(x) + T_0 M_1(x)}{L_2(x) + T_0 M_2(x)} \int_{t_0}^t \frac{\partial}{\partial t} \right], \tag{31}$$

in NLO.

Similarly using equations (16), (18) and (17), (19) in equations (25), (26) and (27) we get the t - evolutions of proton, neutron, and difference and ratio of proton and neutron structure functions at low- x in LO and NLO as

$$F_2^p(x, t) = F_2^p(x, t_0) \int_{t_0}^t \frac{\partial}{\partial t} \tag{32}$$

$$F_2^p(x, t) = F_2^p(x, t_0) \frac{t^{b/t+1}}{t_0^{b/t_0+1}} \exp\left[-\frac{1}{t_0} \frac{t}{t_0}\right] \quad (33)$$

$$F_2^n(x, t) = F_2^n(x, t_0) \frac{t^b}{t_0^b} \quad (34)$$

$$F_2^n(x, t) = F_2^n(x, t_0) \frac{t^{b/t+1}}{t_0^{b/t_0+1}} \exp\left[-\frac{1}{t_0} \frac{t}{t_0}\right] \quad (35)$$

$$F_2^p(x, t) - F_2^n(x, t) = [F_2^p(x, t_0) - F_2^n(x, t_0)] \left(\frac{t}{t_0}\right), \quad (36)$$

$$F_2^p(x, t) - F_2^n(x, t) = [F_2^p(x, t_0) - F_2^n(x, t_0)] \frac{t^{b/t+1}}{t_0^{b/t_0+1}} \exp\left[-\frac{1}{t_0} \frac{t}{t_0}\right] \quad (37)$$

and

$$\frac{F_2^p(x, t)}{F_2^n(x, t)} = \frac{F_2^p(x, t_0)}{F_2^n(x, t_0)} = R(x). \quad (38)$$

where $R(x)$ is a constant for fixed- x . It is observed that ratio of proton and neutron is same for both NLO and LO and it is independent of t for fixed- x . We also observed that unique solutions of GLDAP evolution equations in LO and NLO are same with particular solutions in LO and NLO for y maximum in $\beta = \alpha^y$ relation [1-4].

III. RESULTS AND DISCUSSION

In the present paper, we compare our results of t -evolution of deuteron, proton, neutron and difference and ratio of proton and neutron structure functions with the HERA [9] and NMC [10] low- x and low- Q^2 data and results of x - evolution of deuteron structure functions with NMC low- x and low- Q^2 data. In case of HERA data proton and neutron structure functions are measured in the range $2 \leq Q^2 \leq 50 \text{ GeV}^2$. Moreover here $P_T \leq 200 \text{ MeV}$, where P_T is the transverse momentum of the final state baryon. In case of NMC data proton and neutron structure functions are measured in the range $0.75 \leq Q^2 \leq 27 \text{ GeV}^2$. We consider number of flavours $N_f = 4$. We also compare our results of t -evolution of proton - structure functions with recent global parameterization [11]. This parameterization includes data from H1-96 \ 99, ZEUS- 96/97(X0.98), NMC, E665, data.

In Fig. 1(a), (b), (c), (d), we present our results of t -evolutions of deuteron, proton, neutron, and difference of proton and neutron structure functions (solid lines for NLO and dashed lines for LO) for the representative values of x given in the figure. Data points at lowest- Q^2 values in the figures are taken as inputs to test the evolution equations. Agreement with the data [9-10] is found to be good. We observe that t -evolutions are slightly steeper in LO calculations than those of NLO.

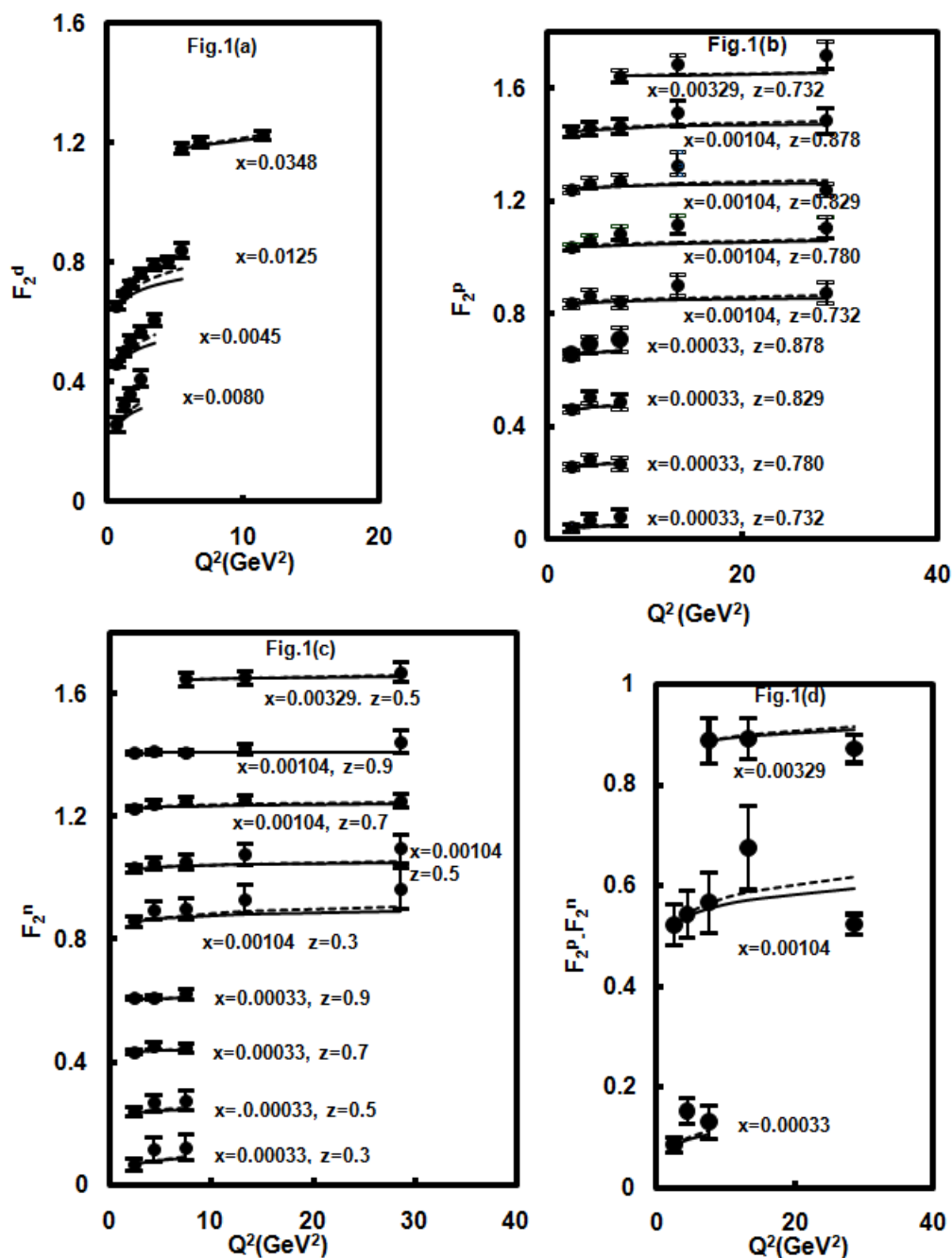


Fig.1: Results of t-evolutions of deuteron, proton, neutron and difference of proton and neutron structure functions (dashed lines for LO and solid lines for NLO) for the representative values of x in LO and NLO for NMC data. For convenience, value of each data point is increased by adding $0.2i$, where $i = 0, 1, 2, 3 \dots$ are the numberings of curves counting from the bottom of the lowermost curve as the 0-th order. Data points at lowest- Q^2 values in the figures are taken as input.

In fig. 2, we compare our results of t-evolutions of proton structure functions F_2^p (solid lines for NLO and dashed lines for LO) with recent global parameterization [11] (long dashed lines) for the representative values of x given in the figure. Data points at lowest- Q^2 values in the figures are taken as input to test the evolution equation. We observe that t-evolutions are slightly steeper in LO calculations than those of NLO. Agreement with the LO results is found to be better than with the NLO results.

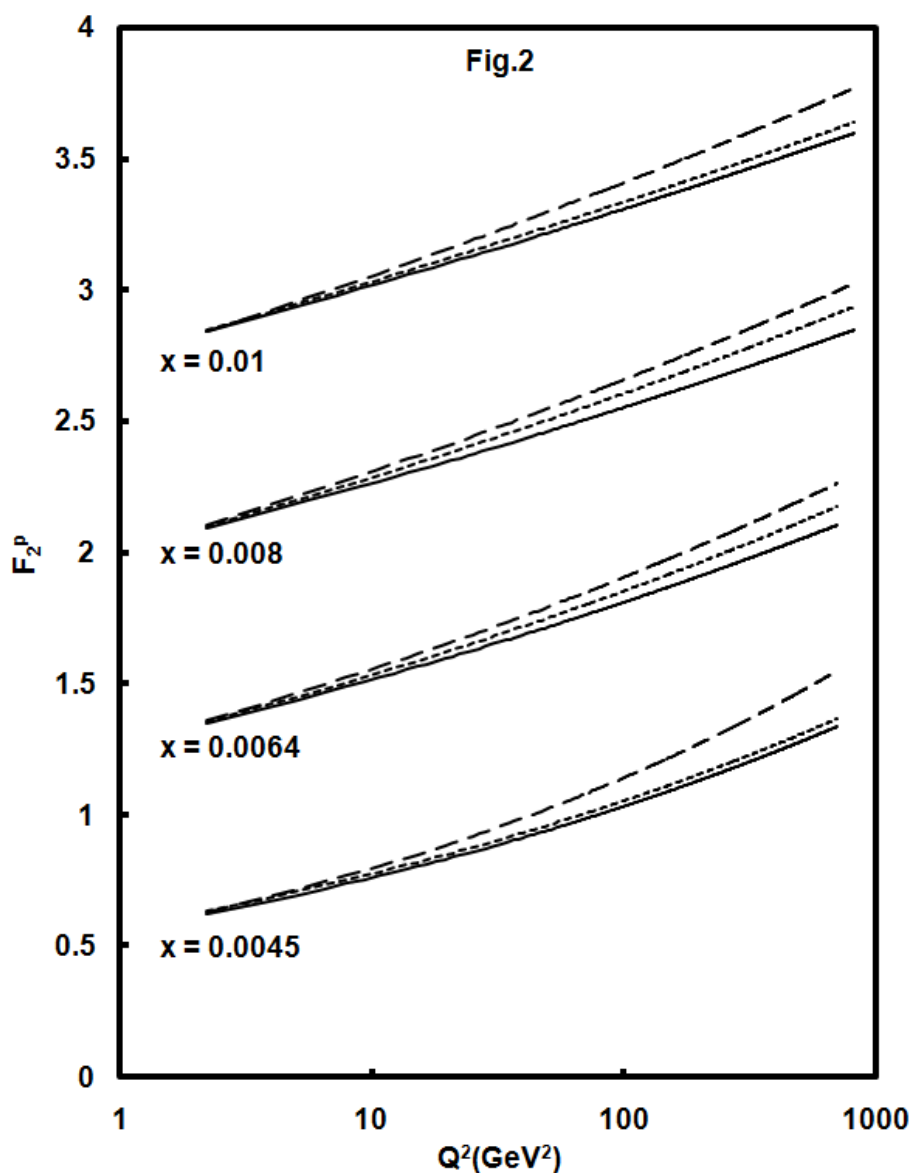
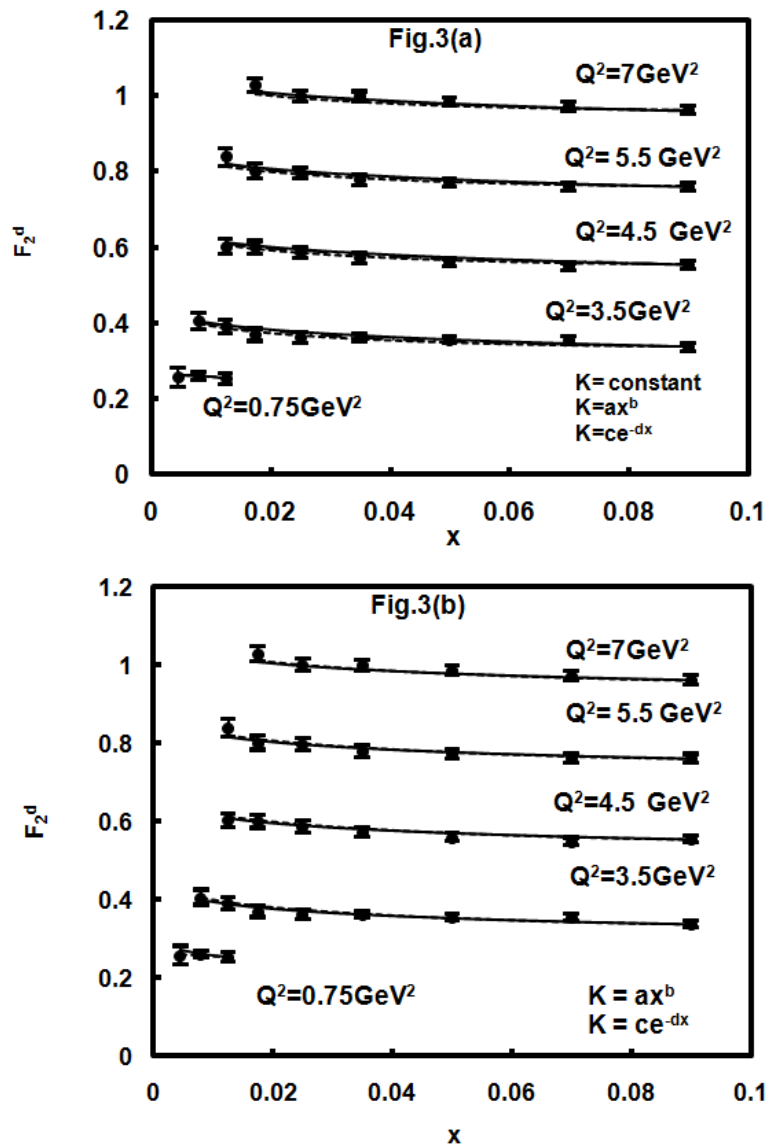


Fig.2: Results of t-evolutions of proton structure functions F_2^p (dashed lines for LO and solid lines for NLO) with recent global parametrization (long dashed lines) for the representative values of x given in the figures. Data points at lowest- Q^2 values in the figures are taken as input. For convenience, value of each data point is increased by adding $0.5i$, where $i = 0, 1, 2, 3, \dots$ are the numberings of curves counting from the bottom of the lowermost curve as the 0-0-th order. Data points at lowest- Q^2 values in the figures are taken as input.

In figs.3(a), 3(b) we present our results of x -distribution of deuteron structure functions F_2^d in LO for $K(x) = \text{constant}$ (solid lines), $K(x) = ax^b$ (dashed lines) and for $K(x) = ce^{-dx}$ (dotted lines), and in NLO for $K(x) = ax^b$ (solid lines) and for $K(x) = ce^{-dx}$ (dashed lines) where a, b, c and d are constants and for representative values of Q^2 given in each figure, and compare them with NMC deuteron low- x low- Q^2 data [10]. In each data point for x -value just below 0.1 has been taken as input $F_2^d(x_0, t)$. In case of LO, if we take $K(x) = 4.5$, then agreement



Figs.3(a) and 3(b): Results of x -distribution of deuteron structure functions F_2^d in LO for $K(x) = \text{constant}$ (solid lines), $K(x) = ax^b$ (dashed lines) and for $K(x) = ce^{-dx}$ (dotted lines), where $K(x) = 4.5$, $a = 4.5$, $b = 0.01$, $c = 5$, $b = 1$ and in NLO for $K(x) = ax^b$ (solid lines), and for $K(x) = ce^{-dx}$ (dotted lines), where $a = 5.5$, $b = 0.016$, $c = 0.28$, and $d = -3.8$ and for representative values of Q^2 given in each figure, and compare them with NMC deuteron low- x low- Q^2 data. In each the data point for x -value just below 0.1 has been taken as input $F_2^d(x_0, t)$. For convenience, value of each data point is increased by adding $0.2i$, where $i = 0, 1, 2, 3, \dots$ are the numberings of curves counting from the bottom of the lowermost curve as the 0-th order.

of the result with experimental data is found to be excellent. On the other hand, if we take $K(x) = ax^b$, then agreement of the results with experimental data is found to be good at $a = 4.5$, $b = 0.01$. Again if we take $K(x) = ce^{-dx}$, then agreement of the results with experimental data is found to be good at $c=5$, $b=1$. For x - evolutions of deuteron structure function, results of unique solutions and results of particular solutions have not any significance difference in LO [1].

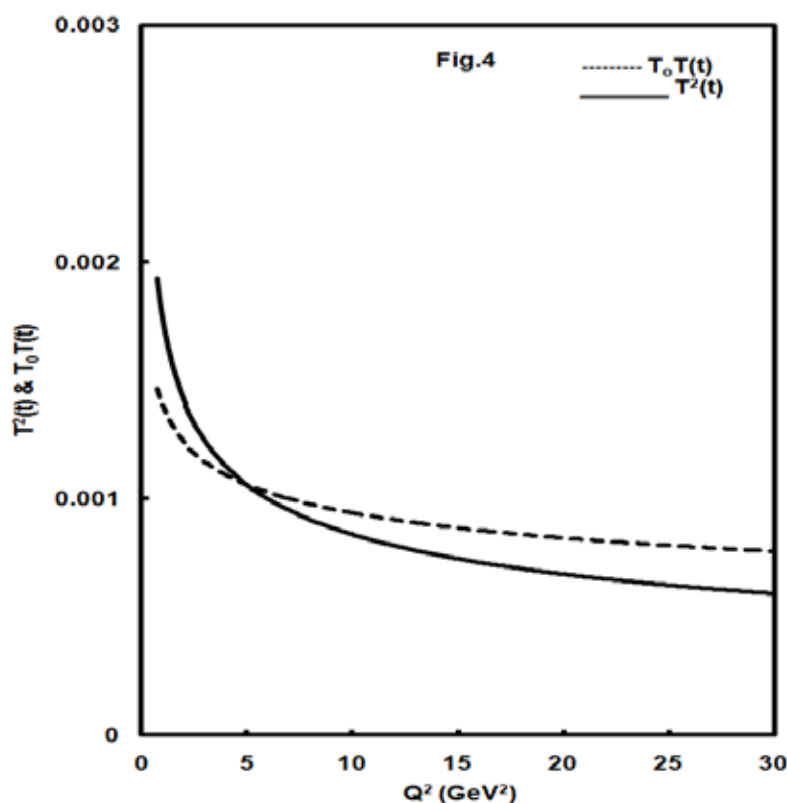


Fig.4: $T(t)^2$ and $T_0 T(t)$, where $T(t) = \alpha_s(t)/2\pi$ against Q^2 in the Q^2 range $0 \leq Q^2 \leq 30 \text{ GeV}^2$.

In case of NLO, if we take $K(x) = ax^b$, then agreement of the result with experimental data is found to be excellent at $a = 5.5$, $b = 0.016$. On the other hand if we take $K(x) = ce^{-dx}$, then agreement of the results with experimental data is found to be good at $c = 0.28$, $d = -3.8$. But agreement of the results with experimental data is found to be very poor for any constant value of $K(x)$. Therefore we do not present our result of x -distribution at $K(x) = \text{constant}$ in NLO.

In fig.4, we plot $T(t)^2$ and $T_0 T(t)$, where $T(t) = \alpha_s(t)/2\pi$ against Q^2 in the Q^2 range $0 \leq Q^2 \leq 30 \text{ GeV}^2$ as required by our data used. Though the explicit value of T_0 is not necessary in calculating t -evolution of, yet we observe that for $T_0 = 0.027$, errors become minimum in the Q^2 range $0 \leq Q^2 \leq 30 \text{ GeV}^2$.

IV. CONCLUSION

We derive t and x -evolutions of various structure functions and compare them with global data and parameterizations with satisfactory phenomenological success. It has been observed that though we have derived a unique t -evolution for deuteron, proton, neutron, difference and ratio of proton and neutron structure functions in LO and NLO, yet we can not establish a completely unique x -evolution for deuteron structure function in LO and NLO due to the relation $K(x)$ between singlet and gluon structure functions. $K(x)$ may be in the forms of a constant, an exponential function or a power function and they can equally produce required x -distribution of deuteron structure functions. But unlike many parameter arbitrary input x -distribution functions generally used in the literature, our method requires only one or two such parameters. On the other hand, our methods are mathematically simpler with less number of approximations. Explicit form of $K(x)$ can actually be obtained only by solving coupled GLDAP evolution equations for singlet and gluon structure functions, and works are going on in this regard.

REFERENCES

- [1] R. Rajkhowa and J. K. Sarma, Indian J. Phys. 78A (3), 367-375 (2004).
- [2] R. Rajkhowa and J. K. Sarma, International Journal of Novel Research in Physics Chemistry & Mathematics Vol. 1, Issue 1, pp: 12-24 (2014); International Journal of Scientific & Engineering Research, vol.4, issue 11, November (2013) 1185.
- [3] R. Rajkhowa, International Journal of Scientific & Research publications, vol.3, issue 11, November (2013) 1; International Journal of Engineering Research & Technology, vol.2, issue 10, oct (2013) 3492.
- [4] R. Rajkhowa and J. K. Sarma, Indian J. Phys. 78 (9), 979-987 (2004)
- [5] R. Rajkhowa and J. K. Sarma, Indian J. Phys. 79(1) (2005) 55-64.
- [6] G. Altarelli and G. Parisi, Nucl. Phys B 126, p298 (1977).
- [7] G. Altarelli, Phy. Rep. 81, p1 (1981).
- [8] V. N. Gribov and L. N. Lipatov, Sov. J. Nucl. Phys. 20, p94 (1975).
- [9] Y. L. Dokshitzer, Sov.Phys. JETP 46, p641 (1977).
- [10] C. Adloff , H1 Collaboration, DESY 98--169, hep-ex/9811013, (1998).
- [11] M. Arneodo, hep/961031,NMC, Nucl.Phys.B.483, p3 (1997).
- [12] A.D. Martin et. al, hep-ph / 0110215 (2001).
- [13] W. Furmanski and R. Petronzio, Nucl. Phys. B 195, p237 (1982).
- [14] W. Furmanski and R. Petronzio, Z. Phys. C11, 293 (1982); Phys. Lett B 97, p437 (1980).
- [15] L. F. Abbott , W.B. Atwood and R.M. Barnett, Phys. Rev. D22 p582 (1980)
- [16] A. Deshamukhya and D. K. Choudhury , Proc. 2nd Regional Conf. Phys. Research in North-East, Guwahati,
- [17] India, October, 2001, p34 (2001).
- [18] S. Gradshteyn and I. M. Ryzhik, 'Tables of Integrals, Series and Products',ed. Alen Jeffrey, Academic
- [19] Press, New York (1965).
- [20] D. K. Choudhury and J. K. Sarma, Pramana-J. Phys. 39, p273(1992).
- [21] J. K. Sarma, D. K. Choudhury, G. K. Medhi, Phys. Lett. B403, p139 (1997).
- [22] J. K. Sarma and B. Das, Phy. Lett. B304, p323 (1993).
- [23] F. Ayres Jr, 'Differential Equations', Schaum's Outline Series, McGraw-Hill (1952).
- [24] F. H. Miller, 'Partial Differential Equation', John and Willey (1960).
- [25] F. Halzen, A. D.Martin, 'Quarks and Leptons: An Introductory Course in Modern Particle Physics', John
- [26] and Wiley (1984).
- [27] B.Badelek et. al, 'Small x physics' DESY 91-124, October 1991 p17 (1991).
- [28] G Grammer and J D Sullivan: in Electromagnetic Interactions of Hadrons, eds A Donnachie and G Shaw,
- [29] Plenum Press, 1978.
- [30] T H Bauer et al.: Rev. Mod. Phys. 50 (1978) 261 and references therein.
- [31] E Reya : Perturbative Quantum Chromodynamics, DESY 79/88, DO-TH 79/20 (1979)
- [32] P.D.B Collins, A.D. Martin, R.H. Dalitz, 'Hadron Interactions', Adam Hilger Ltd., Bristol (1984).

Biographical Notes

Dr. R. Rajkhowa is working as a Assistant Professor in Physics Department, T. H. B College, Jamugurihat, Sonitpur-784189, Assam, India

N J Hazarika is working as a Assistant Professor in Mathematics Department, T. H. B College, Jamugurihat, Sonitpur-784189, Assam, India and presently pursuing Ph. D. from Rajiv Gandhi University, Assam.

MANAGEMENT LESSONS FROM SWACHH BHARAT MISSION

Dr. ShailjaBadra¹, Vivek Sharma²

^{1,2} Assistant Professor, Sheila Raheja School of Business Management & Research, Mumbai (India)

ABSTRACT

The world order is rapidly changing. India is finding itself as an epicenter of development. Cleanliness is the stark reality which the nation cannot ignore any further. Clean initiatives are often seen as a Western way of life. It is therefore important to peep into ancient Indian tradition to find that it was considered next to Godliness. The change happened over the last thousand years when subsequent rulers left the country reeling under poverty, over-population and lack of proper hygiene. Mahatma Gandhi used cleanliness as a potent tool to integrate larger sections of society during the freedom struggle. But Independence came with inherent challenges and contradictions. As successive governments grappled with larger issues of development, the cleanliness agenda took a backseat. Swachh Bharat Mission is not an old ideology in a new frame. It represents the collective aspiration of a nation to transform progress beyond mind and mindset. Swachh Bharat is the brainchild of the new PM and his Central Government. It is set to provide the much needed acceleration to become a developed nation by 2025. In a world where boundaries get blurred with technological advancement, the perception of India as nation committed to cleanliness has to find a substantial number of takers. The reality check shall happen in 2019 when the campaign ends. The issues of good governance and welfare of the people are linked to this clean drive. It is also strong rebuttal to the belief that India is resistant to change. Swachh Bharat is the game changer which tries to pool and integrate every effort under one umbrella. Government agencies, non-profit organizations, community leaders, religious groups, students and children have come together in a unified drive on cleanliness. The gamut of activities taken up by different agencies in the clean drive showcases the diversity of India. This paper attempts to study the impact of the managerial push by the government. It tries to find whether the impact is at many levels. The method used is a structured questionnaire administered to a set of 108 management students.

Keywords: *Clean India, Management Insight, Swachh Bharat Mission*

I. INTRODUCTION

The focus on cleanliness is not new to successive governments. It was Nirmal Bharat Abhiyan which became an integral part of Total Sanitation Campaign (TSC) launched an earlier UPA Government. The aim was to provide universal household sanitation coverage by 2012. It did not create the desired impact even though money poured from government coffers. The Prime Minister led the launch of Swachh Bharat Mission on Mahatma Gandhi's birthday (October 2, 2014) He quoted the words of M.K. Gandhi "Sanitation is more important than Independence." The impact was bound to be immediate. The plans are ambitious and the scale of the cleanliness mission is huge. Out of 2.00 lakh crores to be spent over next five years, the urban part would be 62009 crores. The bigger allocation of Rupees 1.34 lakh crores would be the rural component. The effort is to transform

sanitation in these areas by constructing 11.11 crore toilets, eliminate manual scavenging and sensitizing rural folks to the benefits of living healthier lives, reducing disease and death which arises out of bad management of solid waste. In a country where pilferage of funds is an accepted way of life, the effort is to account for every rupee spent in the Swachh Bharat Mission. India has the dubious distinction of being a leader in bad sanitation practices. The scourge of manual scavenging is a blot in the process of a country trying to find a place among developed nations. The experiences of developed countries in solid waste management are many and varied. Even in metropolitan areas, the segregation of garbage, the disposal of wet and dry waste is far from the minimal accepted standards worldwide. Government estimate pin it around 6500 per person per year to provide a clean neighborhood. The move of the Government has caught the imagination of different agencies, private firms, multinationals and Indian companies, and their involvement is increasing with every passing day. The Government of Maharashtra decided that each college adopts one village in the state. National Service Scheme volunteers would actively participate in cleanliness. However, it is the citizen involvement which makes any initiative successful. Early reports have suggested that people involvement is high. It is an area of tremendous interest whether it can integrate the efforts of State governments, NGO's and multinationals into the mission.

II. LITERATURE REVIEW

The endeavor of the Government is to turn it into a mass movement requiring not just toilets, but also a change in behavior and mindsets of people (The Hindu, October 4, 2014)

Expatriates are getting involved in the campaign. In South Africa, the Indian community decided to support small neighborhood projects, placing garbage where it is required, promotion and separation of waste (The Times of India, December 6' 2014) According to Government estimates, urban India generates 68.8 million tonnes of solid waste per year (1.88 lakh tonnes everyday) It is estimated to touch 160 million tonnes by 2041. One-third of the garbage in urban areas is untreated. About 14 million tonnes is left to rot. The problem is compounded by about 38 billion litres of sewage generated everyday in 498 Tier I cities (2009 figures). Out of this, 26 billion is left in the open untreated. Rural India generates 0.4 million tonnes of solid waste. According to a UN report, India leads the world in open defecation. 68% rural households are without toilets. 88% of disease in rural India is due to lack of clean water, sanitation and solid waste management. The drive shall use 1.34 lakh crores to construct 11.11 crore toilets. It is proposed that all 2.47 lakh panchayats will be given 20 lakh each over the next five year period to maintain clean surroundings. The alignment towards the Campaign drive is gaining steam. In a major policy shift, the Chief Minister of Maharashtra launched "Munjian"- a cleanliness initiative that involves all the 18 Universities and its affiliated colleges. Each college shall adopt one village where National Service Scheme volunteers would actively participate in cleanliness drive. The move made University of Mumbai the first in the country to align itself with the mission. (The Times of India, 4th December, 2014) International studies have tried to understand the effect of cleanliness on natural and man-made environment. Micheal A. Berry found that air, water, land and energy have to be kept clean. His research found that humans manage their life by managing the environment. The Partnership for Clean Air Inc. (PLC) in Philippines found that when institutions come together, they play a big role in cleaning air of pollutants. It suggested governments to keep a check on pollutants in the air. Many countries including India & China are actively involved in the movement. A research done at University of Ontario found that traditional cleaning chemicals have given way to new products

III. PROBLEM STATEMENT

The focus on cleanliness is the pressing issue as India tries to moves from developing to developed nation. Managerial focus and clinical execution are key drivers to the cleanliness drive. This study focuses on the issue of cleanliness in modern India.

IV. OBJECTIVES

1. To understand the managerial implications of Swachh Bharat Campaign.
2. To find the current level of respondent participation in the cleanliness initiative.
3. To suggest measures that increase participation & effectiveness of Swachh Bharat drive.

V. HYPOTHESIS

The proposed research has following set hypothesis

H₁: Swachh Bharat campaign shall impact cleanliness in India.

H₂: Swachh Bharat campaign would help to increase people participation in the clean drive.

VI. METHODOLOGY

- a) **TOOLS:** Qualitative as well as quantitative method of data collection was used. Analysis was done using structured Questionnaire method to conclude the paper.
- b) **Sample Size:** 108 respondents
- c) **Sampling Method:** Random Sampling
- d) **Sampling Place:** Mumbai, Maharashtra (India)

VII. ANALYSIS AND INTERPRETATION OF DATA

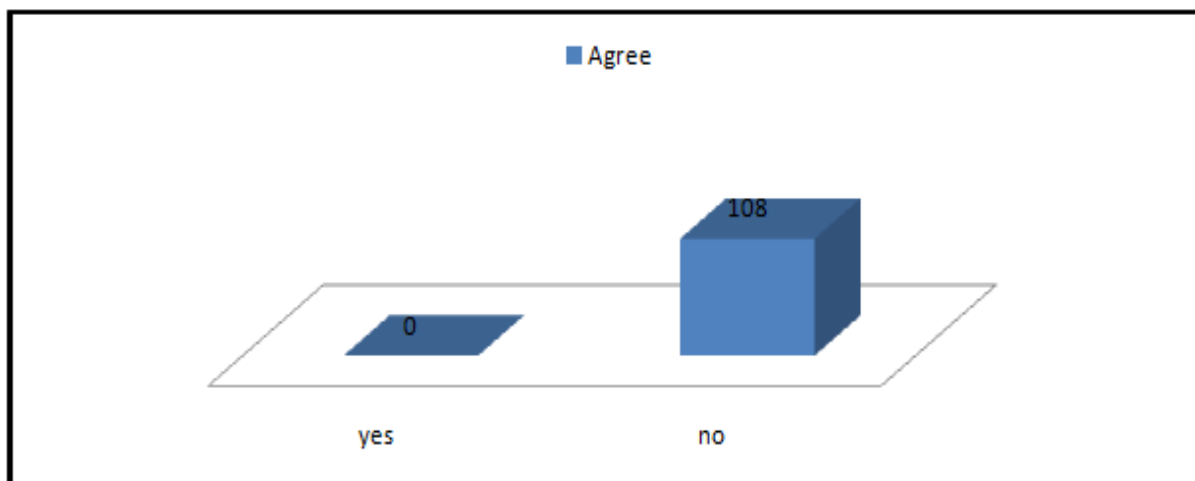


Fig. 1: Respondents Perception on the City Cleanliness Initiative

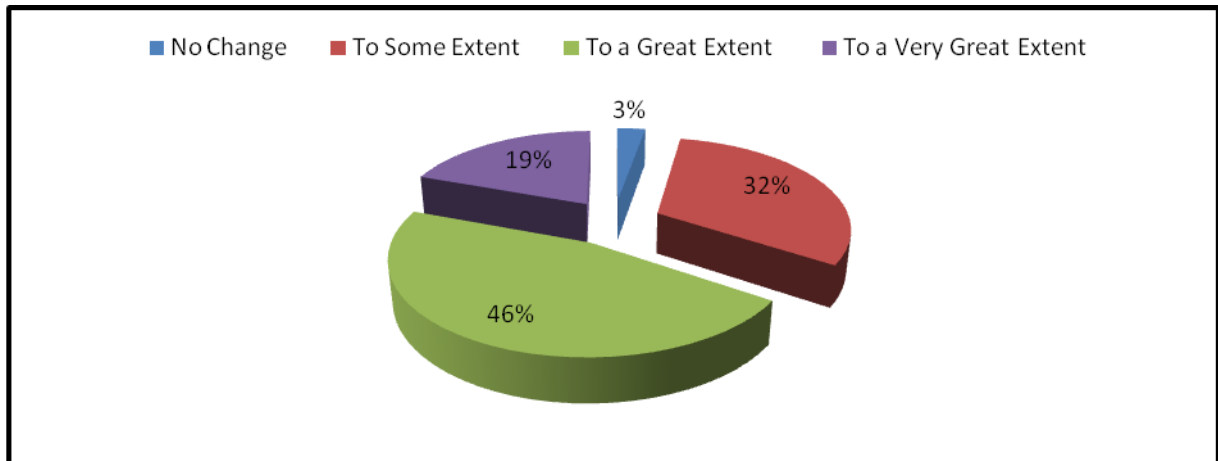


Fig. 2: Impact of Swachh Bharat Campaign on Management Students Perception about Cleanliness

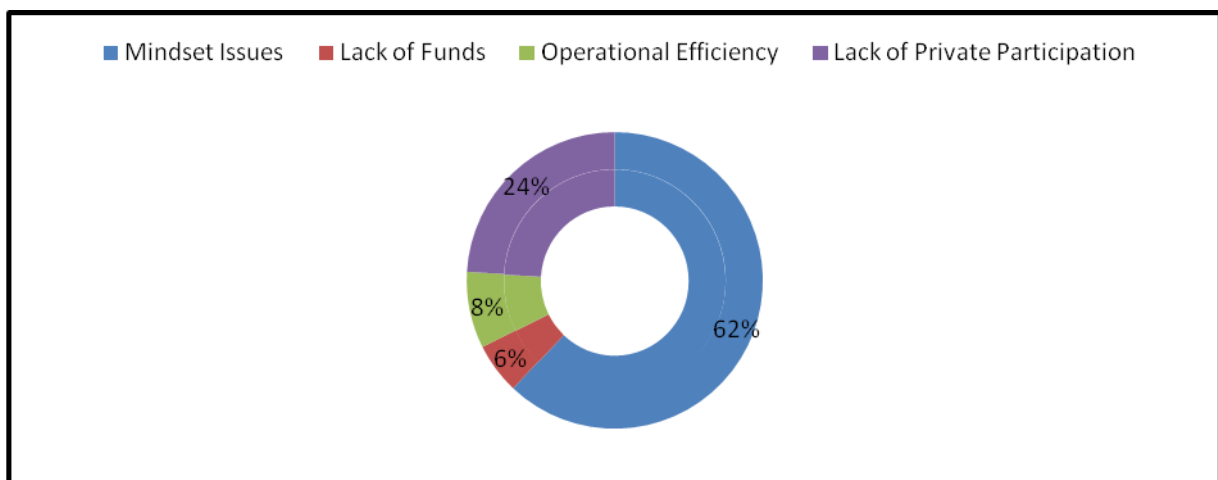


Fig. 3: Problems in Implementing Swachh Bharat Campaign

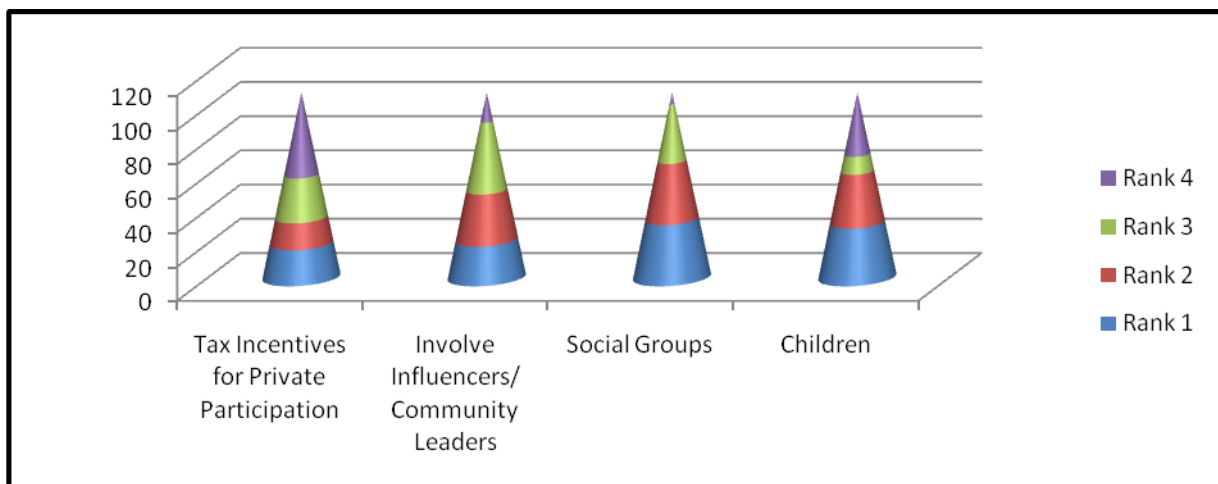


Fig. 4: Factor Contributing to the Cleanliness Drive in the Order of Preference

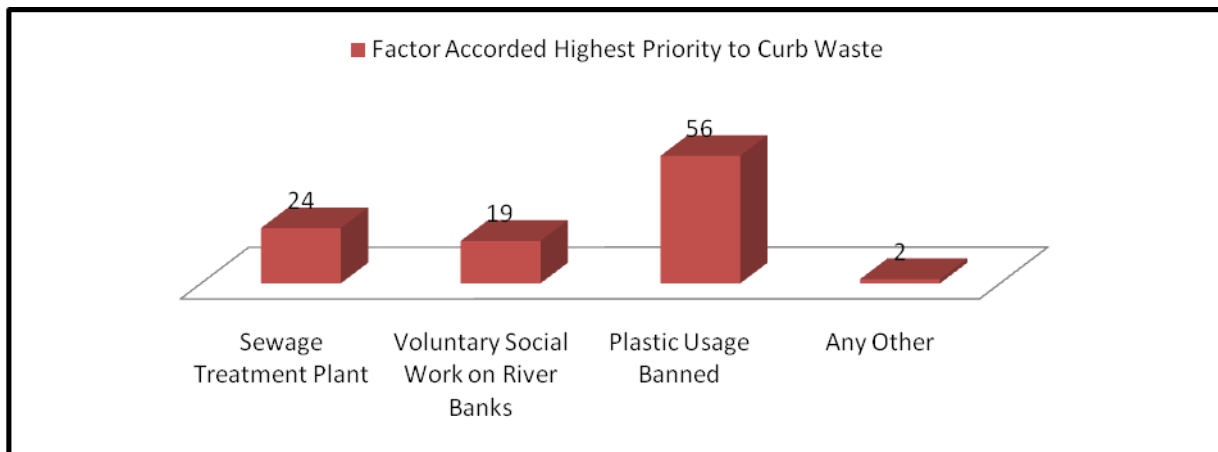


Fig. 5: Factors Accorded Highest Priority to Help Curb Waste in Your City

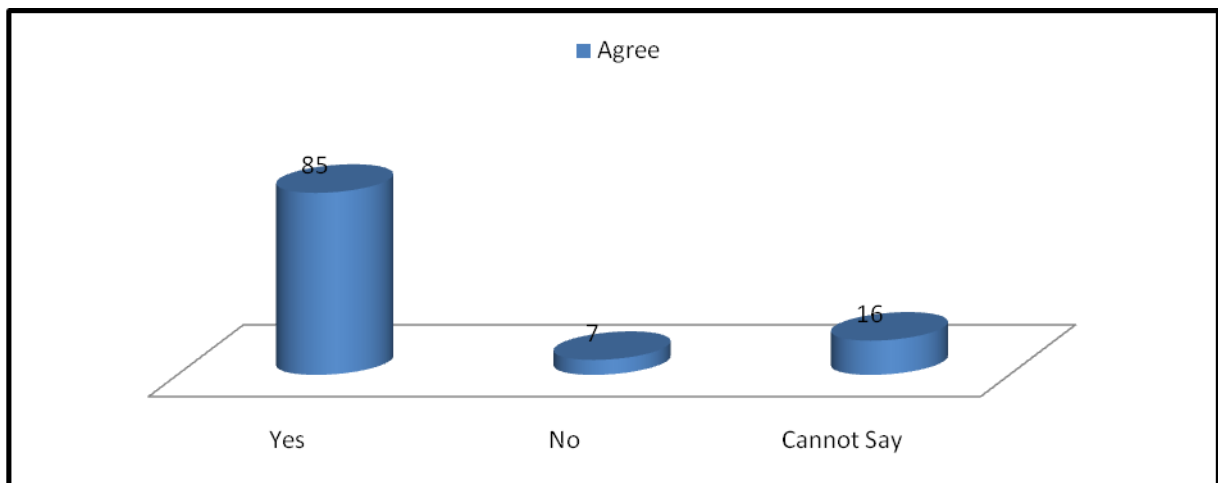


Fig. 6: Effect of Swachh Bharat Campaign to Change the Indian Perception of Cleanliness in the Eyes of the Western World

Fig. 1 above reveals that all the 108 management trainees agreed that keeping public places clean is as much as their duty as keeping their houses clean. The overwhelming majority of management students also believe that Swachh Bharat campaign has changed their perception about cleanliness. However very few (3%) of them considered it to be one of the events which resulted in no change as shown in Fig. 2. Thus, Hypothesis **H₁**: Swachh Bharat campaign shall impact cleanliness in India **holds TRUE**. Majority (62%) of the management students believe that cleaning is the job of specific class of people. It is the biggest problem in implementing the cleanliness campaign. Lack of private participation (24%) is considered to be the second big problem in the cleanliness drive followed by operational efficiency (8%) and lack of funds as represented by Fig. 3.

Fig. 4 shows that social groups are accorded the highest preference, followed by involving & educating children, involving community leaders and influencers and tax incentives for private participation respectively for garnering mass support for the campaign. Hypothesis **H₂**: Swachh Bharat campaign would help to increase people participation in the clean drive **holds TRUE**.

Majority of the management students (Fig. 5) felt that there should be a ban on plastic usage. Sewage treatment was accorded the second place, followed by voluntary social work on river banks. The avoidance of tobacco, garbage maintenance by municipal corporation and strict fine for habitual offenders especially in public places,

were also mentioned by few management trainees as few other initiatives. Management students felt that corporates should also take up few initiatives to promote and strengthen Swachh Bharat Campaign such as creating social awareness; various seminars, workshops, awards, marathon and campaigns in societies, colleges and schools; controlling level of pollution through curbing Industrial waste; incentives and recognition for employee participation in cleanliness drive.

Fig. 6 depicts majority (85%) of the management students were of the view that Swachh Bharat campaign would change the perception of cleanliness in the eyes of the western world. Few (16) said that it is too early to say if there would be any change. They believed that such campaigns need to be on continuous basis to stir the soul of each and every individual to create the impact.

VIII. CONCLUSIONS

The managerial focus on Swachh Bharat campaign attempts to gauge the mood of the country. The campaign brings focus to the pressing transformational need of the nation. The change is perceptible as India embarks on its journey to create a clean and hygienic environment. But orthodox mindset is a hindrance to the drive. Cleanliness is still considered a job performed by a specific set of persons. The alignment of children and youth in such campaigns creates a ripple effect. Teamwork and patriotism are value which the Government wishes to inculcate among students. The findings are in consonance with Maharashtra Government plan to inculcate feelings of patriotism through adoption of one village by every college affiliated to 18 Universities of the state. The ideamooted to devote 100 hours per person per year on cleanliness is an extension of the same premise. Initiatives from campus to corporate is a welcome step. Management trainees today are future corporate leaders. It is important to sensitize them during their two year management course. Indian companies and multinationals are more forthcoming. The effort has begun to make a difference. It is common knowledge that many companies have pledged support in the cause of rural sanitation. Many brainstorming sessions in boardrooms have moved to the next level of implementation. They are generating excitement and funding. Segregation of wet and dry waste is a step forward. Solid waste management will have to be streamlined to make it as effective as in developed countries. Voluntary social work on river banks is worth considering in the light of the assertion that they have become a major hazard for clean environment. Sewage and other waste are dumped in rivers causing irreparable damage to riverbeds, fishes and life in water. Respondents advocated a ban on plastic. It has been the view of many that ban is not a piecemeal initiative. It requires a comprehensive amendment and rigorous penalties. It shall require a shift in public policy. The move will help the management of non-biodegradable waste better. Pollution by way of burning plastic or leaving it untreated requires attention to make cleanliness drive successful. Teamwork and patriotism are values which the Government wishes to inculcate among students and ordinary citizens. The active involvement of celebrities in neighborhood initiatives lends credence to the drive. Youngsters are sensitized to the benefits of course correction on cleanliness. The biggest beneficiary is Brand India. And the ripple effect is strong. The campaign unifies people from diverse backgrounds, uses raw energy and technology. This paper found results on similar lines as Government approach on cleanliness.

IX. SUGGESTIONS

- I. It is important to create a fund for Swachh Bharat campaign as the movement gains steam. Indian and multinational companies, government departments and not for profit organizations can pool resources for the movement.

- II. Tax breaks and financial incentive to organizations working closely with the campaign is needed. It shall help the campaign to gain critical volume with the inflow of big contributions.
- III. Industry can help by apportioning a small portion of profit for Swachh Bharat Campaign. It may be similar to P&G support on every product sold.
- IV. Asian countries and Europe levy strict monetary fine to perpetual offenders. India can take a cue from the West while implementing the law.
- V. Acceptance to change is easier when presented in short films and street plays. Mass movements begin with genuine and honest efforts in this direction.
- VI. It is critical to bring behavioral changes in people regarding healthy sanitation practices.
- VII. The role of local bodies to design, execute and operate robust system on managing waste is pivotal. It is therefore necessary to strengthen their hands with key initiatives.
- VIII. It is important for the incumbent government to encourage public-private participation to give an impetus to the movement.
- IX. The drive on Swachh Bharat Campaign can be linked to CSR initiatives.
- X. Social media platforms can exchange ideas and share pictures of collective efforts.
- XI. The role of emerging technologies is vital to a managerial focus.

X. LIMITATIONS OF THE RESEARCH

The research was limited to the island city of Mumbai. Another perspective could be added by expanding the study beyond the students of management. A logical extension could be including the views of a cross section of society.

XI. SCOPE FOR FUTURE STUDY

The campaign can become effective with the involvement of masses in Tier I, Tier II and Tier III cities. Rural folks and their contribution to the process of change is important. The problems present a big opportunity for experts from industry to make a difference and help the Government stay its trajectory in Swachh Bharat Mission. The role of media as a catalyst for change is the scope of another interesting research.

REFERENCES

- [1] Kotler, Philip (2013), Marketing Management, Pearson Publication, 13 Edition, Page 77-78
- [2] Chatterji, Madhumita, Corporate Social Responsibility, Oxford University Press, Page 271-275
- [3] Jadhav, H.V., Advanced Environmental Management, Himalaya Publishing House, Page 1-18

Biographical Notes

Dr. Shailja Badra is Ph.D. (Education) from Himachal Pradesh University, Shimla and Masters in Financial Management from Jannalal Bajaj Institute of Management Studies, Mumbai (India).

She has worked as Curriculum Developer for Pre-school Children and Teachers for the past 10 years and currently working as Assistant Professor.

Prof. Vivek Sharma is M.Statistics (Gold Medalist) from Allahabad University, Allahabad and MBA(Marketing) from G.G.D. Central University, Bilaspur (India).

He has 17 years of experience in Banking and Financial Services Insurance Sector and currently working as Assistant Professor.

LONG TERM HYDROLOGICAL SIMULATION MODELLING BASED ON PHYSICAL CHARACTERISTICS OF WATERSHED

Dilip G. Durbude¹, B. B. Jadia², R. S. Sontakke³

¹Associate Professor, Engineering Faculty, WALMI, Aurangabad, (India)

²Professor and Head, IWDM Faculty, WALMI, Aurangabad, (India)

³Joint Director and S. E., WALMI, Aurangabad, (India)

ABSTRACT

The physical characteristics of watershed play a vital role in generating runoff and significantly affect the hydrological behavior of the watershed. The future performance of this hydrological behavior of watershed can be predicted by conceptually modelling. But, in the conceptual rainfall-runoff modelling, finding the value of conceptual model parameters is a challenging task particularly in ungauged basins or basins where very less measurements are available. Hence, it has been the endeavor of many hydrologists to quantify and relate geomorphological characteristics of ungauged watersheds to their hydrologic response characteristics. Very recently developed Jain et al.(2012) Modified Long Term Hydrologic Simulation Advance Soil Moisture Accounting (MLTHS ASMA) 15-parameters model performed better than the existing LTHS models to simulate total stream flow, but for its pragmatic application, it is required to correlate model parameters with some measurable physical characteristics of the watersheds. Therefore, in the present study, the measurable physical characteristics of the seventeen watersheds lying in various agro-climatic zones of India are correlated with model parameters using step-wise backward elimination procedure via p-value of F-statistic of multiple regression analysis. In the majority cases of the watershed under study, the model parameters exhibited a significant relationship with physical characteristics of the watersheds.

Keywords: Advance Soil Moisture Accounting, Geomorphological Characteristics, Hydrologic Modeling, Runoff, Watershed.

I. INTRODUCTION

The conceptual rainfall-runoff models generally involves certain parameters relating to watershed characteristics such as size, shape, orientation, topography, geology, geomorphology, land use and soil characteristics etc. play very important role in generating runoff and affect significantly the hydrological response of a watershed. Finding the value of these parameters is a challenging task particularly in ungauged basins or basins where very less measurements are available. Hence, it has been the endeavor of many hydrologists to quantify and relate geomorphological parameters of these watersheds to their hydrologic response characteristics (Chandra, 1993). As such, Horton (1945) pioneered the hydro-geomorphologic analysis of watershed and provided a rational and systematic base, rather a framework of outlines of geomorphological characteristics to relate them to various hydrological properties of the watershed. Strahler's (1952) modification of this technique has generally been adopted for use in hydrologic study. Potter (1953) and Benson (1962) related peak discharge to watershed area, a

topographical factor, and a rainfall frequency factor. Boyd (1978) developed a conceptual model using watershed geomorphological properties. Using a probabilistic framework, Rodriguez-Iturbe and Valdes (1979) and Gupta et al. (1980) presented a geomorphological instantaneous unit hydrograph with the exponential probability distribution for the time of travel of water drops which is essentially equivalent to using a linear reservoir. Rosso (1984) derived the Nash IUH parameters as functions of Horton's ratios. Hydro-geomorphological analysis was carried out in a number of Indian watersheds to compute the runoff in water resources development and management projects (Roohani and Gupta, 1988; Karnieli et al. (1994); Chalam et al., 1996; Chaudhary and Sharma, 1998; Hsieh and Wang (1999); Kumar et al., 2001; Ali and Singh, 2002; Durbude and Kumar, 2002; Durbude (2004); Singh et al., 2003; Suresh et al., 2004; Durbude, 2005; Durbude and Chandramohan, 2007; Dabral and Pandey, 2007; etc.).

A general fact is that the model containing too many parameters for simulation of limited components of hydrological processes exhibit difficulty in field applications. Usability of a model can be enhanced if its parameters can be related to measurable catchment characteristics. The physical characteristics of the watersheds which are measurable entities and influencing the runoff characteristics of watershed can be correlated with the model parameters by means of some techniques such as regression analysis. In regression analysis, investigations are made to relate dependent variable (Y) for example model parameters to independent predictors (Xs) such as physical characteristics of watershed. It can be used for modeling causal relationships between model parameters and physical characteristics of watershed.

Therefore, in the present study, parameters of the recently developed long term hydrological simulation Jain et al. (2012) MLTHS ASMA model is correlated with the measurable physical characteristics of the watershed by using the multiple regression technique.

II. MATERIAL AND METHODS

2.1 Existing MLTHS ASMA Model

The existing MLTHS ASMA model proposed by Jain et al. (2012) is primarily based on the physical concepts that describe water movement through a watershed; the total runoff of the catchment is quantified by incorporating sub-modules for direct surface runoff, lateral flow, and base flow. The accounting for soil moisture and ground water store is considered on daily basis. The initial soil moisture store level is used to calculate the space available for water retention, which is updated on daily basis using evapotranspiration, drainage from soil moisture store and level of soil moisture. Direct surface runoff is computed using modified formulation of the Soil Conservation Service Curve Number (SCS-CN) method given by Michel et al. (2005) and Durbude et al. (2011). The sub-surface drainage flow is modeled using the formulations based on concepts given by Yuan et al. (2001) for computation of the sub-surface drainage flow (Jain et al., 2012). Jain et al. (2012) MLTHS ASMA model uses the ASMA procedure both for surface and sub-surface flow components by formulating sub-surface drainage flow component based on the modification in SCS-CN method through theoretical analogy. As this model operates on daily time step, it requires daily rainfall as input and the observed runoff is used only to calibrate parameters of the model and its validation.

The mathematical formulations for computation of the surface flow and sub-surface flow components and losses (such as evapotranspiration and deep percolation) involved in the MLTHS ASMA (Jain et al., 2012) model are again reproduced here, as follows.

2.1.1 Surface Flow Components

The surface flow, which occurs only when the rainfall rate is greater than the rate of infiltration. It is modeled using the ASMA procedure proposed by Durbude et al. (2011), in which soil moisture store at time t is computed by using equation 1 as (Michel et al., 2005);

$$V_t = V_{0(t)} + P_t - RO_t \quad (1)$$

where $V_{0(t)}$ is initial soil moisture store level (mm) at time ' t ', P_t is accumulated rainfall at time ' t ' along a storm (mm), RO_t is direct runoff at time ' t ' along a storm (mm), and V_t is soil moisture store level at time ' t ', i.e. when the accumulated rainfall is equal to P_t (mm).

The direct surface runoff (RO), a component of surface flow can be computed based on AM (Durbude et al., 2011) as;

$$\text{If } V_{0(t)} \leq S_{a(t)} - P_t, \text{ then } RO_t = 0 \quad (2)$$

If $S_{a(t)} - P_t < V_{0(t)} < S_{a(t)}$, then

$$RO_t = \frac{(P_t + V_{0(t)} - S_{a(t)})^2}{P_t + V_{0(t)} - S_{a(t)} + SM_t} \quad (3)$$

If $S_{a(t)} \leq V_{0(t)} \leq S_{a(t)} + SM_t$, then

$$RO_t = P_t - \frac{(SM_t + S_{a(t)} - V_{0(t)})^2}{SM_t^2 + (SM_t + S_{a(t)} - V_{0(t)})P_t} \quad (4)$$

In this model, it was assumed that the current space available for water retention (S_t) is constant for the first 5 days of simulation. The value of S_t for the first day of simulation ($S_t=S_0$) is computed from Eq. (5) by using the initial value of CN (i.e. CN_0 to be determine by optimization). Afterwards, S_t is modified based on antecedent moisture (AM) into modified water retention (SM_t) to avoid the sudden variation in the daily curve number that may affect the performance of model (Geetha et al., 2007; Durbude et al., 2011) as follows;

$$SM_t = \frac{(S_t)^2}{(AM_t + S_t)} \quad (5)$$

Where AM can be computed using the following expression.

$$AM_t = \delta \sqrt{P_{5(t)}} \quad (6)$$

Here $P_{5(t)}$ is the 5 days antecedent rainfall at time ' t ' and δ is the coefficient of antecedent moisture to be determined by optimization.

The next parameter S_a (Eqs.7-9) is set as a fraction of S (as per the Michel et al., 2005), as follows;

$$S_{a(t)} = \alpha S_t \quad (7)$$

Where α is a parameter (fraction) of S_a , which is treated as calibration parameter and obtained through optimization.

Similarly, the initial soil moisture store level (V_0) can be computed as follows (Durbude et al., 2011);

$$\text{If } V_{0(t)} \leq S_{a(t)} - P_{5(t)}, \text{ then}$$

$$V_{0(t)} = V_{00(t)} + \beta (P_5)_t \quad (8)$$

If $S_{a(t)} - P_{5(t)} < V_{00(t)} < S_{a(t)}$, then

$$V_{0(t)} = V_{00(t)} + \beta \frac{(P_{5(t)} + V_{00(t)} - S_{a(t)})^2}{P_{5(t)} + V_{00(t)} - S_{a(t)} + SM_t} \quad (9)$$

If $S_{a(t)} \leq V_{00(t)} \leq S_{a(t)} + SM_t$, then

$$V_{0(t)} = V_{00(t)} + \beta \frac{(SM_t + S_{a(t)} - V_{00(t)})^2}{SM_t^2 + (SM_t + S_{a(t)} - V_{00(t)})P_{5(t)}} \quad (10)$$

Where β is a model parameter obtained through optimization, and V_{00} is pre-antecedent moisture level defined as (Durbude et al., 2011)

$$V_{00(t)} = \gamma SM_t \quad (11)$$

Here γ ranges from 0.0 to 1.0 and can be obtained by optimization.

2.1.2 Routing of Direct Runoff

The direct surface runoff RO_t (Eqs. 7-9) is routed using a single linear reservoir to produce the surface runoff (SRO_t) at the outlet of the basin after the number of days exceeds 5 (Nash, 1957) to account for catchment induced storage effects as follows;

$$SRO_t = C_0 \cdot RO_t + C_1 \cdot RO_{(t-1)} + C_2 \cdot SRO_{(t-1)} \quad (12)$$

Where

$$C_0 = \frac{(1/K)}{2 + (1/K)} \quad (13)$$

$$C_1 = C_0 \quad (14)$$

$$C_2 = \frac{2 - (1/K)}{2 + (1/K)} \quad (15)$$

K is the storage coefficient determined from optimization. In linear reservoir routing, the amount of attenuation is a function of $\Delta t/K$. Values of $\Delta t/K$ greater than 2 can lead to negative attenuation, therefore due care was taken during optimization to restrict value of $\Delta t/K$ to not to exceed 2.

2.1.3 Evapotranspiration

Evapotranspiration (ET) is the amount of water that goes back or lost to the atmosphere. It is the combination of evaporation from the soil surface and transpiration from the vegetation and can be obtained by the summation of daily evaporation from the water bodies and transpiration from the soil zone in the watershed. Since, in the evapotranspiration process, the transpiration process is more dominant than evaporation process, hence, the evapotranspiration is assumed equivalent with transpiration and expressed as follows:

$$ET_t = P_1 \cdot (\theta_t - \theta_w) \quad (16)$$

Where P_1 =coefficient of transpiration from soil zone, θ_t = soil moisture at time 't', θ_w = wilting point of the soil.

2.1.4 Sub-Surface Flow Components

Sub-surface flow occurs beneath the ground surface, when infiltrated rainfall meets an underground zone of low transmission and travels above the zone to the soil surface downhill, and appears as a seep or spring. In this

model, the expression for sub-surface drainage flow (DR_t) at time 't' is derived based on theoretical analogy (Yuan et al., 2001) as follows;

$$DR_t = \frac{(P_t - (S_{a(t)} - V_{0(t)}) - SRO_t - I_{d(t)})^2}{(P_t - (S_{a(t)} - V_{0(t)}) - SRO_t - I_{d(t)} + S_{d(t)})} \quad (17)$$

The Eq. (22) is valid for $(P_t - S_{a(t)} + V_{0(t)} - SRO_t) \geq I_{d(t)}$; $DR_t = 0$, otherwise. Here,

$$I_{d(t)} = \lambda_d \cdot S_{d(t)} \quad (18)$$

$$S_{d(t)} = \frac{25400}{CN_{d(t)}} - 254 \quad (19)$$

I_d is initial abstraction in saturated zone at time 't'; λ_d is coefficient of initial abstraction in saturated zone (I_d); $S_{d(t)}$ is potential maximum retention in saturated zone at time 't'; and $CN_{d(t)}$ is curve number for sub-surface (drainage) flow at time 't'.

The sub-surface drainage flow is further partitioned into two components: (i) sub-surface drainage flow in lateral direction as lateral flow and (ii) sub-surface drainage flow in vertical direction as percolation into ground water zone.

2.1.4.1 Lateral Flow

Fraction of sub-surface drainage flow moving in lateral direction (Putty and Prasad, 1994, 2000) is given as:

$$THR_t = P_3 \cdot DR_t \quad (20)$$

Where THR_t is lateral flow at time 't' and P_3 is unsaturated soil zone runoff coefficient.

The remaining portion of sub-surface drainage flow moving in the vertical direction to meets the ground water store (GWS) due to the permeability of the soil is considered as percolation and modeled as follows (Mishra et al., 2005, Putty and Prasad, 1994, 2000):

$$PR_t = (1 - P_3) \cdot DR_t \quad (21)$$

Where PR_t = percolation at time 't'.

The saturated store GWS is considered as a non-linear reservoir from which the outflow occurs at an exponential rate in the form of deep seepage as follows:

$$DSP_t = (y_t - y_f)^{E_g} \quad (22)$$

Where DSP_t = deep seepage at time 't', y_t = ground water at time 't', y_f = field capacity of the soil in the ground water zone and E_g = exponent of ground water zone

The deep seepage which travels in lateral as well as vertical direction through GWS is further bifurcated into active ground water flow (base flow) and inactive ground water flow (deep percolation) into the aquifers.

2.1.4.2 Base Flow

The base flow (BF_t) or delayed flow, which is an active ground water flow, is modeled as outflow from a non-linear storage as follows:

$$BF_t = P_4 \cdot DSP_t \quad (23)$$

Where P_4 =ground water zone runoff coefficient.

The inactive sub-surface flow into aquifers is termed as deep percolation and occurs from the saturated ground water zone in vertical direction, and is considered as a loss from the saturated store which is modeled as:

$$DPR_t = (1 - P_4) \cdot DSP_t \quad (24)$$

Where DPR_t = deep percolation at any time 't' and P_4 = ground water zone runoff coefficient. Here, it is worth emphasizing that the proposed model considers deep seepage which is partitioned into two components, base flow and deep percolation.

2.1.5 Total Stream Flow

The total stream flow (TRO_t) at time 't', is the sum of the surface runoff, lateral flow, and base flow (Eqs. 4, 17, 25, and 28).

$$TRO_t = RO_t + THR_t + BF_t \quad \text{if } t \leq 5 \text{ days} \quad (25)$$

$$TRO_t = SRO_t + THR_t + BF_t \quad \text{if } t > 5 \text{ days} \quad (26)$$

The daily water balance can be maintained by daily water retention storage or soil moisture budgeting from both the SMS and GWS by defining the lower and upper limits of wilting point and field capacity of the soil. The current space available for retention of water S_t in unsaturated zone and $S_{d(t)}$ in saturated zone is upgraded on daily basis by taking into account the changes in SMS and GWS as:

$$S_{t+1} = S_t + q_t - q_{(t+1)} + y_t - y_{(t+1)} \quad (27)$$

$$S_{d(t+1)} = S_{d(t)} + q_t - q_{(t+1)} + y_t - y_{(t+1)} \quad (28)$$

were, $S_{(t+1)}$ is the next day's potential maximum retention (mm); $S_{d(t+1)}$ is the next day's potential maximum retention (mm) in saturated zone; $q_{(t+1)}$ is the next day's soil moisture (mm); $y_{(t+1)}$ is the next day's ground water (mm). The soil moisture store (SMS) and ground water store (GWS) are upgraded on daily basis as:

$$q_{(t+1)} = q_t + V_t - V_{0(t)} - ET_t - DR_t \quad (29)$$

$$y_{(t+1)} = y_t + PR_t - BF_{(t)} - DPR_t \quad (30)$$

2.2 Multiple Regression Technique

In the multiple regression, the multiple correlation coefficient (R) is Pearson's product moment correlation between the predicted values (Y') and the observed values (Y). Just as coefficient of determination (r^2) is the proportion of the total variance (s^2) of Y that can be explained by the linear regression of Y on X, R^2 is the proportion of the variance explained by multiple regressions. The significance of R can be tested by the F-statistic of the analysis of variance for the regression. The basic idea is to select the most significant regression equation, which corresponds to the minimum p-value of F-test. In regression analysis, selecting variables is very important. As a matter of fact, the first problem that has to be solved in practice is to determine which variables should be included in the model. Obviously, the goodness of regression model depends on the selection of variables. How to select variables that can yield the best regression equation? Aitkin (1974) defined a class of "adequate" regression equations, characterized by a lower bound on the multiple correlation coefficients. Here "adequate" means that each member of the class is not significantly poorer than the complete equation. As Aitkin pointed out, this does not solve the problem of finding the "best" equation for prediction. Besides, Spjotvoll (1972) constructed a multiple comparison method, which usually gives a set of many equations none of which is significantly better than any other. Many criteria have been presented by Draper and Smith (1981) for the selection of the "best" regression equation, but none of these has been considered as the best one. Using different criteria, one gets different (the "best") regression equations. Among these criteria are residual mean square (s^2), adjusted multiple correlation coefficient (R), Cp-statistic (Mallows, 1964) and so on. In order to develop a good model based on these criteria, it is necessary to select the best subset.

2.2.1 Best Subset Selection

A problem arises frequently in multiple regression analysis how to predict the value of a dependent variable when there are a number of variables available to choose as independent variables. Though the high speed of modern algorithms is available to perform the multiple linear regression calculations, it is tempting to select a subset instead of just using all the variables in the model. It is always better to make predictions with models that do not include irrelevant variables. Dropping independent variables that have small (non-zero) coefficients will improve the predictions as it will reduce the mean square error (MSE). Hence, there is a need for selecting subset of the independent parameters to correlate with the dependant parameters. There are several methods for selecting a subset of predictors that produce the "best" regression. Many statisticians discourage general use of these methods because they can detract from the real-world importance of predictors in a model. Examples of predictor selection methods are step-up selection, step-down selection, stepwise regression, and best subset selection. The fact that there is no predominant method indicates that none of them are broadly satisfactory (Draper and Smith, 1998).

2.2.2 Algorithms for Subset Selection

Selecting subsets to improve MSE is a difficult computational problem for large number of independent variables. The most common procedure for more than 20 independent variables is to use heuristics to select "good" subsets rather than to look for the best subset for a given criterion. The heuristics most often used and available in statistics software are step-wise procedures. There are three common procedures: forward selection, backward elimination, and step-wise regression (Draper and Smith, 1998). In forward selection procedure, the variables are kept on adding one at a time to construct what we hope is a reasonably good subset (Draper and Smith, 1998). Starting with constant term only in subset, compute the reduction in the sum of squares of the residuals (SSR) obtained by including each variable that is not presently in S . For the variable, say, i that give the largest reduction in SSR compute as:

$$F_i = \text{Max}_{i \notin S} \frac{SSR(S) - SSR(S \cup \{i\})}{s^2(S \cup \{i\})} \quad (31)$$

If $F_i > F_{in}$, where F_{in} is a threshold (typically between 2 and 4) add i to S . Repeat until no variables can be added.

The backward elimination started with all variables in S . Compute the increase in the sum of squares of the residuals (SSR) obtained by excluding each variable that is presently in S (Draper and Smith, 1998). For the variable, say, i that give the smallest increase in SSR compute as:

$$F_i = \text{Min}_{i \in S} \frac{s^2(S)}{SSR(S - \{i\}) - SSR(S)} \quad (32)$$

If $F_i < F_{out}$, where F_{out} is a threshold (typically between 2 and 4) then drop i from S . Repeat until no variable can be dropped. Backward Elimination has the advantage that all variables are included in S at some stage. This addresses a problem of forward selection that will never select a variable that is better than a previously selected variable that is strongly correlated with it. The disadvantage is that the full model with all variables is required at the start and this can be time-consuming and numerically unstable.

The step-wise regression procedure is like forward selection except that at each step we consider dropping variables as in backward elimination. Convergence is guaranteed if the thresholds F_{out} and F_{in} satisfy: $F_{out} < F_{in}$. It is possible, however, for a variable to enter S and then leave S at a subsequent step and even rejoin S at a

yet later step. As stated above these methods pick one best subset. There are straightforward variations of the methods that do identify several close to best choices for different sizes of independent variable subsets.

None of the above methods guarantees that they yield the best subset for any criterion such as adjusted R^2 . These are reasonable methods for situations with large number of independent variables. Hence, in the present study, stepwise multiple regressions with p-value of F-statistic were followed to select the best subset of various combinations of measurable characteristics of study watersheds by using EXCEL 2007: Multiple regression and statistical software, namely SYSTAT.

2.2.3 Stepwise Multiple Regression

Stepwise regression was introduced by Efraymson (1960). This method is an automated procedure used to select the most statistically significant variables from a large pool of explanatory variables. The method does not take into account industrial knowledge about the process, and therefore, other variables of interest may be later added to the model, if necessary. If properly used, the stepwise regression option in EXCEL 2007 and SYSTAT (or other stat packages) puts more power and information than does the ordinary multiple regression option, and it is especially useful for shifting through large number of potential independent variables and/or fine-tuning a model by poking variables in and/or out. If improperly used, it may converge on a poor model while giving a false sense of security. The stepwise regression option either begins with no variables in the model or proceeds forward (adding one variable at a time) or start with all potential variables in the model and proceed backward (removing one variable at a time). At each step, the SYSTAT program performs various calculations via for each variable currently in the model, it computes the t-statistic for its estimated coefficient, squares it, and reports this as its "F-to-remove" statistic; for each variable not in the model, it computes the t-statistic that its coefficient would have if it were the next variable added, squares it, and reports this as its "F-to-enter" statistic. At the next step, the program automatically enters the variable with the highest F-to-enter statistic or removes the variable with the lowest F-to-remove statistic in accordance with certain control parameters that have been specified. Under the forward method, at each step, it enters the variable with the largest F-to-enter statistic, provided that this is greater than the threshold value for F-to-enter. When there are no variables left to enter whose F-to-enter statistics are above the threshold, it checks to see whether the F-to-remove statistics of any variables added previously have fallen below the F-to-remove threshold. If so, it removes the worst of them, and then tries to continue. It finally stops when no variables either in or out of the model have F-statistics on the wrong side of their respective thresholds. The backward method is similar in spirit, except it starts with all variables in the model and successively removes the variable with the smallest F-to-remove statistic, provided that this is less than the threshold value for F-to-remove. Whenever a variable is entered, its new F-to-remove statistic is initially the same as its old F-to-enter statistic, but the F-to-enter and F-to-remove statistics of the other variables will generally all change. Similarly, when a variable is removed, its new F-to-enter statistic is initially the same as its old F-to-remove statistic. Until the F-to-enter and F-to-remove statistics of the other variables are recomputed, it is impossible to tell what the next variable to enter or remove will be. Hence, this process is myopic, looking only one step forward or backward at any point. There is no guarantee that the best model that can be constructed from the available variables (or even a good model) will be found by this one-step-ahead search procedure. Hence, when the procedure terminates, one should study the sequence of variables added and deleted, think about whether the variables that were included or excluded make sense. For example, the variable with the lowest F-to-remove or highest F-to-enter may have just missed the threshold value, in which case one may wish to tweak the F-values and see what happens. Sometimes adding a variable with a

marginal F-to-enter statistic, or removing one with a marginal F-to-remove statistic, can cause the F-to-enter statistics of other variables not in the model to go up and/or the F-to-remove statistics of other variables in the model to go down, triggering a new chain of entries or removals leading to a very different model. The selection of stepwise forward or backward multiple regression method depends on the set of independent variables. If a very large set of potential independent variables is available from which one has to extract a few, i.e. one is on fishing expedition, one should generally go forward. On the other hand, if one has a modest-sized set of potential variables from which one wishes to eliminate a few, i.e. one is fine-tuning some prior selection of variables, one should generally go backward. As noted above, after SYSTAT completes a forward run based on the F-to-enter threshold, it takes a backward look based on the F-to-remove threshold, and vice versa. Hence, both thresholds come into play regardless of which method are using, and the F-to-enter threshold must be greater than or equal to the F-to-remove threshold (to prevent cycling). Usually the two thresholds are set to the same value. Keeping in mind that the *F*-statistics are squares of corresponding *t*-statistics, an *F*-statistic equal to 4 would correspond to a *t*-statistic equal to 2, which is the usual rule-of-thumb value for "significance at the 5% level." (4 is the default value for both thresholds.). It is always better using a somewhat smaller threshold value than 4 for the automatic phase of the search-for example 3.5 or 3. Since the automatic stepwise algorithm is myopic, it is usually OK to let it enter a few too many variables in the model, and then one can weed out the marginal ones later on by hand. However, beware of using too low an *F*-threshold if the number of variables is large compared to the number of observations or if there is a problem with multicollinearity in data.

III. RESULTS AND DISCUSSION

The optimized values of parameters of MLTHS ASMA (Jain et al., 2012) model applied to the daily data of rainfall and stream flow of the 17 watersheds varying in size/shape, physical properties and situated in different agro-climatic zones of India are presented in Table 1.

Table 1. Optimized Values of Parameters of MLTHS ASMA (Jain et al. 2012) Model

Sr. No.	Name of Watershed	Model Parameters														
		CN ₀	δ	α	β	γ	K	P ₁	P ₃	P ₄	θ _w	ψ _r	E _s	ψ ₀	CNd ₀	λ _d
1.	Hemavati	30.5	2.33	0.41	0.14	0.44	1.52	0.01	0.11	0.99	40.3	300.0	0.32	300.3	64.7	0.01
2.	Hridaynagar	27.5	0.01	0.54	0.01	0.52	1.23	0.04	0.00	0.59	299.7	496.2	0.26	253.6	60.7	0.01
3.	Mohegaon	37.0	0.05	0.46	0.01	0.50	5.00	0.03	0.60	0.16	119.7	395.3	0.32	469.4	58.3	0.07
4.	Manot	35.3	6.63	0.85	0.00	0.95	3.02	0.02	0.60	0.48	298.9	413.8	0.36	377.1	56.6	0.57
5.	Amachi	17.4	0.10	0.40	0.02	0.42	2.00	0.01	0.20	0.44	80.0	310.0	0.34	242.9	32.3	0.02
6.	Anthrolli	28.6	4.92	0.43	0.01	0.46	1.69	0.01	0.39	0.10	220.0	259.8	0.54	358.8	78.2	0.13
7.	Attigundi	20.0	0.02	0.45	0.001	0.58	5.98	0.05	0.24	0.98	162.5	373.9	0.38	199.4	44.8	0.26
8.	Barchi	38.1	0.01	0.53	0.01	0.54	2.00	0.01	0.35	0.50	148.9	279.2	0.38	551.5	55.4	0.09
9.	Khanapur	11.3	0.14	0.46	0.02	0.57	3.18	0.01	0.60	0.99	179.9	405.0	0.50	198.3	18.3	0.15
10.	Hirehalla	14.6	0.06	0.48	0.10	0.50	2.07	0.09	0.80	0.06	130.3	300.0	0.49	350.0	35.8	0.03
11.	Sagar	21.4	0.21	0.50	0.01	0.54	0.64	0.01	0.59	0.54	45.5	400.0	0.90	191.0	50.8	0.09
12.	Sorab	52.8	0.13	0.53	0.01	0.61	1.63	0.01	0.50	0.84	105.0	302.3	0.40	397.0	51.9	0.05
13.	Dasanakatte	15.6	0.11	0.59	0.24	0.61	0.76	0.00	0.40	0.99	123.6	399.9	0.38	394.4	20.4	0.02
14.	Haladi	25.6	0.02	0.56	0.23	0.60	1.66	0.01	0.47	0.99	103.8	400.0	0.35	389.1	37.1	0.05
15.	Jadkal	30.8	0.98	0.47	0.34	0.53	0.53	0.05	0.48	0.99	160.0	400.0	0.39	405.7	42.2	0.06
16.	Kokkarne	15.8	4.99	0.57	0.18	0.56	2.06	0.00	0.55	0.99	127.4	407.9	0.30	220.2	25.9	0.01
17.	Halkal	26.5	0.01	0.65	0.30	0.66	1.34	0.01	0.47	0.99	240.0	262.9	0.38	303.4	33.5	0.01

As stated earlier, the geomorphological characteristics of the watersheds that significantly affect the runoff are geographical area, length, slope, shape, land use, and soil characteristics of watershed. The various geomorphological characteristics of study watersheds were extracted from the Survey of India (SOI) toposheets. The toposheets were scanned and projected into Universal Traverse Mercator (UTM) projection system into zone (43-in which the study area lies), using Everest (India, 1956) Ellipsoid and Everest (India, Nepal) datum using image processing utilities of Integrated Land and Water Information System (ILWIS) software. The rectified toposheets were further used for the delineation of different features in the study watersheds like contour lines and drainage networks etc. The base map of the watershed boundary at 1:50,000 scale was prepared using the location of various contour and drainage lines. Different thematic maps, viz., contour map and drainage map were prepared using the base map. Digital Elevation Models (DEMs) were created using the contour maps, which were further used for the assessment of relief aspects. The mathematical expressions given by various researchers such as Horton (1945), Miller (1953), and Schum (1956) were used to compute geomorphological characteristics of watershed as shown in Table 2.

Table 2. Geomorphological Characteristics of Study Watersheds

Sr. No.	Name of Watershed	Geomorphological characteristics of the watershed								
		Area	Perimeter	Length	Hydrologic length	Form factor	Circulatory ratio	Elongation ratio	Total relief	Vegetation
		(A)	(P)	(Lb)	(Lm)	(Rf)	(Rc)	(Re)	(H)	(V)
		(Km ²)	(Km)	(Km)	(Km)				(m)	(%)
1	Hirehalla	1296.00	162.23	55.49	51.31	0.42	0.62	0.73	150	6
2	Hridaynagar	3370.00	402.42	182.92	215.20	0.10	0.26	0.36	228	65
3	Amachi	87.00	33.74	11.28	11.51	0.68	0.96	0.93	224	70
4	Barchi	4661.00	326.97	148.62	174.85	0.21	0.55	0.52	391	58
5	Mohegaon	14.50	20.81	8.18	8.60	0.22	0.42	0.53	254	94
6	Anthroli	503.00	98.21	35.47	24.23	0.40	0.66	0.71	246	57
7	Manot	5032.00	503.03	228.65	269.00	0.10	0.25	0.35	660	35
8	Sorab	96.00	45.30	15.81	24.61	0.38	0.59	0.70	266	60
9	Khanapur	320.00	143.74	30.83	48.08	0.34	0.19	0.65	146	63
10	Sagar	75.00	33.56	11.84	10.92	0.54	0.84	0.83	108	55
11	Attigundi	4.51	8.81	3.47	2.34	0.37	0.73	0.69	188	85
12	Hemavati	600.00	127.35	57.89	55.13	0.18	0.46	0.48	350	12
13	Kokkarne	343.00	116.94	34.35	53.17	0.29	0.32	0.61	1147	82
14	Halkal	108.00	48.23	18.39	17.64	0.32	0.58	0.64	1101	92
15	Dasanakatte	135.00	57.95	19.92	28.56	0.34	0.50	0.66	869	92
16	Jadkal	90.00	39.45	13.12	18.75	0.52	0.73	0.82	1142	85
17	Haladi	505.00	105.07	34.79	42.75	0.05	0.57	0.73	968	87

The multiple regression analysis was carried out to develop the relation between the MLTHS ASMA model parameters and the geomorphological characteristics of the watershed. For this purpose, the regression matrix was prepared to have an idea about the poorly correlated geomorphological characteristics of study watersheds with model parameters as shown in Table 3. This analysis helps to take decision for carrying out multiple linear regression analysis. The multiple regressions were performed using the Data Analysis Add-in facilities of EXCEL 2007. The regression matrix (Table 3) was used for choosing the best subset of the watershed

characteristics to correlate with model parameters. Since EXCEL 2007 has limited facilities and required several trials to select the

Table 3. Regression Matrix between MLTHS ASMA Model Parameters and Geomorphological Characteristics of Study Watersheds

Sr. No.	Model Parameters	Regression coefficient (r^2)								
		A	P	Lb	Lm	Rf	Rc	Re	H	V
1	CNd ₀	0.178	0.146	0.196	0.145	0.090	0.001	0.170	0.089	0.175
2	α	0.181	0.261	0.244	0.264	0.307	0.366	0.293	0.218	0.003
3	β	0.160	0.154	0.149	0.138	0.000	0.022	0.057	0.628	0.168
4	γ	0.171	0.221	0.212	0.238	0.300	0.310	0.280	0.131	0.000
5	δ	0.014	0.024	0.025	0.022	0.079	0.027	0.016	0.001	0.024
6	P ₃	0.001	0.003	0.014	0.010	0.034	0.004	0.075	0.005	0.012
7	P ₄	0.173	0.093	0.101	0.068	0.048	0.071	0.003	0.281	0.191
8	K	0.032	0.079	0.060	0.060	0.124	0.166	0.073	0.127	0.060
9	P ₁	0.041	0.029	0.026	0.017	0.011	0.014	0.001	0.043	0.120
10	θ_w	0.262	0.385	0.368	0.370	0.142	0.285	0.291	0.028	0.006
11	ψ_f	0.222	0.329	0.283	0.334	0.221	0.324	0.179	0.085	0.001
12	ψ_0	0.094	0.038	0.050	0.045	0.159	0.032	0.084	0.072	0.000
13	E _g	0.147	0.205	0.190	0.207	0.486	0.483	0.418	0.236	0.000
14	CN ₀	0.053	0.011	0.036	0.033	0.062	0.001	0.088	0.010	0.001
15	λ_d	0.172	0.163	0.173	0.173	0.028	0.023	0.079	0.021	0.017

best subset of watersheds characteristics, the multiple regressions using stepwise backward elimination procedure based on p-value of F- statistics (Zhang and Wang, 1997) is performed in SYSTAT 10. Here, the p-value is the probability (prob(F)) of obtaining a test statistic at least an extreme as the one that was actually observed, assuming that the null hypothesis is true. Generally, one rejects the null hypothesis if the p-value is smaller than or equal to the significance level (α). If the level is 0.05, then results that are only 30% likely or less are deemed extraordinary, given that the null hypothesis is true. The calculated p-value exceeds 0.05, so the observation is consistent with the null hypothesis. Likewise, if $\text{prob}(F) < 0.05$, then the model is considered significantly better that would be expected by chance and reject the null hypothesis of no linear relationship of model parameters to the measurable physical characteristics of the watersheds. Some of the statisticians also considered the model is highly significant if p-value is less than or equal to 0.001.

The various combination of p-value -to enter and p- value-to remove and/or F-value-to enter and F-value to remove were tried in SYSTAT 10 to choose the correct combination to develop the regression equations. The regression statistics along with analysis of variance (ANOVA) for correct combination of physical characteristics of watersheds to estimate the various model parameters are computed. As seen from the ANOVA, the multiple correlation coefficient (multiple R) for most of the model parameters such as CN₀, α , β , P₃, P₄, θ_w , ψ_f , ψ_0 , E_g, and CNd₀, are more than 0.60, which indicates that there exists a good correlation between model parameters and measurable physical characteristics of the watersheds. A very good correlation (multiple R=0.95) is found between initial ground water content (ψ_0) and physical characteristics of the watershed such as A, P, Lb, Lm, Rf, Rc, and Re. From the p-value of F-statistics, it is found that the regression equation developed for β , θ_w , ψ_0 , and E_g parameters are highly significant (level of significance or p- value is more than 0.001), while some parameters such as δ , K, P₁, and λ_d are very poorly significant (or insignificant) at 95% confidence interval

(level of significance or p-value is less than 0.05). From the ANOVA, the regression equations for various model parameters were formulated as shown in Table 4.

Table 4. Regression Equations Showing Relationship between LTHS ASMA II Model Parameters and Geomorphological Characteristics of Watersheds

Model Parameter	Multi-linear Regression Equation	Multiple (R ²)
CN ₀	CN ₀ =31.991-0.317P+0.702Lb	0.39
α	α=0.64-0.424Rc+0.0001H	0.52
β	β =0.022-0.001L+0.0003H	0.76*
γ	γ =0.751-0.37Rc	0.31
δ	δ =0.023Lb+10.38Rf-2.75	0.24**
P ₃	P ₃ =0.45+0.0003A+0.005P-0.02Lb	0.56
P ₄	P ₄ =1.38-0.0001A-0.018Lb+0.017Lm-1.125Rf+0.0001H	0.74
K	K=1.27-0.011H+0.147V	0.40**
P ₁	P ₁ =0.02+0.001P-0.002Lb-0.0002Lm+0.17Rc-0.18Re	0.24**
θ _w	θ _w =10.968Lb-8.248Lm+275.567Rf-481.685Rc+319.221Re+2.709V-133.414	0.85*
ψ _f	θ _f =180.578+0.835Lm-330.33Rc+444.463Re	0.54
ψ ₀	ψ ₀ =0.26A-15.69P+48.91Lb-17.0Lm-320.07Rf-3144.86Rc+4051.43Re-207.56	0.91*
λ _d	λ _d =0.056+0.001Lm	0.17**
CNd ₀	CNd ₀ =36.79+1.51Lb-1.19Lm	0.52
E _g	E _g =0.242+0.601Rc-0.0001H	0.65*

Note: * highly significant at 95% confidence interval

** not significant at 95% confidence interval

As seen from Table 4, the multi-linear regression equations developed for some of the model parameters of MLTHS ASMA model are highly significant, while there exists a significant relationship for most of the parameters. Hence, the multi-linear regression equations developed for these model parameters (except for those parameters for which regression equations are found insignificant) may be used for parameter estimation using the measurable physical characteristics of watersheds. Thus, many parameters of MLTHS ASMA model could be estimated from catchment characteristics and could potentially be used for field application when sufficient data for better calibration of parameters of the model do not exist.

IV. CONCLUSIONS

The relationship between model parameters and measurable geomorphological characteristics of the watersheds using multiple regression analysis is developed in this paper. The step-wise regression with backward elimination on p-value of F-statistics is followed to develop regression equations. In most of the cases, a significant relationship is found between the model parameters and geomorphological characteristics of study watersheds at 95% confidence interval. The multi-linear equations thus developed for various parameters of MLTHS ASMA model can be used to estimate the total runoff from the ungauged watershed in various agro-climatic zones of India.

REFERENCES

- [1] M. K. Jain, D. G. Durbude and S. K. Mishra, SCS-CN based modified long term hydrologic simulation model for daily stream flow simulation, *Journal of Hydrologic Engineering (ASCE)*, 17(11), 2012, 1204–1220.
- [2] S. Chandra, *Geomorphology of Sabarmati basin up to Dharoi*, Rep. National Institute of Hydrology, Roorkee, TR-138, 1993, 3-5.
- [3] R. E. Horton, Erosional development of streams and their drainage basins-hydrophysical approach to quantitative morphology, *Bull. Geol. Soc. of Ame.*, 56, 1945, 275-370.
- [4] A. N. Strahler, Hypsometric (area-altitude) analysis of erosional topography, *Bull. Geol. Soc. Ame.*, 63, 1952, 1117-1142.
- [5] W. D. Potter, Rainfall and topographic features that affects runoff.” *Trans. Ame. Geophys. Un.*, 34, 1953, 67-73.
- [6] M. A. Benson, Flood peaks related to hydrological factors in the south-west, *USGS Prof. Paper 450 E*, 1962, 161-163
- [7] M. J. Boyd, A storage-routing model relating drainage basin hydrology and geomorphology, *Water Resour. Res.*, 14 (15), 1978, 921-928.
- [8] I. Rodriguez-Iturbe, and J. B. Valdes, The geomorphologic structure of hydrology response, *Water Resour. Res.* 15(6), 1979, 1409-1420.
- [9] V. K. Gupta, E. Waymire and C. T. Wang, A representation of an instantaneous unit hydrograph from geomorphology, *Water Resour. Res.*, 16 (5), 1980, 855–862.
- [10] R. Rosso, Nash model relation to Horton order ratios, *Water Resour. Res.*, 20(7), 1984, 914-920.
- [11] M. S. Roohani, and R. P. Gupta, Quantitative hydrogeomorphic investigations in the Chenab catchment, Himalayas, *J. Hydro. (IAH)*, 11(4), 1988, 25-43.
- [12] A. M. Karnieli, M. H. Diskin, and L. J. Lane, CELMOD 5-A semi-distributed cell model for conversion of rainfall into runoff in semi-arid watersheds, *J. Hydro.*, 157 (1-4), 1994, 61–85.
- [13] B. N. S. Chalam, M. Krishnaveni, and M. Karmegam, Correlation of runoff with geomorphic parameters, *J. Appl. Hydro.*, 9 (3-4), 1996, 24-31.
- [14] R. S. Chaudhary and P. D. Sharma, Erosion hazard assessment and treatment prioritization of Giri River catchment, North Western Himalayas, *Indian J. Soil Cons.*, 26(1), 1998, 6-11.
- [15] L. S. Hsieh, and R. Y. Wang, A semi-distributed parallel-type linear reservoir rainfall– runoff model and its application in Taiwan, *Hydrol. Process.*, 13(8), 1999, 1247–1268.
- [16] R. Kumar, A. K. Lohani, S. Kumar, C. Chatterjee, and R. K. Nema, GIS based morphometric analysis of Ajay river basin up to Sarthgauging site of South Bihar, *J. Appl. Hydrol. (AHI)*, 14(4), 2001, 45-54.
- [17] S. Ali, and R. Singh, Morphological and hydrological investigation in Hirakud catchment for watershed management planning, *J. Soil Water Cons. (India)*, 1(4), 2002, 246-256.
- [18] Dilip G. Durbude, and C. P. Kumar, Application of GIS for the determination of morphological characteristics of a watershed, *Proc. National Conf. on Modern Trend in Water Resources Development and Environmental Management*, Vellore, India, Vellore Institute of Technology, Vellore, March 2002, 11-17.
- [19] Dilip G. Durbude, Remote sensing application for hydro-geomorphological analysis of a watershed, *Proc. National Conf. on Hydraulic. Water Resour. (HDRO 2004)*, ISH & VNIT, Nagpur, December, VNIT, Nagpur, India, 2004, 42-49.
- [20] R. K. Singh, C. M. Bhatt, and V. H. Prasad, Morphological study of a watershed using remote sensing and GIS techniques, *Hydro. J. (IAH)*, 26(1&2), 2003, 55-66.

- [21] M. Suresh, S. Sudhakar, K. N. Tiwari and V. M. Chowdary, Prioritization of watersheds using morphometric parameters and assessment of Surface Water Potential using Remote Sensing, *J. Indian Soc. Rem. Sens.*, 32(3), 2004, 249-259.
- [22] Dilip G. Durbude, Remote sensing and GIS approach for land use, soil texture and morphological characteristics of a watershed, *J. Appl. Hydrol. (AHI)*, 18(3), 2005, 42-50.
- [23] Dilip G. Durbude and T. Chandramohan, Morphometric analysis of a forested watershed using GIS technique, In: *Forest Hydrology*, (Ed.) Venkatesh, B., Purandara, B. K. and Ramasastri, K. S., Capital Publishing, New Delhi, 2007, 130-136.
- [24] P. P. Dabral and A. Pandey, Morphometric analysis and prioritization of a eastern Himalayan river basin using satellite data and GIS, *Asian J. Geoinformatics*, 7(3), 2007, 3-14.
- [25] C. Michel, A. Vazken and C. Perrin, Soil conservation service curve number method: how to mend a wrong soil moisture accounting procedure, *Water Resour. Res.*, 41:W02011, 2005, 1-6.
- [26] Dilip G. Durbude, M. K. Jain and S. K. Mishra, Long term hydrologic simulation using SCS-CN based improved soil moisture accounting procedure, *Hydrol. Process.*, 125, 2011, 561-579.
- [27] Y. Yuan, J. K. Mitchell, M. C. Hirschi and R. A. C. Cooke, Modified SCS curve number method for predicting subsurface drainage flow, *Trans. ASAE*, 44(6): 2001, 1673-1682.
- [28] K. Geetha, S. K. Mishra, T. I. Eldho, A. K. Rastogi and R. P. Pandey, Modification to SCS-CN method for long-term hydrologic simulation, *J. Irrig. Drain. Engg.*, 133(5), 2007, 475-486.
- [29] S. K. Mishra, K. Geetha, A. K. Rastogi and R. P. Pandey, Long-term hydrologic simulation using storage and source area concepts, *Hydrol. Process.*, 19, 2005, 2845-2861.
- [30] M. R. Y. Putty and R. Prasad, Understanding runoff processes using a watershed model—a case study in the Western Ghats in South India, *J. Hydro.*, 228, 2000, 215-227.
- [31] M. R. Y. Putty, and R. Prasad, Stream flow generation in Western Ghats, In: 6th National Sympo., Hydrology, Shillong, 1994.
- [32] M. A. Aitkin, A general linear model approach to data analysis, Symposium on Statistical Computing, Sydney, August 1974.
- [33] E. Spjotvoll, On the optimality of some multiple comparison procedure, *The Annals of Math. Statistics*, 43(2), 1972, 398-411.
- [34] N. R., Draper and H. Smith, *Applied regression analysis, 2d Edition*, New York: John Wiley & Sons, Inc., 1981.
- [35] C. L. Mallows, Choosing variables in a linear regression: a graphical aid, Presented at the Central Regional Meeting of the Institute of Mathematical Statistics, Manhattan, Kansa, 1964.
- [36] N. R. Draper and H. Smith, *Applied regression analysis (3rd edition)*, New York: John Wiley and Sons, Inc., 1998.
- [37] M. A. Efronson, *Multiple regression analysis*, In Ralston, A. and Wilf, HS, editors, *Mathematical Methods for Digital Computers*. Wiley, 1960.
- [38] Jin, Zhang, and X. Wang, Selecting the best regression equation via the p-value of F-test, *Metrika*, 46: 1997, 33-40.
- [39] V. C. Miller, A quantitative geomorphic study of drainage basin characteristics in the Clinch mountain area, Virginia and Tennessee, Proj. NR 389-402, Tech Rep 3, Columbia Univ., Deptt. Geol., ONR, New York, 1953.
- [40] S. A. Schum, Evaluation of drainage systems and slopes in badlands at Perth Amboy, New Jersey, *Geol. Soc. Ame. Bull.*, 67, 1956, 597-646.
- [41]

ONLINE SHOPPING IN PRESENT SCENARIO: A BOON OR CURSE

Ms. Neha Jain

Assistant Professor, Department of Management, Jtuniversity, Rajasthan, (India)

ABSTRACT

Online shopping or e-shopping is a form of electronic commerce which allows consumers to directly buy goods or services from a seller over the Internet using a web browser. Alternative names are: e-web-store, e-shop, e-store, Internet shop, web-shop, web-store, online store, online storefront and virtual store. The act of purchasing or services over the Internet. Online shopping has grown in popularity over the years, mainly because people find it convenient and easy to bargain shop from the comfort of their home or office. One of the most enticing factor about online shopping, particularly during a holiday season, is it alleviates the need to wait in long lines or search from store to store for a particular items. This research paper is based on online shopping in current scenario it is a boon or curse. The research paper is based on information collected from primary and secondary sources after the detailed study. An attempt has been made to present comprehensive analysis of online shopping. A good number of respondents showed their interest regarding online shopping.

Keywords: *Analysis, Boon, Curse, Methodology, Scenario.*

I. INTRODUCTION

1.1 Traditional Shopping

Imagine going to a store, think of your favorite store in the nearest mall to where you live. You get into the store, slowly walking from rack to rack, checking out the display, putting a dress over your body and trying to check out your reflection on one of the nearby full-view mirrors that are placed all around the store. You move on to the next display rack, and probably make another selection and do the same thing you did earlier. This is what traditional shopping is about. Having the ability to physically choose and check out what an item or product is like, would look like, and what its features are. This is why some consumers still prefer the traditional type of shopping over online shopping because for one, it allows them to meticulously check out an item. Some consumers are not quite certain with their own size, sometimes fitting a size that would normally be bigger or smaller than their actual size. So in retrospect, while online shopping has not just numerous benefits and advantages as explained by many online consumers as well as studies and surveys, there are still conventional shoppers who like to check out the product that they are interested in buying.

1.2 Online Shopping

Simply put, it is any form of sale that is done over the internet. Shopping has certainly gotten a new definition since the arrival of the internet. Because of what the internet has to offer, that is, any person or company from any part of the world who is able to post and sell goods on the internet via a website is able to sell. What's more, any consumer does not have to worry about having to find means to exchange monetary paper because not just online banking is made available; the consumer is given the option to pay through different payment methods.

These days, it is even easier to find the most difficult of all products, by easily typing in the product or item that you are looking for. One doesn't have to worry about location because logistic companies are also joining the bandwagon, so to speak, and helps in making sure that their products would be available to any and all destinations in the world. In fact, there are more and more advantages and benefits to online shopping and why people choose to do this type of shopping over traditional shopping.

1.3 Online Vs. Traditional Shopping

Shopping is probably one of the oldest terms used to talk about what we have all been doing over the years, if possible, eras. Then again, in ancient times, the terms that would have been used would be 'trading' or 'bartering' and probably even 'market.'

1.4 Statement of the Problem

What has traditional shopping have to offer now that the internet has opened up a wider and more enticing market to the current consumers.

1.5 Objective of the Study

The major objective of this study is to understand for the respondents online shopping it is an advantage or curse.

To uncover the problems they face while selecting online shopping.

To understand their shopping mode.

To come up with solutions to minimize the problems faced by them.

II. RESEARCH METHODOLOGY

The sources of data used in this research are primary as well as secondary data.

Primary Data: Primary data is original data collected by a person for the purpose of some research .In this study, the primary data is collected from respondents with the help of a questionnaire. The respondents were requested to answer the questions in their questionnaire and their responses were recorded. The questionnaire was prepared keeping in the mind the objectives of the research.

The research paper is based on information collected from primary sources. After the detailed study, an attempt has been made to present comprehensive analysis of the respondents view about online shopping. In collecting requisite data and information regarding the topic selected, I approached the respondents at Jhunjhunu and observed the impact of online shopping.

Secondary Data: Secondary Data is the data which is readily available in various sources such as Magazines, journals, books, internet etc.

Research Tool: Questionnaire is the tool used in this study. Questionnaire is a set of questions to be asked to the respondent. It also contains suitable spaces where answers can be recorded.

Research Method: A survey was conducted to collect the data .The data hence collected was analyzed and the findings were collected.

Sample size: 100 respondents

Samples design: were taken on the basis of convenience

Sampling Method: The data was collected through structured questionnaire which consisted of 12 questions with multiple choice answers. The respondents choose one option which they felt was the right answer or at least closest to the right answer.

Research Period: Research was done over a period of 1 month

Research Instrument This work was carried out through self administered questionnaires.

Various sites of online shopping as follows-

Amazon.in is operated by Amazon Seller Services Private Ltd, an affiliate of Amazon.com, Inc. (NASDAQ: AMZN). Amazon.com, Inc. is a Fortune 500 company based in Seattle, that opened on the World Wide Web in July 1995; and today offers Earth's Biggest Selection. Amazon and its affiliates operate websites, including www.amazon.com, www.amazon.co.uk, www.amazon.de, www.amazon.co.jp, www.amazon.fr, www.amazon.ca, www.amazon.cn, www.amazon.it, www.amazon.es and www.amazon.com.br. As used herein, "Amazon.com", "we", "our" and similar terms include Amazon.com, Inc., and its subsidiaries, unless the context indicates otherwise.

Products on amazon.in range from; Books, Music, Movies & TV shows; the Kindle family of E-Readers, Tablets and eBooks; Computers & Accessories; Mobiles & Accessories; Cameras & Photography; Portable Media Players; Toys & Games; Video Games; Baby Products; Personal Care Appliances; Health Care Devices; Gourmet & Specialty Foods; Pet Supplies; Clothing & Accessories; Sunglasses; Watches; Fashion; Precious Jewellery; Shoes; Handbags & Clutches; Luggage & Bags; Home & Kitchen; Beauty; Luxury Beauty; Sports, Fitness & Outdoors, Health & Personal Care products, Musical Instruments & Professional Audio, Office and Stationery Products and e-Gift Cards. It is still "Day 1" and Amazon.in is relentlessly focused on expanding selection and raising the bar for customer experience in India.

In Feb 2012, Amazon Seller Services made its foray into the Indian market with the launch of Junglee.com, enabling retailers in India to advertise their products for free to millions of Indian shoppers and drive targeted traffic to their stores. With the introduction of the Amazon.in marketplace and launch of two new programmes – 'Sell on Amazon' and 'Fulfilment by Amazon' – sellers across India now have access to unlimited and free 'virtual shelf space' and a scalable, pay-as-you-go fulfilment and customer service offerings.

Jabong.com is a young and vibrant company that aims to provide good quality branded products. Jabong.com caters to the fashion needs of men, women and kids across footwear, apparel, jewellery and accessories. At Jabong.com we strive to achieve the highest level of "Customer Satisfaction" possible. Our cutting edge E-commerce platform, highly experienced buying team, agile warehouse systems and state of the art customer care centre provides customer with:

- Broader selection of products
- Superior buying experience
- On-time delivery of products
- Quick resolution of any concerns

Launched in February 2010, **Snapdeal.com** is India's largest e-commerce marketplace. Snapdeal provides a platform for vendors across the country to connect with millions of customers. Our online shopping platform has the widest assortment of products from thousands of national, international and regional brands across diverse categories like Mobiles, Laptops, Cameras, Appliances, Women's Apparel, Men's Apparel, Watches, Home &

Kitchen, Automotive and Health. Grab your favorite products at best prices and save the one thing that matters most to you-"Your, Money".

Snapdeal.com has a network of more than 50000 Merchants/Brands, and has over 20 million members (which is 1 out of every 6 internet users in the country) and caters to the shopping needs of customers across 4000+ towns and cities

Naaptol.com is one of India's leading online shopping websites that hosts a variety of products from hundreds of different brands. At Naaptol, we have always understood the value of your hard earned money and this is for the reason why we withstand with you in the company of bulky discounts to satisfy your shopping needs on every go. No matter what your cravings are, we have almost everything that you might fall in need for.

We have a whole lot of all the latest and in-fashion gears and accessories to enhance your everyday shopping experience. At Naaptol, we understand that your needs may be endless and that's how we have slated ourselves to match with almost every needs of yours. Like you, we too have a keen eye over the best products and 100% customer satisfaction, which is however, our craving.

Ever since the **online shopping** has taken off, we have modulated ourselves to offer you nothing but the best and with our best in class service, we promise to get through you no matter where you live. There is always a Naaptolite knocking at your doorstep in pursuit of your happy shopping experience with us. We strictly don't believe in making tall promises or building castles in the air, but what we really believe is our quality service should always be a reason enough to make you smile. After all, we know how delighted it feels when you save some additional bucks on your shopping.

Online shopping in India

is a growing phenomenon and we have taken utmost care to offer you with simple checkouts that are just couple of clicks away from you. Moreover, the ISO certification that we have earned for our quality makes us stand apart from our peers and close to you. Encapsulating all your needs to a digital cart, your shopping quest will always be high on smiles and less on banks.

Discover fashion at **Yebhi.com**, your one-stop shop for fashion. Get all the online fashion stores, all the coupons and prices on one site. Thousands of designs in shoes and clothing from Flipkart, Myntra, Jabong, Amazon, Snapdeal and many more. Why go everywhere, when the world of fashion is now at Yebhi.

Get the best discounts and the latest coupons, plus get extra cash back when you shop via Yebhi. Save more and even more. Use cash back to buy vouchers and exclusive deals on Yebhi.

Find new stores, trending merchandise and create your collections. All this and more, on your favorite online fashion store, Yebhi.com.

Flipkart is an Indian E-Commerce company established in 2007 by Sachin Bansal and Binny Bansal. It operates exclusively in India, with headquarters at Bangalore, Karnataka.Wikipedia

1. **Customer service:** 080 4940 0000
2. **Founded:** September 5, 2007
3. **CEO:** Sachin Bansal
4. **Founders:** Sachin Bansal, Binny Bansal

Flipkart is a leading destination for online shopping in India, offering some of the best prices and a completely hassle-free experience with options of paying through Cash on Delivery, Debit Card, Credit Card and Net Banking processed through secure and trusted gateways. Now shop for your favorite books, apparel, footwear, lifestyle accessories, baby care products, toys, posters, sports and fitness, mobile phones, laptops, cameras,

movies, music, health and beauty, televisions, refrigerators, air-conditioners, washing machines, MP3 players and products from a host of other categories available. Some of the top selling electronic brands on the website are Samsung, HTC, Nokia, Dell, HP, Sony, Canon, Nikon, LG, Toshiba, Philips, Braun, Bajaj and Morphy Richards. Browse through our cool lifestyle accessories, apparel and footwear brands featured on our site with expert descriptions to help you arrive at the right buying decision. Flipkart also offers free home delivery for many of our products along with easy EMI options. Get the best prices and the best online shopping experience every time, guaranteed.

eBay Inc. (stylized **ebay**) is an American multinational corporation and e-commerce company, providing consumer-to-consumer & business-to-consumer sales services via Internet. It is headquartered in San Jose, California, United States. eBay was founded by Pierre Omidyar in 1995, and became a notable success story of the dot-com bubble; it is a multi-billion dollar business with operations localized in over thirty countries.

OLX (OnLine eXchange) operates as a national online classifieds marketplace for used goods such as furniture, musical instruments, sporting goods, cars, kids and baby items, motorcycles, cameras, mobile phones, property and much more. It is accessible through the internet and through native apps on smartphones. OLX has a presence in over 106 countries with offices and local operations in Angola, Argentina, Bangladesh, Brazil, India, Indonesia, Portugal, Poland, Peru, Romania, Hungary, Bulgaria, Panama, Switzerland, South Africa, Kenya, Nigeria, Thailand, Philippines, Pakistan, Ghana and others.^[1]

Originally founded in March 2006 by Internet entrepreneurs Fabrice Grinda and A.C.F

HomeShop18 is an online and on-air retail and distribution venture of Network 18 Group, India. HomeShop18 was launched on 9 April 2008 as India's first 24-hour Home Shopping TV channel, where anchors performed live demonstration of products on sale similar to HSN or QVC in USA. The television channel established HomeShop18's foothold in Indian retail because of high television penetration. Later, as the internet reach grew all over the country, HomeShop18 launched www.homeshop18.com which was ranked as the No. 5 most trafficked Ecommerce portal in India by Comscore in July 2013. **FreeKaaMaal** is India's largest bargain hunting site where you will find online deals, discount coupons, promo codes, lowest price items and much more.

III. QUESTIONNAIRE & GRAPH & FIGURES

3.1 Questionnaire

Q-1 Your preference of products while shopping.

Home Appliances Apparel Grocery Mobile & Accessories

Q-2 Your frequency of shopping.

Weekly Bi-Monthly Monthly Window shopping

Q-3 Your ways of shopping.

Unorganized Organized online other sources

Q-4 Important factor you feel while shopping.

Satisfaction Value for money Payment flexibility Durability

Q-5 Preferred mode of payment while shopping.

Cash Credit card Debit card Cash on delivery

Q-6 Your expectation regarding delivery of the product.

Hand to hand within seven days with in fifteen days 2-4 weeks

Q-7 While shopping and purchase of a product, which factor seems most important to you.

Friend's Opinion Past experience Advertisement Direct marketing

Q-8 Your Monthly income (RS).

Upto 10,000 Above 10,000

Q-9 Your age.

20-30 30-40

Q-10 Your gender.

Male Female

Q-11 Your Occupation.

Part time full time

Q-12 your opinion regarding online shopping.

Not satisfactory Satisfactory Good First preference

Name- _____ Area _____ City _____

3.2 Graphs

Q-1 your preference of products while shopping

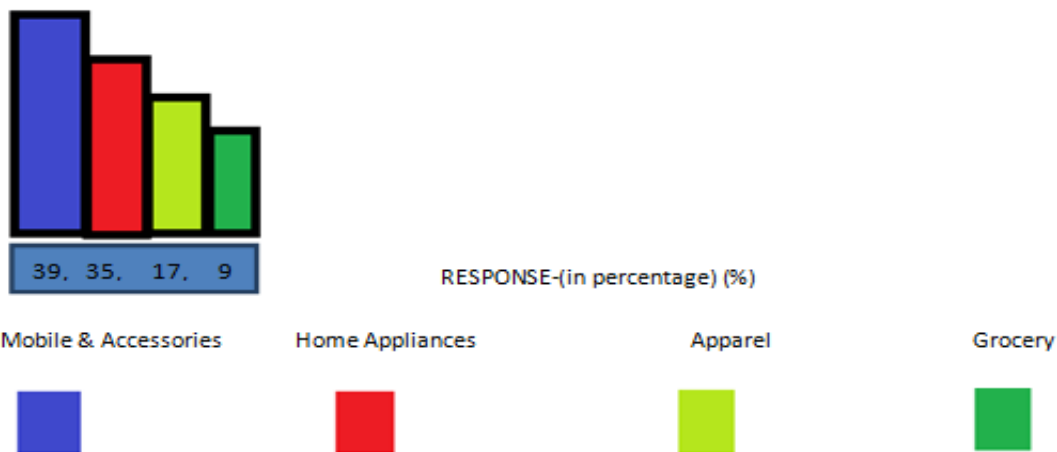


Fig.1: Analysis: Respondents liked Mobile & Accessories as their first preference while shopping 39% then home appliances 35%, apparel 17% & least liked grocery 9 %.

Q-2 Your frequency of shopping.

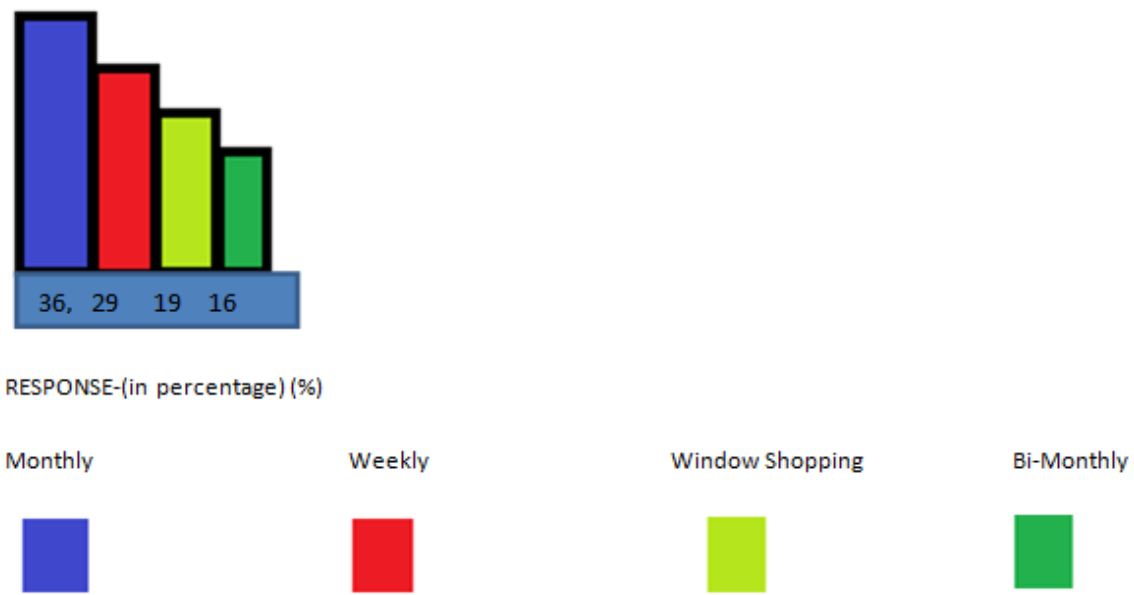


Fig. 2: Analysis: Respondents showed monthly as a frequency of shopping 36 %,weekly 29%,window shopping 19%,bi-monthly 16 %.

Q-3 Your ways of shopping.

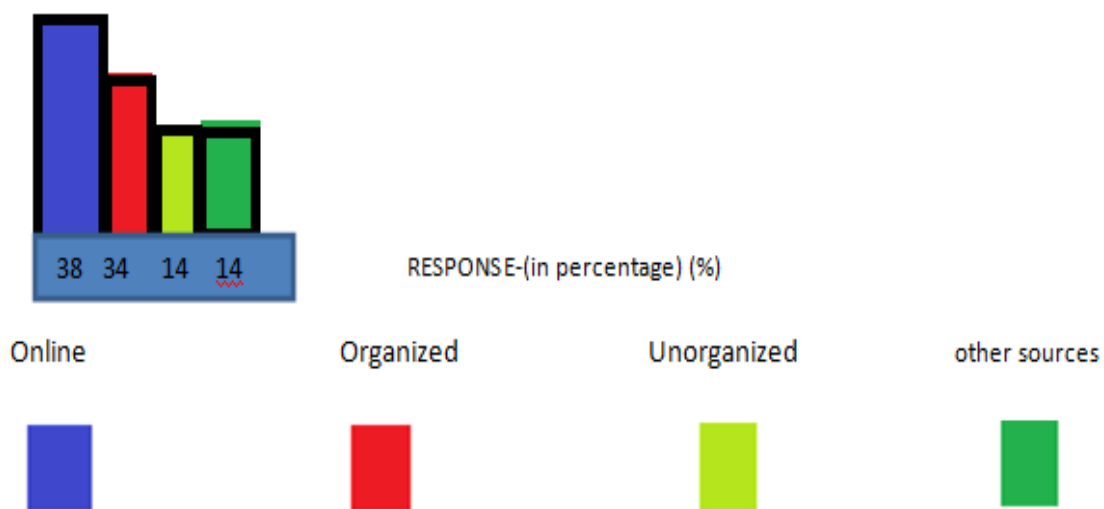


Fig. 3: Analysis: Respondents shopped from online 38%, organized from retail outlets 34%, unorganized 14% & from other sources 14%.

Q-4 Important factor you feel while shopping.

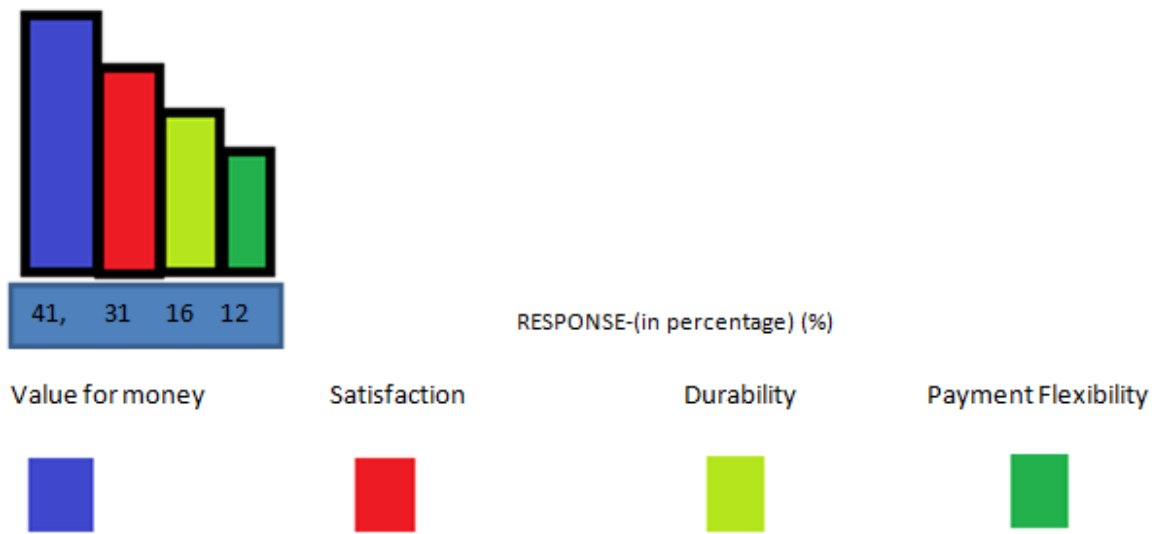


Fig.4: Analysis: Respondents felt important factor while shopping firstly was Value for money 41 %, satisfaction 31%, and durability 16 % & at last payment flexibility 12 %.

Q-5 Preferred mode of payment while shopping

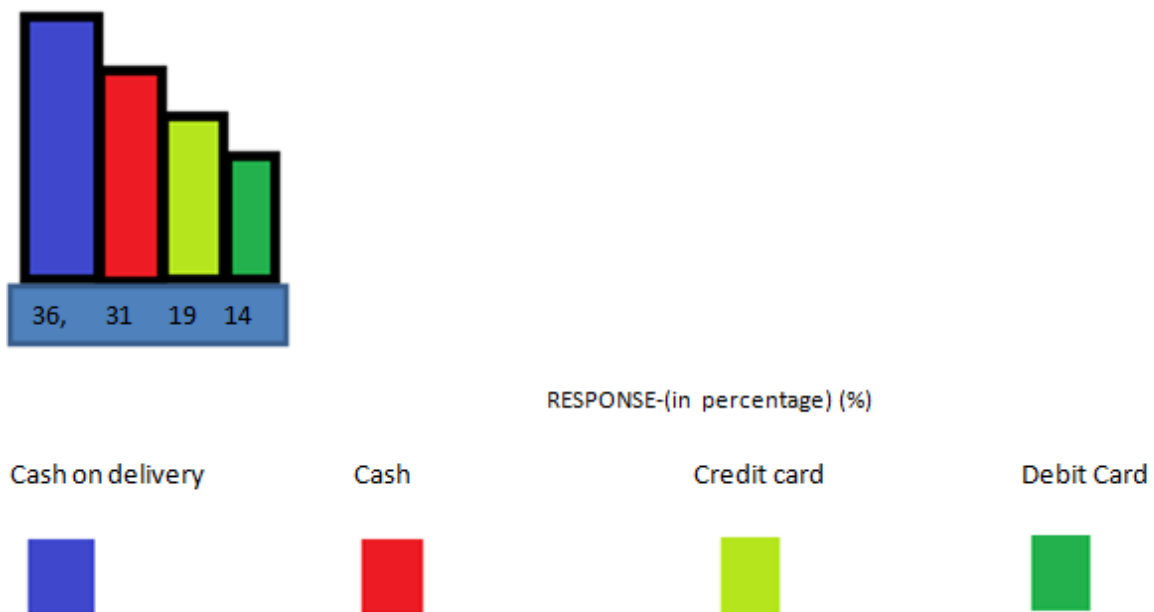


Fig. 5: Analysis: Respondents liked 36% to cash on delivery mode of payment while shopping, cash 31%, credit card 19%, debit card 14 %.

Q-6 your expectation regarding delivery of the product.

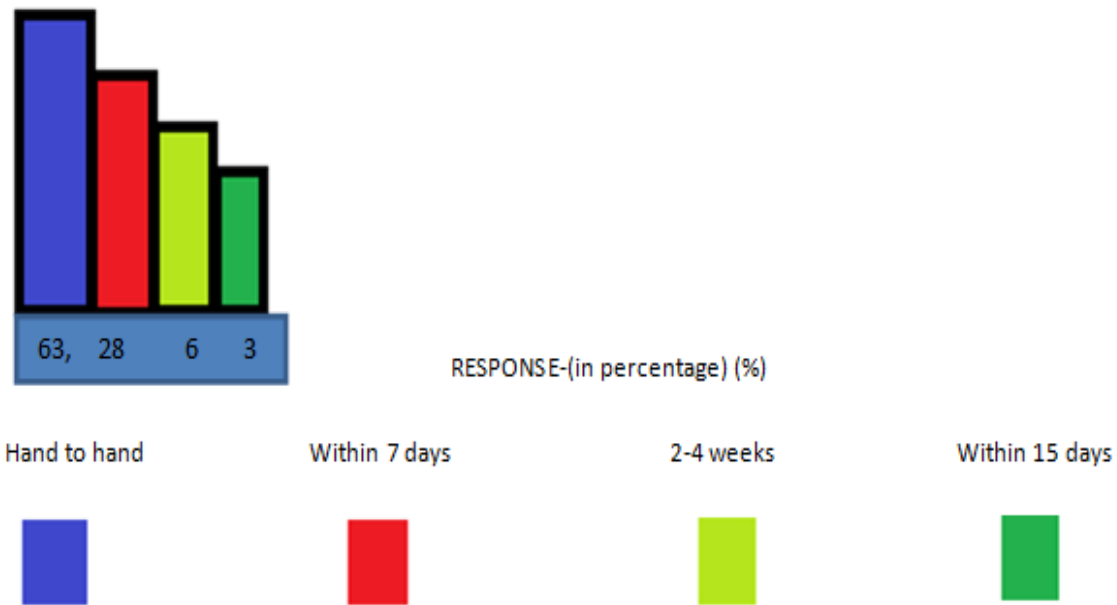


Fig.6: Analysis: Respondents first expectation regarding delivery of the product was hand to hand 63%, within 7 days 28%, 2-4 weeks 6%, within 15 days 3 %.

Q-7 while shopping and purchase of a product, which factor seems most important to you.

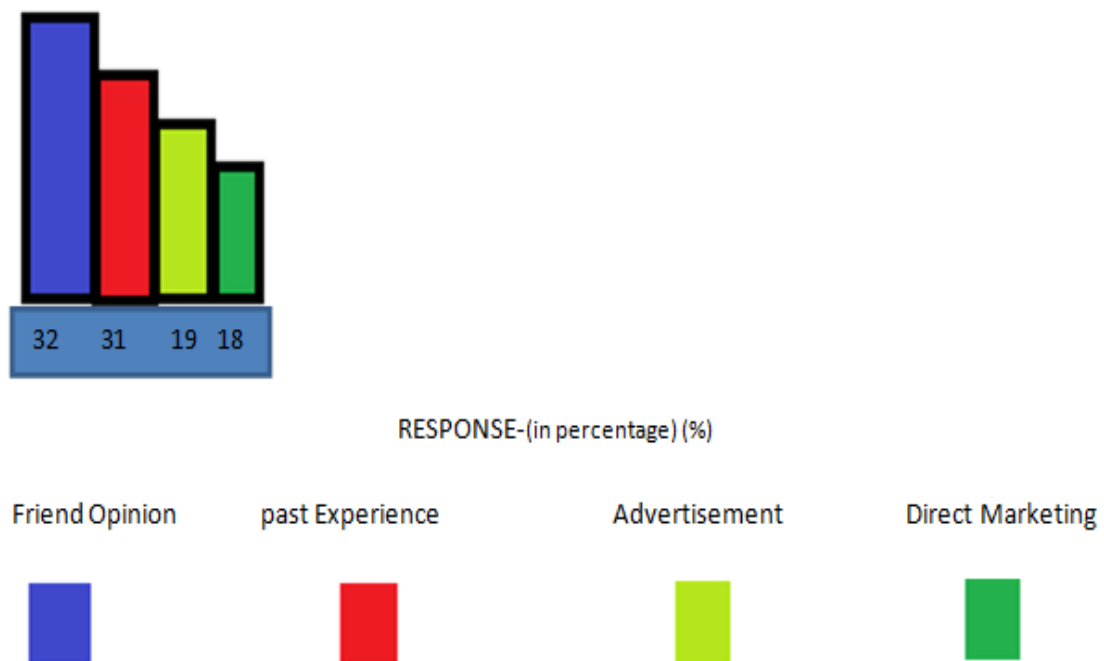


Fig.7: Analysis: While shopping and purchase of a product for respondents friend opinion 32% was important, past experience 31%, advertisement 19%, direct marketing 18%.

Q-8 Your Monthly income (RS).

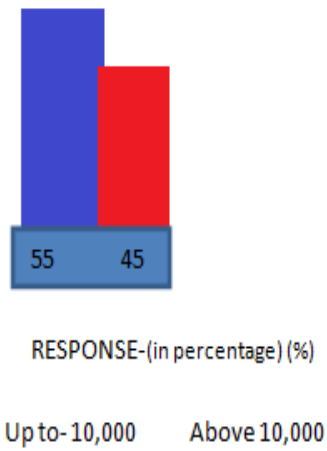


Fig. 8: Analysis: Respondents monthly income Up to-10,000 in rupees was 55% & above 10,000 rupees 45%.

Q-9 Your age.

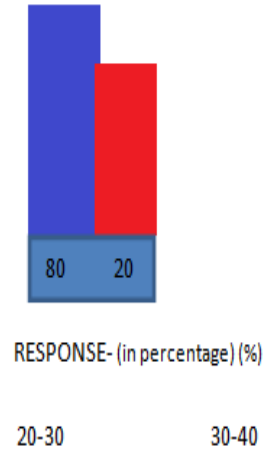


Fig. 9: Analysis Respondents age 20-30 was 80% & 30-40 was 20 %.

Q-10 Your gender.

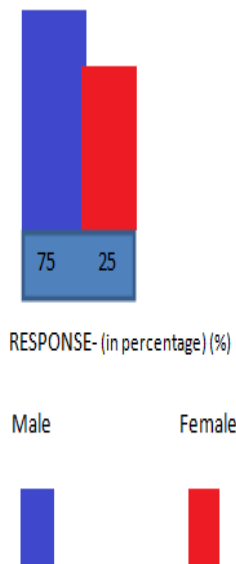


Fig. 10: Analysis: Respondents of male gender % was 75 & female 25 % it showed that male gender as comparison to female done more online shopping.

Q-11 Your Occupation

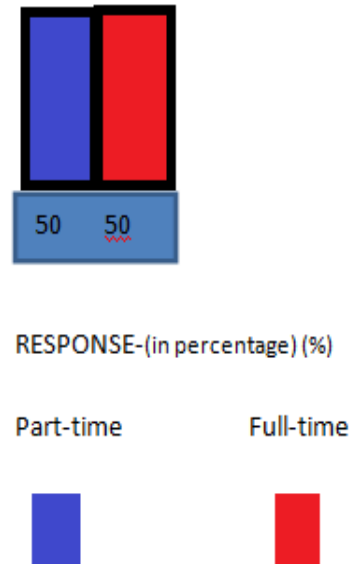


Fig. 11: Analysis: Respondents occupation of part time job & full time job was 50-50%.

Q-12 your opinion regarding online shopping.

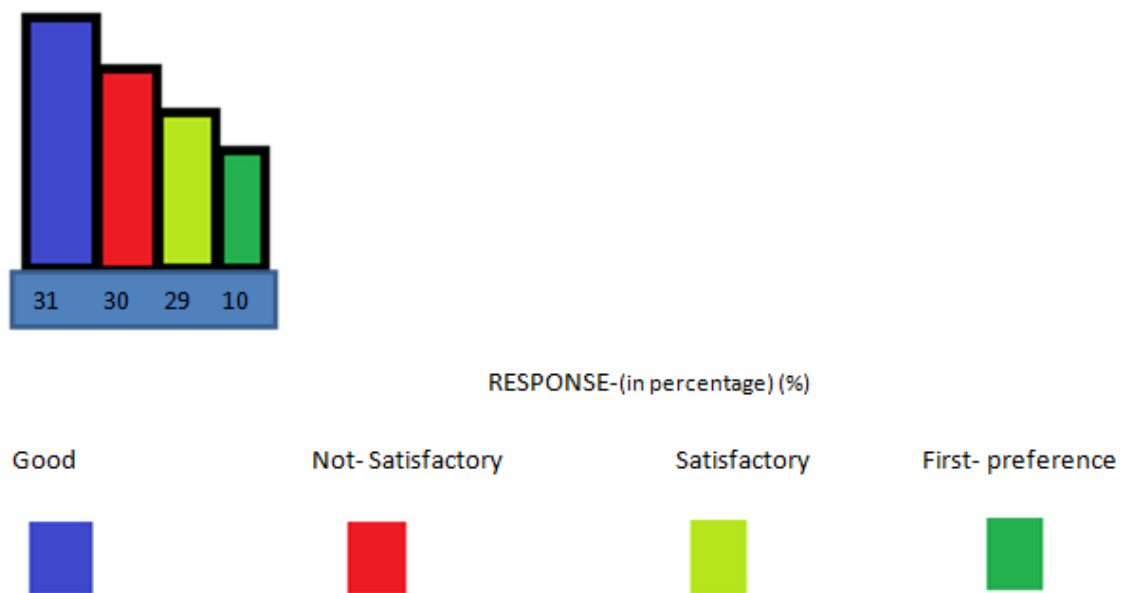


Fig. 12: Analysis: Respondents opinion regarding online shopping was good of 31%, not satisfactory 30%, satisfactory 29%, first preference 10 %

IV. CONCLUSION

Online shopping has given any and all types of consumers the ability of being able to buy anything, that is, any type of item or product, regardless of where its location is in any part of the world. What's more, the consumer does not have to leave the confines of his house or current location to be able to own and purchase the merchandise, item, or product that he wants.

Traditional shopping still allows for more ground to the consumer in terms of being able to physically check out and even try out the merchandise that he wants.

So if they have certain peculiarities, quirks, or habits that you, as a consumer, would have, no matter what type of shopping you choose, whether you would go for online shopping or traditional shopping, the bottom line is that they would always be able to find the best means to whatever suits them in both the money factor and the need or want factor.

On the other hand online shopping having some curse for the respondents

The online shopping sites do not provide fix time of delivery. These generally mention within 15 days of order for national delivery and 30 days for international delivery. But, actually it takes more than the estimated time in most of the cases for delivery of heavy products.

Respondents might be charged with high shipping cost for delivery of items like furniture, heavy electrical appliances and lots more.

Respondents do not have the option of testing the product before its delivery. The product might have some faults.

Respondents can only see the visuals of product online but not the actual product. What is shown in the picture might not be similar to what delivered to you.

Advantage

Respondents can search the exact product which they are searching for.

There are heavy discounts on online products.

Respondents can find variety of option at one place.

Respondents need not to go anywhere for shopping. They can easily shop while sitting at home.

Respondents can get the cheapest deal for the product online

Limitation

Although this study was conducted with the aim of providing accurate and authentic information, the research is subject of a few practice constraints that constitute the limitations of the study.

The sample is limited to 100 respondents only.

Convenience methods of sampling have been used which may lead to bias.

The interaction with the respondents was limited due to their work.

The study is limited to respondents in JHUNJHUNU city only.

Suggestions

Respondents should make aware about the online shopping.

They should try and understand online shopping.

Respondents who are depressed or stressed out can be counseled

V.ACKNOWLEDGEMENT

The author is thankful to the respondents of Jhunjhunu city, Rajasthan for giving their time and showing interest in this research.

REFERENCES

Journal Papers

- [1] The research development research foundation, Jaipur .Journal of banking, information technology & management, vol-11(02), July-December 2014.
- [2] JJT University, Jhunjhunu .Multi –Disciplinary Bi-annual research Journal, Vol-7 (02) June -2014 centum.
- [3] JJT University, Jhunjhunu .Research Journal of Commerce & management (Bi-annual), (spark), volume-3, (02) July 2014.
- [4] Management ideas, a monthly journal, comdex times, volume-(xx1), (01) Jan 2015.
- [5] Yadav .S.K, research methodology (Shri JJT University) Jhunjhunu.